KONINKLIJKE AKADEMIE VAN WETENSCHAPPEN TE AMSTERDAM

PROCEEDINGS

VOLUME XXXV

No. 8

President: J. VAN DER HOEVE
Secretary: B. BROUWER

CONTENTS

ERNST COHEN und L. C. J. TE BOEKHORST: "Die vermeintliche Allotropie des flüssigen Nitrobenzols", p. 1016.

L. S. ORNSTEIN und J. J. WENT: "Bemerkung über den Oberton $\triangle\nu = 1539$ im Ramanspektrum von $C\,Cl_4$", p. 1024.

R. WEITZENBÖCK: "Die projektiven Invarianten von vier Ebenen im R_5", p. 1026.

A. A. NIJLAND: "Mittlere Lichtkurven von langperiodischen Veränderlichen. IX. χ Cygni", p. 1030. (With one Plate).

F. A. H. SCHREINEMAKERS: "Osmotic systems in which non-diffusing substances may occur also", p. 1038.

F. A. H. SCHREINEMAKERS and L. J. VAN DER WOLK: "Osmotic systems with water, NaCl and Na_2CO_3 in which one invariant liquid" II, p. 1046.

F. M. JAEGER and E. ROSENBOHM: "The Exact Measurement of the Specific Heats of Solid Substances at High Temperatures. XI. On the Remarkable Behaviour of Beryllium after preliminary Heating above 420°", p. 1055.

P. H. VAN CITTERT: "The "VAN LEEUWENHOEK Microscope" in possession of the University of Utrecht". (Communicated by Prof. L. S. ORNSTEIN), p. 1062. (With one Plate).

H. I. WATERMAN, A. J. TULLENERS and J. DOOREN: "The Thermal decomposition of Paraffin wax in the Presence and in the Absence of Hydrogen of High Pressure". (Communicated by Prof. J. BÖESEKEN), p. 1063. (With one Table).

M. ZIEGLER: "On the Directional Effect of the Single Hot Wire Anemometer". (Communicated by Prof. J. M. BURGERS), p. 1067.

W. HUREWICZ: "Ueber die henkelfreien Kontinua". (Communicated by Prof. L. E. J. BROUWER), p. 1077.

C. S. MEIJER: "Asymptotische Entwicklungen von BESSELschen, HANKELschen und verwandten Funktionen". IV. (Communicated by Prof. J. G. VAN DER CORPUT), p. 1079.

G. L. SMIT SIBINGA: "The interference of meridional and transversal stress in the southeastern part of Borneo". (Communicated by Prof. H. A. BROUWER), p. 1090.

U. HAANSTRA und E. SPIKER: "Ueber Fossilien aus dem Altmiozän von Rembang (Nord Java)". (Communicated by Prof. L. RUTTEN), p. 1097. (With one Plate).

T. H. VAN DEN HONERT: "On the Mechanism of the Transport of Organic Materials in Plants". (Communicated by Prof. F. A. F. C. WENT), p. 1104.

Chemistry. — *Die vermeintliche Allotropie des flüssigen Nitrobenzols.*

Von ERNST COHEN und L. C. J. TE BOEKHORST.

(Communicated at the meeting of October 29, 1932.)

Einleitung.

In einer Anzahl kürzerer Mitteilungen [1] über die Temperaturabhängigkeit gewisser physikalischer Eigenschaften des Nitrobenzols, Aethyläthers und des Schwefelkohlenstoffs, welche sie in einer längeren Abhandlung unter dem Titel „Ueber zwei verschiedene Flüssigkeitszustände" zusammenfassten, kamen M. WOLFKE und J. MAZUR [2] zu dem Schlusse, dass die genannten Flüssigkeiten den allotropen Stoffen zuzuzählen sind. Gewisse Zweifel an der Zuverlässigkeit der Versuche, welche am Nitrobenzol angestellt waren, veranlassten uns zunächst an diesem Stoffe eine Nachprüfung von einigen der von den genannten Autoren mitgeteilten Ergebnissen zu unternehmen. Während unserer Untersuchung erschienen von mehreren Seiten [3] Mitteilungen über den nämlichen Gegenstand, der ja für unsere Kenntnisse über den Molekularzustand der Flüssigkeiten von hoher Bedeutung ist. Wir haben unsere Arbeit fortgesetzt, weil die von uns angestrebte Genauigkeit eine grössere war als die in den bisher veröffentlichten Arbeiten erreichte. Während wir die ausführliche Beschreibung unserer Versuche demnächst an anderer Stelle zu bringen gedenken, teilen wir hier kurz die wichtigsten Resultate unserer Messungen am Nitrobenzol mit. Auch die ausführlichere Besprechung der Arbeiten anderer Autoren, welche sich mit den von WOLFKE und MAZUR am Nitrobenzol erhaltenen Ergebnissen befassen. verschieben wir auf später.

1. *Darstellung von reinem Nitrobenzol.*

1. Es liegt auf der Hand sich in einem Falle, wie dem vorliegenden, nicht zufriedenzugeben mit der Darstellung auf nur *einem* Wege. Wir

---

[1] Nature **126**, 649, 684, 993 (1930); **127**, 236, 270, 741, 893, 927 (1931); **128**, 584, 673, 761, 871 (1931). Auch Acta physica polonica **1**, 47, 53, 63, 71 (1932).

[2] Z. Physik **74**, 110 (1932).

[3] MASSY, WARREN und WOLFENDEN, J. Chem. Soc. 91. (1932); NEWTON FRIEND, Nature **129**, 471 (1932); PIEKARA, Nature **130**, 93 (1932); LOTHAR MEYER, Z. Physik **75**, 421 (1932); THORNE und BAYLEY, Phys. Rev. **41**, 376 (1932); SMITS, Z. physik. Chem. (A) **160**, 225 (1932); SMITS und GERDING, Z. physik. Chem. (A) **160**, 231 (1932); MURAKAMI, Bull. Chem. Soc. Japan **7**, 216 (1932); BRAUNE und GIERTZ, Z. physik. Chem. (A) **161**, 389 (1932); VAN ITTERBEEK, Nature **130**, 389 (1932); WOLFKE und ZIEMECKI, Acta physica polonica **1**, 271 (1932); WELLM, Z. physik. Chem (B) **19**, 113 (1932); TROTTER, Phys. Rev. **40**, 1052 (1932). Vergl. auch MENZIES und LACOSS über die Allotropie des flüssigen Benzols, Proc. Nat. Acad. Sci. **18**, 144 (1932).

arbeiteten dementsprechend mit *zwei* Präparaten. Das erste (*A*) war erhalten aus einem Handelspräparat, welches Wasser und eine geringe Menge Dinitrothiophen enthielt. Nachdem dasselbe viele Male der fraktionierten Kristallisation sowie einer mehrmals wiederholten fraktionierten Destillation unter vermindertem Druck und der scharfen Trocknung über P_2O_5 unterworfen worden war, der nochmals fraktionierte Kristallisation folgte, wobei durch geeignete Wahl der Apparate dafür gesorgt wurde, dass auch geringe Spuren Wasser nicht aufgenommen werden konnten, erhielten wir schliesslich etwa 0.5 Kilo eines Präparates, mit dem die Versuche, von denen später die Rede sein wird, ausgeführt wurden. In demselben liess sich Dinitrothiophen nicht mehr nachweisen.

2. Die von diesem Präparate erhaltenen Kristallisationsfraktionen zeigten einen unveränderlichen Schmelzpunkt von 5.77° ± 0.01 C. Dieses Präparat wurde sorgfältigst unter den nötigen Kauteln gegen Wasseraufnahme in vorher scharf getrocknete Glaskölbchen gegeben. Sodann schmolzen wir dieselben zu und hoben sie im Dunkeln auf. Eine spätere Kontrolle ergab, dass der Schmelzpunkt auch während fünf Monaten innerhalb 0.01° C. unverändert blieb.

3. Unser zweites Präparat (*B*) stellten wir her durch Nitrieren (nach MASSON[1])) von (thiophenfreiem) Benzol p. A. für Molekulargewichtsbestimmung (MERCK), welches wir zuvor der fraktionierten Kristallisation unterwarfen. Nachdem das erhaltene Produkt in derselben Art und Weise wie unser Präparat *A* gereinigt war, änderte sich der Schmelzpunkt bei weiteren Kristallisationen nicht mehr. Derselbe ergab sich zu 5.77° ± 0.01 C., war also der ähnliche wie der unseres Präparates *A*.

B wurde wie *A* aufgehoben und änderte auch während acht Monaten seinen Schmelzpunkt nicht.

2. *Die verwendeten Thermometer.*

4. Merkwürdigerweise teilen die meisten Autoren, die sich mit einer Nachprüfung der von WOLFKE und MAZUR erhaltenen Ergebnisse befasst haben, nichts Näheres mit über die von ihnen benutzten Thermometer, während der Temperaturmessung bei der Feststellung der Temperaturabhängigkeit bestimmter physikalischer Eigenschaften einer Flüssigkeit doch die grösste Bedeutung beizulegen ist.

5. Wir verwendeten ein in Hundertstel Grade geteiltes Normal-Beckmannthermometer, welches von der Physikalisch-technischen Reichsanstalt in Berlin-Charlottenburg geeicht war. Die Temperatur, welche dieses Instrument im schmelzenden Eise angab, wurde genau ermittelt. Wir benutzten hierzu reines Eis, welches wir durch Gefrieren von reinstem destilliertem Wasser hergestellt hatten. Bei der monatlichen Wieder-

---

[1]) **Nature 128, 726 (1931).**

holung der betreffenden Bestimmung erhielten wir stets innerhalb 0.01° C. denselben Wert. Das betreffende Instrument wurde stets in schmelzendem Eis aufbewahrt. Die weiteren Thermometer, deren wir uns bedienten, waren mit einem von der *P. T. R.* kontrollierten Instrument verglichen worden.

3. *Die verwendeten Gewichte.*

6. Die bei unseren Messungen benutzten Gewichte hatten wir zuvor in bekannter Weise nach TH. W. RICHARDS [1]) kontrolliert.

4. *Die Temperaturabhängigkeit der Dichten des Nitrobenzols im Intervall 1—20° C.*

7. Zur Dichtebestimmung unserer beiden Präparate bei verschiedenen Temperaturen verwendeten wir zwei Dilatometer von der von ANDREAE [2]) beschriebenen Form. Das Volumen der Kugeln betrug etwa 35 cc., das Lumen der Kapillare 2 mm. Eine besondere Vorrichtung setzte uns in Stand die Einführung der Flüssigkeit unter Vermeidung jeglicher Berührung derselben mit der Luft auszuführen. Nachdem die beiden Dilatometer durch Auswägen mit luftfreiem Wasser in geeigneter Weise sorgfältigst geeicht waren, schritten wir zu den Dichtebestimmungen. Die Dilatometer befanden sich dabei in einem grösseren, mit Wasser gefüllten Thermostaten, dessen Temperatur innerhalb 0.01° C. konstant gehalten wurde. Die Wägungen (auf einer BUNGEschen Wage mit Spiegelablesung) fanden statt bis auf $^1/_{10}$ Milligramm.

8. Nach jeder Messungsreihe bei verschiedenen Temperaturen pressten wir die Flüssigkeit unter Vermeidung jeglicher Berührung derselben mit der Luft, in einen scharf getrockneten Beckmannschen Gefrierpunktsbestimmungsapparat und ermittelten ihren Schmelzpunkt aufs Neue. Derselbe war *stets* innerhalb 0.01° C. derselbe geblieben.

9. Unsere Tabelle 1 enthält die in der beschriebenen Art und Weise ermittelten Dichten (bezw. das spezifische Volumen) des Nitrobenzols. Die Werte $D^{t°}_{4°}$ sind die Mittelwerte der an unseren Präparaten *A* und *B* mittels der Dilatometer I und II gefundenen Dichten bei den in Kolumne 1 (Tabelle 1) aufgeführten Temperaturen.

So sind z.B. die Werte $D^{5°.93}_{4°}$ bezw. $D^{14°.44}_{4°}$ entstanden aus den in Tabelle 2 verzeichneten Einzelbestimmungen.

10. Die in Kolumne 3 der Tabelle 1 verzeichneten *V*-Werte lassen sich darstellen mittels der Gleichung:

$$V_t = 0.81759^3 + 0.0_3663\,t + 0.0_648\,t^2 \quad . \quad . \quad . \quad . \quad . \qquad (1)$$

welche nach der Methode der kleinsten Quadrate berechnet ist.

---

[1]) Z. physik. Chem. **33**, 605 (1900).

[2]) Z. physik. Chem. **82**, 109 (1913).

TABELLE 1.

Dichte und spezifisches Volumen des Nitrobenzols zwischen 1 und 20° C.

Temp. in ° C.[1]	Dichte $D^{t^\circ}_{4^\circ}$	Spez. Vol. V gef.	Spez. Vol. V ber.	Diff. (gef.—ber.) $\times 10^5$
1.36	1.22175	0.81850	0.81850	± 0
2.35	1.22076	0.81916	0.81916	± 0
2.95	1.22017	0.81956	0.81955	+ 1
3.54	1.21959	0.81995	0.81995	± 0
3.94	1.21919	0.82022	0.82021	+ 1
4.44	1.21869	0.82055	0.82055	± 0
4.75	1.21840	0.82075	0.82076	— 1
4.95	1.21819	0.82089	0.82089	± 0
5.45	1.21769	0.82123	0.82122	+ 1
5.95	1.21721	0.82155	0.82156	— 1
6.43	1.21672	0.82188	0.82188	± 0
6.94	1 21623	0.82221	0.82222	— 1
7.44	1.21571	0.82256	0.82256	± 0
7.94	1.21522	0.82290	0.82289	+ 1
8.44	1.21472	0.82323	0.82323	± 0
8.93	1.21427	0.82354	0.82356	— 2
9.43	1.21375	0.82389	0.82389	± 0
9.93	1.21327	0.82422	0.82423	— 1
10.43	1.21278	0.82455	0.82456	— 1
10.92	1.21228	0.82489	0.82489	± 0
11.43	1.21178	0.82523	0.82524	— 1
12.44	1.21079	0.82591	0.82592	— 1
13.44	1.20978	0.82660	0.82660	± 0
14.44	1.20879	0.82727	0.82727	± 0
15.45	1 20781	0.82794	0.82796	— 2
16.35	1.20690	0.82857	0.82857	± 0
16.45	1.20681	0.82863	0.82864	— 1
17.45	1.20582	0.82931	0.82931	± 0
19.96	1.20336	0.83101	0.83102	— 1

---

[1] Das Nitrobenzol blieb auch im unterkühlten Zustande (1.36° bis 5.45°) völlig flüssig.

TABELLE 2.

Temp. in ° C	$D^{t^\circ}_{4^\circ}$ Mit Dilatometer I		$D^{t^\circ}_{4^\circ}$ Mit Dilatometer II		Mittel
	Präparat A	Präparat B	Präparat A	Präparat B	
9.93	1.21325	1.21326	1.21331	1.21327	1.21327
14.44	1.20875	1.20878	1.20881	1.20881	1.20879

Hierin stellt V_t das spez. Volumen des Nitrobenzols, t die entsprechende Temperatur in C°. dar.

Kolumne 5 enthält die Differenz ($\times 10^5$) zwischen den experimentell von uns gefundenen und den nach dieser Gleichung berechneten V-Werten. Es ergibt sich also, dass ein Knick in der Dichte-Temperatur-Kurve des Nitrobenzols, wie derselbe von Wolfke und Mazur[1]) gefunden wurde, nicht auftritt.

Sollte den von Wolfke und Mazur in ihrer Figur 5 (zwischen 9.40° und 10.76° C.) als *unregelmässig* liegend bezeichneten Punkten auf der Dichte-Temperatur-Kurve reelle Bedeutung zukommen, so wäre an die Möglichkeit zu denken, dass das von ihnen untersuchte Präparat irgend welche Verunreinigung enthalten hat, welche in dem Sinne eines „agent minéralisateur" wirkend, die Bildung einer zweiten Form des flüssigen Nitrobenzols begünstigt hätte. Bei festen Stoffen sind ja derartige Wirkungen bekannt.

11. Berechnet man nach Gleichung (1) die Dichte bei den Temperaturen, bei welchen Wolfke und Mazur ihre Bestimmungen ausführten, so entstehen die in Tabelle 3 eingetragenen Werte.

TABELLE 3.

Temperatur in ° C	$D^{t^\circ}_{4^\circ}$ nach Wolfke und Mazur	$D^{t^\circ}_{4^\circ}$ nach Cohen und te Boekhorst
6.43	1.2413	1.21672
7.16	1.2351	1.21600
8.54	1.2246	1.21463
9.02	1.2205	1.21416
9.40	1.2173	1.21378
9.60	1.2145	1.21358
10.76	1.2130	1.21244
15.72	1.2075	1.20753
19.65	1.2033	1.20364

---

[1]) Z. Physik 74, 110 (1932).

12. Um ferner festzustellen, ob die bedeutenden Abweichungen, welche zwischen den von WOLFKE und MAZUR bestimmten D-Werten und den unsrigen vorliegen, sich durch einen Wassergehalt ihres Präparates erklären lassen, haben wir ein Präparat untersucht, dessen Schmelzpunkt durch Wasserzusatz ungefähr auf den von WOLFKE und MAZUR[1]) gefundenen (5.50° C.), gebracht war. Zu diesem Zwecke setzten wir unserem reinen Präparat soviel Wasser zu (etwa 0.05 Gew. Proz.) bis der Schmelzpunkt 5.55° C. geworden war. Die an diesem Gemisch ermittelten spezifischen Volumina lassen sich mittels folgender Gleichung darstellen:

$$V_t = 0.81778^3 + 0.0_3663\,t + 0.0_6 48\,t^2 \quad . \quad . \quad . \quad . \quad . \quad (2)$$

also mittels einer Kurve, welche der durch die Gleichung (1) dargestellten parallel geht.

13. Auch in diesem Falle tritt somit ein Knick nicht auf. Damit wird der von SMITS und GERDING[2]) gegebenen Erklärung der von WOLFKE und MAZUR beschriebenen Erscheinung beim Nitrobenzol der Boden entzogen; dies entspricht dem bereits von BRAUNE und GIERTZ[3]) Mitgeteilten.

5. *Die Temperaturabhängigkeit der Viskosität des Nitrobenzols im Intervall 3—20° C.*

14. Auch die Temperaturabhängigkeit der Viskosität (Fluidität) unserer beiden Präparate haben wir studiert. Dabei wurden dieselben Fürsorgen getroffen betreffs der Wasseraufnahme, wie bei den Dichtebestimmungen, nur wurde hier nicht nach jeder einzelnen Serie von Messungen der Schmelzpunkt aufs Neue ermittelt sondern erst nachdem sämtliche Reihen abgeschlossen waren. Wiederum zeigte sich, dass der Schmelzpunkt 5.77° ± 0.01 C. geblieben war.

15. Bei den Viskositätsmessungen an unseren beiden Präparaten bedienten wir uns des von ERNST COHEN und BRUINS früher ausführlich beschriebenen[4]) Präzisionsverfahrens. Die zu untersuchende Flüssigkeit pressten wir durch zwei Schichten gehärteten Filtrierpapiers zwecks Entfernung eventuell vorhandener Stäubchen.

16. Die Art und Weise in der wir die absoluten Viskositäten des Nitrobenzols bei den verschiedenen Temperaturen ermittelten, ergibt sich aus folgendem Beispiel, in dem es sich um die Bestimmung der absoluten Viskosität bei 7.93° C. handelt.

---

[1]) Nature **127**, 893 (1931).

[2]) Z. physik. Chem. (A) **160**, 231 (1932).

[3]) Z. physik. Chem. (A) **161**, 389 (1932).

[4]) Z. physik. Chem. **103**, 404 (1923). Speziell S. 432 ff.

Dichte bei 7.93° C. des Nitrobenzols in der Luft 1.21398
Ausflusszeit 644.7 Sek. (Mittel aus 644.5; 644.8; 644.9; 644.5 Sek.).
Dichte bei 20.00° C. des Nitrobenzols in der Luft 1.20212
Ausflusszeit 510.4 Sek. (Mittel aus 510.3; 510.4; 510.3; 510.5 Sek.).
Dichte bei 20.00° C. des Wassers in der Luft 0.99703
Ausflusszeit 304.4 Sek. (Mittel aus 304.4; 304.3; 304.4 Sek.).

Das Verhältnis zwischen den Viskositäten des Nitrobenzols bei 7.93° und bei 20.00° C. ergibt sich zu:

$$\frac{644.7 \times 1.21398}{510.4 \times 1.20212} = 1.2756$$

Setzen wir die absolute Viskosität des Wassers[1]) bei 20.00° C. 0.01006, so finden wir für die absolute Viskosität des Nitrobenzols bei 20.00° C.:

$$[\eta]_{20.00^\circ} = \frac{510.4 \times 1.20212}{304.4 \times 0.99703} \times 0.01006 = 0.02034$$

Es ergibt sich nunmehr die absolute Viskosität des Nitrobenzols bei 7.93° C. zu

$$[\eta]_{7.93^\circ} = 1.2756 \times 0.02034 = 0.02594$$

also dessen Fluidität bei jener Temperatur zu:

$$\varphi_{7.93^\circ} = \frac{1}{[\eta]_{7.93^\circ}} = 38.54$$

17. Unsere Tabelle 4 enthält die so erhaltenen Werte bei siebzehn Temperaturen zwischen 2.95° und 20.00° C. Mittels der Methode der kleinsten Quadrate findet man:

$$\varphi_t = 31.98^9 + 0.80348\, t + 0.002742\, t^2 \quad . \; . \; . \; . \; . \; . \quad (3)$$

Aus der fünften Kolumne ergibt sich, dass diese Gleichung die Temperaturabhängigkeit der Viskosität im genannten Intervall vorzüglich beschreibt. Auch hier verläuft die Kurve kontinuierlich.

18. Ein Präparat, dem absichtlich eine geringe Menge Wasser zugesetzt und dessen Schmelzpunkt infolgedessen auf 5.57° C. gefallen war, haben wir in genau derselben Weise untersucht. Die gefundenen Fluiditäten lassen sich mittels folgender Gleichung darstellen:

$$\varphi_t = 31.92^9 + 0.80348\, t + 0.002742\, t^2 \quad . \; . \; . \; . \; . \; . \quad (4)$$

Offenbar geht diese Kurve der in Gleichung (3) dargestellten parallel: dieselbe verläuft kontinuierlich.

---

[1]) HOSKING, Phil. Mag. (6) **18**, 260 (1909).

TABELLE 4.

Absolute Viskosität und Fluidität des Nitrobenzols im Intervall 3—20° C.

Temp. in ° C.	Abs. Viskosität	Fluidität φ gef.	Fluidität φ ber.	Diff. gef.—ber.
2.95	0.02908	34.39	34.38	+ 0.01
3.94	0.02841	35.20	35.20	± 0
4.94	0.02776	36.03	36.03	± 0
5.94	0.02714	36.85	36.86	— 0.01
6.93	0.02655	37.67	37.69	— 0.02
7.93	0.02594	38.54	38 53	+ 0.01
8.92	0.02540	39.38	39.37	+ 0.01
9.42	0.02514	39.79	39.80	— 0.01
9.92	0.02484	40.26	40.23	+ 0.03
10.92	0.02434	41.09	41.09	± 0
11.93	0.02383	41.96	41.96	± 0
12.93	0.02336	42.81	42.83	— 0.02
13.94	0.02286	43.75	43.72	+ 0.03
14.94	0.02242	44.60	44.60	± 0
15.95	0.02197	45.51	45.50	+ 0.01
16.95	0.02155	46.40	46.39	+ 0.01
17.95	0.02114	47.31	47.30	+ 0.01
20.00	0.02034	49.17	49.16	+ 0.01

Zusammenfassung.

Es wurde nachgewiesen, dass sowohl die Dichte-Temperatur-Kurve, wie die Viskosität-Temperatur-Kurve des reinen flüssigen Nitrobenzols im Intervall 1—20° C. kontinuierlich verläuft und dass eine Allotropie dieser Flüssigkeit, wie WOLFKE und MAZUR diese gefunden zu haben glauben, nicht existiert.

Es liegt auf der Hand, dass eine Nachprüfung der Ergebnisse von WOLFKE und MAZUR auch beim Aethyläther und dem Schwefelkohlenstoff not tut.

VAN 'T HOFF-Laboratorium.

Utrecht, im Oktober 1932.

Physics. — *Bemerkung über den Oberton $\triangle\nu = 1539$ im Ramanspektrum von $C\,Cl_4$.* Von L. S. ORNSTEIN und J. J. WENT. (Mitteilung aus dem Physikalischen Institut der Reichs-Universität Utrecht).

(Communicated at the meeting of October 29, 1932.)

Bei $C\,Cl_4$ hat man im Raman-Spektrum vier Grundfrequenzen, wovon zufälligerweise $\triangle\nu = 773\ \mathrm{cm}^{-1}$ genau mit der Kombinationsfrequenz $314 + 459 = 773\ \mathrm{cm}^{-1}$, zusammen fällt, wodurch eine Aufspaltung in zwei gleich starke Komponenten auftritt[1]). Der Oberton $\triangle\nu = 1539\ \mathrm{cm}^{-1}$ sollte nun, wie PLACZEK schon zeigte[2]), keine Aufspaltung geben; die Beobachtung hat ihn denn auch immer als einfach gezeigt.

Hier sollen nun Untersuchungen über das Intensitätsverhältnis Ton-Oberton und die Breite des Obertons gegenüber derjenigen des Tons mitgeteilt werden.

Wegen der geringen Intensität dieses Obertons war eine lichtstarke Aufstellung notwendig. Ein Blechzylinder von 30 cm. Länge und etwa 20 cm. Durchmesser wurde auf der Innenseite mit einer MgO Lack weiss angestrichen der im sichtbaren Teil des Spektrums sehr stark diffus und nicht selektiv reflektiert[3]). In diesen Behälter wurde eine gewöhnliche Heraeus Quarz-Quecksilberlampe und ein Flüssigkeitsrohr (Fig. 1) aufgestellt. Wenn man das Flüssigkeitsrohr gegen direktes Hg Licht schützt hat man also eine volkommen gleichmässige und undefinierte Einstrahlung. Um die Lichtintensität noch zu steigern wurde kein Woodsches Rohr benutzt sondern ein Rohr, das sowohl an Vorder als Hinterseite senkrecht abgeschlossen war. Bei *B* ist noch ein Spiegel angebracht, wodurch auch nach hinten gestreutes Licht nutzbar gemacht wird. Da der Brechungsindex von $C\,Cl_4 > 1.43$ ist, kann durch Totalreflexion kein unzerstreutes Licht das

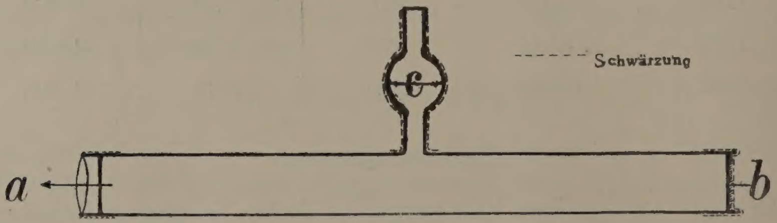

Fig. 1.

---

[1]) E. FERMI Z. f. Phys. 71, 250, 1931.
G. PLACZEK und W. R. VAN WIJK, Z. f. Phys. 67, 582, 1930.

[2]) G. PLACZEK, Leipziger Vorträge 1931.

[3]) Scientific Papers of the Bureau of Standards.

Rohr in der Beobachtungsrichtung *A* verlassen. Bei *C* ist ein kleiner Ballon angeblasen, der die sich beim Erhitzen ausdehnende Flüssigkeit aufnehmen kann; dabei werden auch störende Reflexionen am flachen Flüssigkeitsmeniskus in *C* vermieden. Die Kühlung wurde durch kalte Luft erreicht, die mit einem Ventilator in den Behälter geblasen wurde und wodurch bei konstanter Luftmenge/sec. eine konstante Temperatur von 32° C erreicht werden konnte. Der Spiegel des Rohres wurde mit Linsen auf den Spalt eines kleinen Fuess-Spektrographen abgebildet.

Die Lichtstärke dieser Anordnung war derart, dass bei einer Stromstärke der Hg Lampe von nur 1.9 Amp., drei der vier Raman-Linien von $C\,Cl_4$, angeregt durch $\lambda = 4358$ Å, mit dem kleinen Feuss-Spektrographen visuell zu beobachten und innerhalb einer Minute alle vier Linien zu photographieren waren.

Es wurden verschiedene Aufnahmen von $\triangle\nu = 773$ und $\triangle\nu = 1539$ cm^{-1} (anregende Linie 4358) auf Illford Iso Zenith Platten gemacht mit Spaltbreiten von 0.0125 bis 0.075 mm und Beleuchtungszeiten von 7½ Stunden bis 20 Minuten.

Intensitätsmarken wurden mit den üblichen Utrechter Methoden angebracht. Die Mikrophotogramme der Raman-Linien wurden mit dem Woudaschen apparat[1]) in Intensitäten umgerechnet und für die Intensitätsmessungen die Linien planimetriert.

Tafel 1 gibt die Halbwertsbreiten des Tons und Obertons bei verschiedenen Spaltbreiten in Wellenzahlen.

TAFEL I.

Spaltbreite	Halbwertsbreite Ton	Halbwertsbreite Oberton
0.0125 mm.	51 cm.$^{-1}$	54 cm.$^{-1}$
0.025 „	53 „	54 „
0.050 „	53 „	59 „
0.075 „	64 „	71 „

Man kann also bestimmt sagen dass die Halbwertsbreite des Obertons mindestens ebenso gross ist wie diejenige des Tons, obwohl nur letzterer doppelt sein dürfte.

Für das Intensitätsverhältnis der zwei Linien bekommt man 1 : 5.6. Der Oberton ist also sehr schwach und hat nur eine Intensität von 1×10^{-3} der anregenden Linie[2]). Vielleicht besteht hier auch noch eine kleine

---

[1]) J. Wouda, Z. f. Phys. im Erscheinen.

[2]) A. Carrelli und J. J. Went, Z. f. Phys. **76**, 236, 1932.

Abhängigkeit dieses Verhältnisses von der Spaltbreite, d.h. derart, dass für kleine Spaltbreiten der Oberton verhältnismässig etwas schwächer ist, was auch leicht verständlich wird wenn man berücksichtigt, dass $\triangle\nu = 773$ aus zwei einfachen Frequenzen besteht und $\triangle\nu = 1539$ aus einem Frequenzband aufgebaut ist.

Mathematics. — *Die projektiven Invarianten von vier Ebenen im R_5.* Von R. WEITZENBÖCK.

(Communicated at the meeting of October 29, 1932.)

Im projektiven R_5 ist eine zweidimensionale Ebene a durch ihre 20 homogenen Koordinaten a_{ikl} $(i, k, l = 1, 2, \ldots, 6)$ gegeben. Wir wollen in Folgendem beweisen, dass vier Ebenen a, α, p und π ausser den sechs bilinearen Invarianten der Gestalt

$$A_{12} = (a^3\,\alpha^3) = 36\,\Sigma\, a_{123}\,\alpha_{456}$$

noch eine projektive Invariante $J = J_{1234}$ besitzen, die sich symbolisch durch

$$J_{1234} = (a^3\,\alpha^2\,p)\,(\alpha\,p^2\,\pi^3)$$

darstellen lässt. Jede analog gebaute Invariante $J_{\varkappa\lambda\mu\nu}$, wo $\varkappa\,\lambda\,\mu\,\nu$ eine beliebige Permutation von 1234 bedeutet, ist durch J_{1234} und die A_{ik} ganz und rational ausdrückbar. Die sieben Invarianten J_{1234} und A_{ik} bilden ein kleinstes volles System der vier Ebenen.

§ 1.

Zuerst beweisen wir, dass man stets den Ansatz

$$J = (a^3\,\alpha^2\,p) \quad \ldots\ldots\ldots\ldots \quad (1)$$

machen kann. Ist nämlich $J = (a^3\,x\,y\,z)$ und $x = b$ (aquivalent mit a), so folgt $J = 0$ wegen der zwischen den a_{ikl} geltenden quadratischen p-Relationen. Ebenso führt $(a^3\,\alpha\,\beta\,\gamma)$ zu Null und A_{12}. Bei $(a^3\,\alpha\,\beta\,p)$ gibt das Hineinbringen der zwei weiteren Reihen α in den Klammerfaktor Reduktion und $(\alpha^3\,a^2\,p)$, d.h. also den Typus (1). Somit kann man in $(a^3\,x\,y\,z)$ $x = \alpha$, $y = p$ und $z = \pi$ voraussetzen:

$$K = (a^3\,\alpha\,p\,\pi)\,(\alpha^2\,\ldots\,.).$$

Bringt man hier die Reihe α des ersten Klammerfaktors in den zweiten, so führt dies zu

$$K = (a^3\,\beta\,p\,\pi)\,(\alpha^3\,x\,y\,z)$$

und auch hier müssen x, y und z von drei verschiedenen Ebenen stammen und $\neq \beta$ sein.

Also

$$K = (a^3 \beta p \pi)(\alpha^3 \ldots)(\beta^2 \ldots .).$$

Hier bringen wir wieder die Reihe β des ersten Klammerfaktors in den dritten und erhalten

$$K = (a^3 \gamma p \pi)(\alpha^3 \ldots)(\beta^3 \ldots)(\gamma^2 \ldots).$$

Mit γ verfahren wir genau so. Schliesslich muss in $(a^3 x p \pi)$ die Reihe x von der 1., 3. oder 4. Ebene stammen und das gibt Reduktion. Wir können also in der Tat von (1) ausgehen.

§ 2.

Wenn in $J = (a^3 \alpha^2 p)\ (p^2 \ldots)$ die Reihe p des ersten Klammerfaktors in den zweiten gebracht wird, entsteht $J = (a^3 \alpha^2 \xi)\ (p^3 x y z)$. Ist ξ $(= q$ oder $\pi)$ nicht eine der Reihen x, y, z, so haben wir

$$J = (a^3 \alpha^2 \xi)(p^3 \ldots)(\xi^2 \ldots).$$

Hier bringen wir wieder die erste Reihe ξ in den dritten Klammerfaktor:

$$J = (a^3 \alpha^2 \eta)(p^3 x y z)(\xi^3 u v w).$$

Dies fortgesetzt führt schliesslich zu einem $J = (a^3 \alpha^2 s)$, wo eine zweite Reihe s unter den Reihen x, y, z; u, v, w; ... auftritt, d.h. J hat die Gestalt

$$J = (a^3 \alpha^2 \pi)(p^3 \pi x y) \quad \ldots\ldots\ldots \quad (2)$$

Sind hier x und y von π verschieden, so bringen wir die Reihen π des ersten und zweiten Klammerfaktors in den dritten $(\pi \ldots\ldots)$ und erhalten

$$J = (a^3 \alpha^2 \xi)(p^3 \ldots)(\pi^3 \ldots);$$

hier ist $\xi \neq b, \beta$ und ξ kann also nicht auch im zweiten *und* dritten Klammerfaktor stehen, d.h. wir haben

$$J = (a^3 \alpha^2 \xi)(p^3 \ldots)(\pi^3 \ldots)(\xi \ldots).$$

Hier bringen wir wieder alle drei Reihen ξ in den letzten Klammerfaktor:

$$J = (a^3 \alpha^2 \eta)(p^3 \ldots)(\pi^3 \ldots)(\xi^3 \ldots).$$

Dies fortgesetzt, führt entweder auf eine Invariante der Gestalt

$$J_1 = (a^3 \alpha^2 \pi)(p^3 \pi \ldots)(q^3 \pi \ldots) \quad \ldots\ldots\ldots \quad (3)$$

oder auf den auch aus (2) für $x = \pi$ erhältlichen Typus

$$J_2 = (a^3 \alpha^2 \pi)(p^3 \pi^2 \xi) \quad \ldots\ldots\ldots \quad (4)$$

Auf diesen ist aber auch J_1 sofort reduzierbar, wenn wir z.B. die dritte Reihe π in den zweiten Klammerfaktor hineinbringen.

Wir können somit von (4) aus weiterbauen. Ist $\xi=\alpha$, so erhalten wir die Invariante

$$J_{1243}=(a^3\alpha^2\pi)(\alpha\pi^2p^3);. \quad . \quad . \quad . \quad . \quad . \quad . \quad . \quad . \qquad (5)$$

es bleibt also

$$J_2=(a^3\alpha^2\pi)(p^3\pi^2\xi)(\xi^2\ldots) \quad . \quad . \quad . \quad . \quad . \quad . \quad . \quad . \qquad (6)$$

mit $\xi=b$ oder $\xi=\beta$.

Hier bringen wir die Reihe ξ des zweiten Klammerfaktors in den dritten und erhalten:

$$J_2=(a^3\alpha^2\pi)(p^3\pi^2\eta)(\xi^3\ldots)$$
$$J_2=(a^3\alpha^2\pi)(p^3\pi^2\zeta)(\xi^3\ldots)(\eta^3\ldots)$$

Wir kommen so wie bei (3) auf den Typus

$$J_3=(a^3\alpha^2\pi)(p^3\pi^2x)(\xi^3x\ldots)(\eta^3x\ldots)$$

mit $x, \xi, \eta=b, c, \beta, \gamma$ und durch die analoge Umformung, die von (3) auf (4) führte, auf den Typus

$$J_4=(a^3\alpha^2\pi)(\pi^2p^3b)(b^2\beta^3\eta) \quad . \quad . \quad . \quad . \quad . \quad . \quad . \quad . \qquad (7)$$

mit $\eta=\alpha, q, \varrho$.

Mit η schliessen wir hier so weiter wie bei (6) mit den Reihen ξ. Es ergeben sich dann für J_4 Ketten der Gestalt

$$J_4=(\alpha^2a^3\pi)(\pi^2p^3b)(b^2\beta^3\varrho)\ldots.(\lambda^2\mu^3\alpha)$$

die notwendig mit der letzten Reihe α endigen müssen. Deuten wir diese Ketten durch

$$21\frown 43\frown 12\frown\ldots.\frown\lambda\mu$$

an, so muss J_4 eine gerade Anzahl Indexpaare enthalten; denn die Indizes in jedem Paare sind vertauschbar und endigt J_4 mit 12, so ist $(c^2\gamma^3\alpha)=0$ sein letzter Klammerfaktor. Wir haben also:

$$J_4=12\frown 34\frown 12\frown 34\frown\ldots.34 \quad . \quad . \quad . \quad . \quad . \qquad (8)$$

Das einfachste J_4 ist $12\frown 34$ oder J_{2134} (Vgl. (5)), dann kommt ein J_4 mit vier Klammerfaktoren:

$$J_4=(a^2\alpha^3p)(p^2\pi^3b)(b^2\beta^3q)(q^2\varrho^3a) \quad . \quad . \quad . \quad . \quad . \quad . \qquad (9)$$

Diese Ketten können wir nun wie folgt reduzieren. Wir bringen die zwei Reihen p des zweiten Klammerfaktors in (9) in den ersten hinein (zweimaliges Umformen). Hierdurch entsteht:

$$\left.\begin{array}{r}J_4=12\frown 34\frown 12\frown\ldots\frown 34=\\=-(13\frown 24\frown 12\frown\ldots\frown 34)-2(\alpha^2p^3a)(a\alpha\pi^3b)\frown b\beta\frown\ldots\frown(3^24^3a)+red\cdot\end{array}\right\}(10)$$

Der erste Term rechts ist wegen $24 \frown 12$ reduzibel. Beim zweiten ziehen wir die Reihe a des letzten Klammerfaktors in den zweiten hinein, wodurch Reduktion auf $(\alpha^2 p^3 a)\ (a^2 \alpha \pi^3) = J_{2314}$ entsteht.

§ 3.

Wir haben jetzt noch zu zeigen, dass alle Invarianten $J_{\varkappa\lambda\mu\nu}$ auf J_{1234} und die sechs A_{ik} reduzierbar sind. Stellen wir in $J_{1234} = (1^3\, 2^2\, 3)\ (2\, 3^2\, 4^3)$ die beiden Klammerfaktoren um, so haben wir

$$J_{1234} = J_{4321} \quad . \quad . \quad . \quad . \quad . \quad . \quad . \quad . \quad . \quad (11)$$

Bringen wir die letzte Reihe 2 in den ersten Klammerfaktor, so kommt

$$J_{1234} = J_{2134} + \tfrac{1}{3} A_{12} A_{34} \quad . \quad . \quad . \quad . \quad . \quad . \quad . \quad (12)$$

Ziehen wir hingegen die zwei letzten Reihen 3 in den ersten Klammerfaktor hinein, so entsteht:

$$J_{1234} = 2 J_{1324} - J_{1423} + \tfrac{1}{3} A_{13} A_{42} + \tfrac{1}{3} A_{14} A_{23}$$

Vertauschen wir hier 2 mit 3 und 2 mit 4, so ergibt sich mit Hilfe von (11) und (12):

$$J_{1234} = J_{1324} + \tfrac{1}{9} (A_{12} A_{34} + A_{13} A_{42} + A_{14} A_{23}) \quad . \quad . \quad . \quad (13)$$

Vermöge (11), (12) und (13) lässt sich dann für jede Permutation $\varkappa\lambda\mu\nu$ von 1234 das zugehörige $J_{\varkappa\lambda\mu\nu}$ in der Gestalt

$$J_{\varkappa\lambda\mu\nu} = J_{1234} + Q$$

darstellen, wo Q Null oder linear in den Produkten $A_{ik} A_{rs}$ ist.

Es lässt sich leicht durch spezielle Wahl der vier Ebenen a, α, p und π zeigen, dass die sieben Invarianten A_{ik} und J_{1234} ein *kleinstes volles System von projektiven Invarianten* bilden. Hieraus folgt dann, dass die Figur von vier Ebenen im R_5 *drei absolute projektive Invarianten* besitzt, die z.B. im allgemeinen Falle in rationaler Gestalt durch

$$\frac{J_{1234}}{A_{12} A_{34}}, \quad \frac{J_{1342}}{A_{13} A_{42}}, \quad \frac{J_{1423}}{A_{14} A_{23}}$$

gegeben werden können.

Man kann an Stelle der Invariante J_{1234} auch eine andere Invariante S in das Invariantensystem aufnehmen, die *symmetrisch* in allen vier Ebenen ist:

$$S = J_{1234} - \tfrac{1}{6} A_{12} A_{34} + \tfrac{1}{18} A_{13} A_{42} - \tfrac{1}{18} A_{14} A_{23} \quad . \quad . \quad . \quad (14)$$

Es ist $S = \frac{1}{24} \Sigma J_{\varkappa\lambda\mu\nu}$, wo sich Σ über alle 24 Permutationen erstreckt.

Astronomy. — *Mittlere Lichtkurven von langperiodischen Veränderlichen.* IX. *χ Cygni.* Von A. A. NIJLAND.

(Communicated at the meeting of October 29, 1932).

Instrumente *B*, *S* und *R*. Die Beobachtungen wurden alle auf *R* reduziert; die Reduktion *R—S* beträgt $-0^{m}.43$, die Reduktion *R—B* nicht weniger als $-0^{m}.81$. Spektrum M6—8e (*Harv. Ann.* **79**, 188).

Gesamtzahl der hier zu besprechenden Beobachtungen 962 (von 2416836 bis 2426915). Wie in meinen früheren Publikationen wurden die in zwei Instrumenten angestellten Schätzungen nur einmal gezählt. Tatsächlich ist die Zahl der Schätzungen 1084. Es wurden zwei verdächtige Schätzungen verworfen, bei denen wahrscheinlich die Vergleichsterne falsch identifiziert worden sind. Für den merkwürdigen Fall 2420928 (1916 März 5) s. *Hemel en Dampkring*, **13**, 165. Die daselbst entwickelte Hypothese hat sich als unhaltbar erwiesen; s. auch *Mem. B. A. A.*, **25**, 422.

Karte: HAGEN, *Atlas Stell. var. Series III*; s. auch *Spec. Vat.* XII.

Die Sterne *f*, *i* ($8^{m}.13$) und *p* kommen auch in den *Harv. Ann.* 74 vor. Die Grösse $7^{m}.57$ für *f* fällt aus der Skala heraus, und blieb unberücksichtigt. Es wurde auch *p* von der Diskussion ausgeschlossen, weil die beiden a. a. O. gegebenen Werte $10^{m}.94$ und $11^{m}.62$ schlecht unter sich stimmen.

Die von ROSENBERG in seiner Monographie *Der veränderliche χ Cygni* gegebenen photometrischen Helligkeiten sind scheinbar zum grössten Teil den *Harv. Ann.* entnommen, jedoch mit hier und da nicht unerheblichen Abänderungen. Die in *Harv. Ann.* 98 angeführten Sterne *B*, *c*, *d*, *f*, *h* und *i* kommen auch in Band 37 vor.

Für Stern *p* findet man bei MITCHELL (*Mem. Am. Ac.* **14**, 286) als Mittel mehrerer sehr gut übereinstimmenden photometrischen Messungen (HARVARD, YERKES, LICK, Mc. CORMICK) die Grösse $11^{m}.30$. Stern *o* wurde 7-mal an die Grenze von *S*, *u* 21-mal an die Grenze von *R* angeschlossen.

Die Stufenskala wurde diesmal für die 3 Instrumente getrennt hergestellt, und zwar reduziert auf die Grössen $6^{m}.0$, bezw. $9^{m}.0$ und $11^{m}.0$. Die drei Skalen decken sich teilweise: s. die Tabelle II. Für *S* und *R* ist die Beziehung zwischen Stufenskala und photometrischer Skala nahezu linear; der Stufenwert wird $0^{m}.094$, bezw. $0^{m}.101$. Für das Opernglas *B* ist die bildliche Darstellung deutlich gekrümmt; man kann sie auch in zwei gerade Linien ($4^{m}.2$ bis $6^{m}.0$, TABELLE I. Vergleichsterne.

	BD	HAGEN	PD	PD *red*	HA 29	HA 37	HA 74	ROSENBERG	HA 98	
E	$+29^{\circ}.4057$	—	$4^{m}.32$ GW	$4^{m}.09$	—	—	—	$4^{m}.07$	$4^{m}.09$	F5*p*
D	+31.4062	—	4.65 RG —	4.67	—	—	—	4.54	4.60	K2
C	+34.3590	—	4.88 W	4.59	—	—	—	4.90	4.85	B3
B	+33.3587	—	5.10 WG+	5.04	$5^{m}.01$	$5^{m}.03$	—	5.02	5.03	F5
A	+36.3557	—	5.36 GW —	5.09	—	—	—	[illegible]	5.15	A0*p*
a	+30.3837	—	5.72 GW —	5.44	—	—	—	5.57	5.44	B8
b	+31.3925	—	5.91 WG	5.82	—	—	—	—	5.69	B0
c	+32.3531	—	6.24 GW	5.97	5.92	5.89	—	5.91	5.89	A2
d	+33.3602	3	6.77 GW	6.50	6.45	6.35	—	6.35	6.35	B0
e	+32.3526	—	7.27 W	6.92	—	—	—	—	6.94	F0
f	+31.3765	—	7.67 GW	7.38	7.30	7.28	$[7^{m}.57]$	7.28	7.28	B0
h	+32.3578	6	—	—	7.66	7.62	—	7.53	7.62	K5
i	+32.3589	7	—	—	—	8.10	8.13	8.11	8.03	B8
k	+32.3600	13	—	—	8.63	8.73	—	8.68		
l	+32.3583	20	—	—	9.17	—	—	—		
m	+32.3581	34	—	—	9.67	—	—	9.67		
n	—	51	—	Grenze	—	—	—	10.53		
o	—	62	—	$11^{m}.14$	—	—	—	11.00	MITCHELL	
p	—	67	—	—	—	—	[10,94 11.62]	11.33	$11^{m}.30$	
q	—	87	—	—	12.11	11.72	—	11.92		
r	—	92	—	—	12.37	—	—	12.18		
s	—	107	—	—	—	12.66	—	12.81		
u	—	122	—	13.74	—	—	—	13.40		

Stufenwert $0^{m}.060$ und $6^{m}.0$ bis $7^{m}.0$, Stufenwert $0^{m}.085$) zerlegen. Aus praktischen Gründen empfiehlt es sich aber, auch hier eine für das ganze Intervall von 4^{m} bis 7^{m} geltende lineare Beziehung anzunehmen: der Stufenwert wird dann $0^{m}.068$. Die Wahl zwischen diesen verschiedenen Auffassungen ist schwer zu treffen. In der Tabelle II findet man die drei Stufenskalen nebst den daraus abgelesenen Grössen für die drei Instrumente dargestellt, und zwar für *B* nach dem oben Gesagten sowohl in zwei Teile B_1 und B_2 getrennt, wie auch als ein Ganzes behandelt.

TABELLE II. Stufenskalen.

	Stufenskala			Abgeleitete Grössen					H
	B	*S*	*R*	B_1	B_2	*B*	*S*	*R*	
E	41.3	—	—	$4\overset{\mathrm{m}}{.}19$	—	$4\overset{\mathrm{m}}{.}07$	—	—	$4\overset{\mathrm{m}}{.}13$
D	36.4	—	—	4.48	—	4.40	—	—	4.44
C	32.2	—	—	4.73	—	4.68	—	—	4.71
B	26.0	—	—	5.10	—	5,10	—	—	5.10
A	24.0	—	—	5.22	—	5.24	—	—	5.23
a	20.0	—	—	5.46	—	5.51	—	—	5.48
b	16.0	—	—	5.70	—	5.78	—	—	5.74
c	11.6	44.8	—	5.97	$6\overset{\mathrm{m}}{.}00$	6.08	$5\overset{\mathrm{m}}{.}85$	—	5.97
d	6.2	38.9	—	—	6.45	6.45	6.40	—	6.43
e	1.5	33.4	—	—	6.86	6.77	6.92	—	6.85
f	[0.0]	29.6	—	—	[6.99]	[6.87]	7.26	—	7.26
h	—	25.2	60.1	—	—	—	7.68	$7\overset{\mathrm{m}}{.}40$	7.54
i	—	20.2	52.9	—	—	—	8.15	8.10	8.12
k	—	14.3	46.7	—	—	—	8.70	8.72	8.71
l	—	9.9	41.7	—	—	—	9.12	9.22	9.17
m	—	4.1^{5}	34.8	—	—	—	9.67	9.93	9.80
n	—	[0.0]	28.4	—	—	—	[10.07]	10.58	10.58
o	—	—	26.8	—	—	—	—	10.74	10.74
p	—	—	20.4	—	—	—	—	11.40	11.40
q	—	—	15.2	—	—	—	—	11.93	11.93
r	—	—	11.0	—	—	—	—	12.37	12.37
s	—	—	5.5	—	—	—	—	12.93	12.93
u	—	—	0.0	—	—	—	—	13.50	13.50
1°				$0\overset{\mathrm{m}}{.}060$	$0\overset{\mathrm{m}}{.}085$	$0\overset{\mathrm{m}}{.}068$	$0\overset{\mathrm{m}}{.}094$	$0\overset{\mathrm{m}}{.}101$	

Die *B*- und *S*-Skalen sind bei der unteren Grenze sehr unsicher, da die Zahl der beobachteten Stufendifferenzen hier klein ist. Diese beiden unteren Grenzen blieben daher unberücksichtigt. Es gliedert sich, wie man sieht, Stern *f* vorzüglich in die *S*-Skala, Stern *n* in die *R*-Skala ein, so dass die angenommenen Grössen *H* dieser Sterne (letzte Spalte) als gut verbürgt gelten können. Überhaupt liessen sich die Teilskalen

A. A. NIJLAND: MITTLERE LICHTKURVEN VON LANGPERIODISCHEN VERÄNDERLICHEN. IX. χ CYGNI.

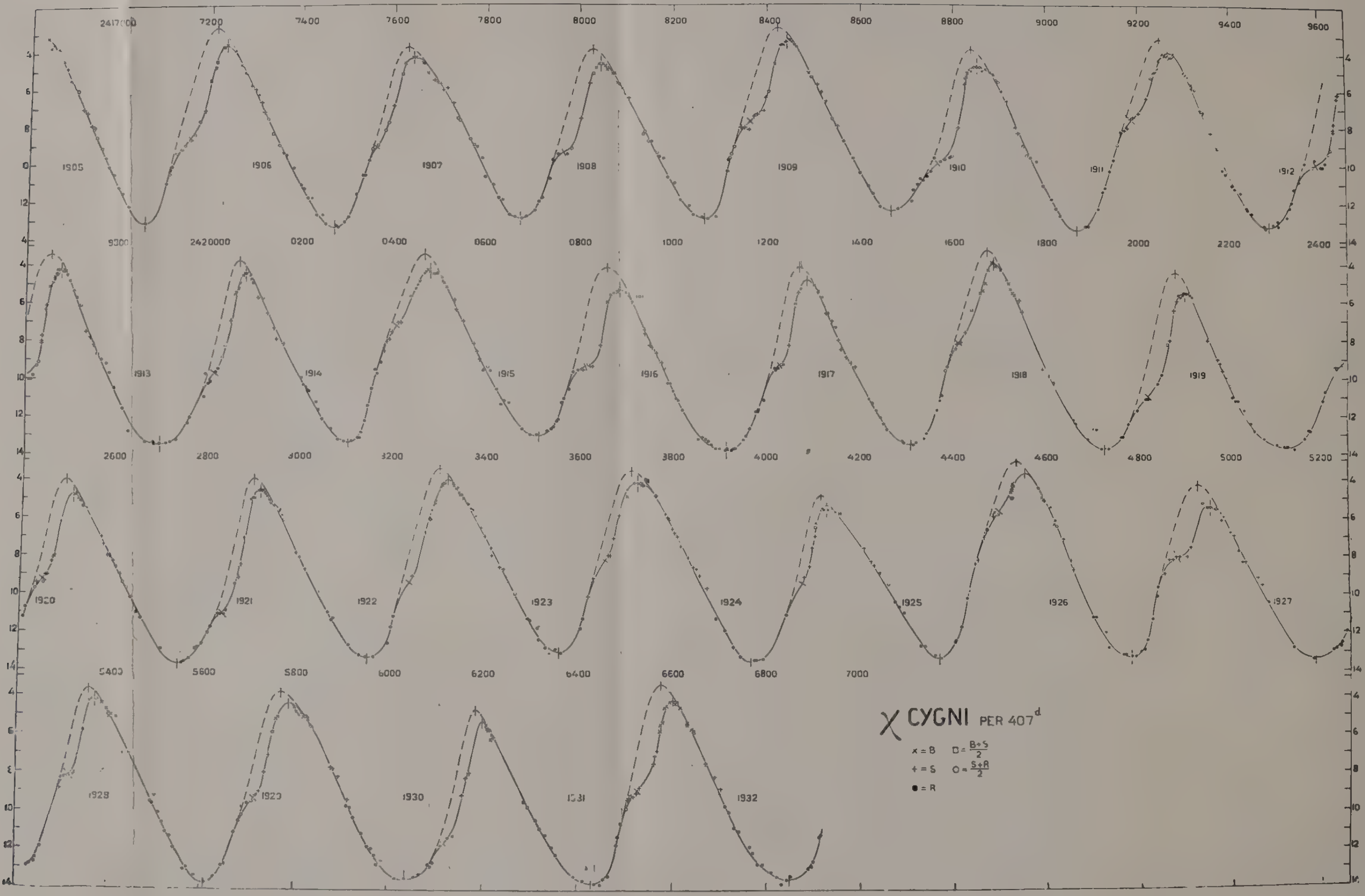

Fig. 1

befriedigend kombinieren. Es wurde das einfache Mittel genommen (letzte Spalte), sogar für die Sterne *h* und *m*, obwohl hier die Differenzen *R—S* ziemlich gross sind.

Es liegen 105 Schätzungen der Farbe vor, welche zum grössten Teil in den Jahren 1905 bis 1909 angestellt wurden. Aus den Tabellen III*a* und III*b* geht hervor, dass sich die Farbenauffassung weder mit der Zeit noch mit der Helligkeit erheblich geändert hat. Das allgemeine Mittel ist $4^{c}.81$.

TABELLEN III*a* und III*b*. Farbenschätzungen.

Zeitraum	*n*	Farbe	Grösse	*n*	Farbe
^{241}6948—7311	20	$5^{c}.15$	$4^{m}.52$	13	$4^{c}.54$
7318—7685	20	4.70	5.30	13	4.88
7691—8134	20	4.40	5.74	13	4.88
8138—8566	21	5.15	6.38	13	4.54
8794—^{242}0516	21	4.81	7.68	13	4.42
3688—4981	3	[5.7]	8.62	13	5.27
	105		9.18	13	4.81
			10.11	14	5.71
				105	4.81

Die Figur 1 enthält die Beobachtungen, alle auf *R* reduziert. Die Reihe der Abweichungen (Beobachtung minus Kurve) zeigt 359 Plus-, 337 Minuszeichen, 266 Nullwerte, 388 Zeichenfolgen, 307 Zeichenwechsel. Das Mittel der absoluten Werte der Abweichungen ist $0^{m}.111$.

Ein Einfluss des Mondscheines auf die Helligkeitsschätzung ist nicht bemerkbar. Es verteilen sich auf 316 bei Mondschein angestellte Beobachtungen die Abweichungen wie folgt: 105 Plus-, 99 Minuszeichen, 112 Nullwerte.

Die Tabelle IV enthält die aus der Kurve abgelesenen Epochen der Minima *m* und der Maxima *M*.

Die Spalte *R* wurde mit den einfachen Elementen:

$2421936^{d} + 407^{d}\,E$ (für die Minima)

und $2422110 + 407\,E$ (für die Maxima)

gerechnet.

Aus den Spalten *B—R* geht hervor, dass die Periode von χ *Cygni*

TABELLE IV.

E	Minima *m*					Maxima *M*				
	B	*v*	*R*	*B—R*	*B—F*	*B*	*v*	*R*	*B—R*	*B—F*
— 12	^{241}7057	$^{\mathrm{m}}$13.1	7052	+ 5	— 10	^{241}7232	$^{\mathrm{m}}$3.7	7226	+ 6	— 10
— 11	7472	13.4	7459	+ 13	+ 2	7640	4.3	7633	+ 7	— 5
— 10	7872	12.8	7866	+ 6	— 2	8043	4.6	8040	+ 3	— 6
— 9	8267	12.8	8273	— 6	— 10	8443	3.3	8447	— 4	— 9
— 8	8667	12.4	8680	— 13	— 15	8852	4.7	8854	— 2	— 5
— 7	9068	13.4	9087	— 19	— 18	9268	4.0	9261	+ 7	+ 7
— 6	9492	13.3	9494	— 2	+ 1	9675	4.2	9668	+ 7	+ 9
— 5	9898	13.5	9901	— 3	+ 2	^{242}0082	4.5	0075	+ 7	+ 11
— 4	^{242}0305	13.5	0308	— 3	+ 3	0480	4.3	0482	— 2	+ 3
— 3	0715	13.0	0715	0	+ 7	0888	5.4	0889	— 1	+ 5
— 2	1115	13.8	1122	— 7	+ 1	1288	4.8	1296	— 8	— 1
— 1	1511	13.5	1529	— 18	— 9	1687	4.0	1703	— 16	— 8
0	1928	13.7	1936	— 8	+ 1	2102	5.5	2110	— 8	0
+ 1	2329	13.7	2343	— 14	— 5	2511	4.8	2517	— 6	+ 2
+ 2	2743	13.7	2750	— 7	+ 1	2918	4.6	2924	— 6	+ 1
+ 3	3152	13.3	3157	— 5	+ 2	3323	4.0	3331	— 8	— 2
+ 4	3560	13.0	3564	— 4	+ 2	3728	4.2	3738	— 10	— 5
+ 5	3972	13.5	3971	+ 1	+ 6	4131	5.5	4145	— 14	— 10
+ 6	4373	13.3	4378	— 5	— 2	4555	3.7	4552	+ 3	+ 5
+ 7	4787	13.3	4785	+ 2	+ 3	4956	5.3	4959	— 3	— 3
+ 8	5189	13.4	5192	— 3	— 5	5364	4.1	5366	— 2	— 5
+ 9	5610	13.7	5599	+ 11	+ 7	5784	4.4	5773	+ 11	+ 6
+ 10	6038	13.5	6006	+ 32	+ 24	6198	5.3	6180	+ 18	+ 9
+ 11	6431	13.7	6413	+ 18	+ 7	6602	4.3	6587	+ 15	+ 3
+ 12	6848	13.5	6820	+ 28	+ 13	—	—	—	—	—
		13.35			± 6		4.48			± 5

für den hier betrachteten Zeitraum in Zunahme begriffen ist. Aus einer graphischen Lösung folgen die Elemente *F*:

$$\left.\begin{array}{l}\text{Maximum: } 2421927^{\mathrm{d}} \\ \text{Minimum: } 2422102\end{array}\right\} + 407^{\mathrm{d}}\, E + 0.165\, E^2.$$

Obwohl die Berücksichtigung des quadratischen Gliedes die Quadratsummen der Abweichungen für die Minima und die Maxima zusammen von 5607 auf 2785 herabdrückt, halte ich die hier angedeutete säkuläre Veränderung nicht für reell. Man könnte die Parabel auch als Teil einer Sinuskurve auffassen; allerdings bleiben dann Periode und Amplitude natürlich unbestimmt. Es lässt sich nun die CHANDLERsche Formel (*G. und L.* II, 224)

$$2565136^d.5 + 406^d.02\,E' + 0^d.0075\,E'^2 + 25^d.0\,sin\,(5^\circ\,E' + 272^\circ),$$

wo $E' = E + 140$, oder

$$2422126^d + 408^d.1\,E + 0^d.0075\,E^2 + 25^d.0\,sin\,(5^\circ\,E + 252^\circ)$$

für kleine Werte von E annähernd auch schreiben in der Form:

$$2422101^d + 408^d\,E + 0^d.095\,(E - 3.6)^2,$$

welche mit verhältnismässig geringfügigen Abänderungen die von mir beobachteten Maxima leidlich gut darzustellen im Stande wäre.

PRAGER's Katalog für 1932 gibt den Periodenwert $412^d.9$, und das aus sämtlichen von mir seit d. J. 1905 in den *Astr. Nachr.* mitgeteilten Epochen der Minima und Maxima abgeleitete allgemeine Mittel ist $407^d.3$. Die extremen Werte des Lichtwechsels sind:

$$\left.\begin{array}{l} \text{Minimum: } v = 13^m.35 \pm 0^m.124 \\ \text{Maximum: } v = 4\ .48 \pm 0\ \ .066 \end{array}\right\}\ \text{(m.F.).}$$

Die Amplitude beträgt somit $8^m.87$. Weder beim Minimum noch beim Maximum zeigen die Abweichungen vom Mittelwert eine deutliche Gesetzmässigkeit.

Wie man sieht (Fig. 1) zeigt χ *Cygni* bei der Aufhellung jedesmal eine Störung, welche ohne den Charakter eines eigentlichen Buckels zu bekommen, den Aufstieg halbwegs verzögert oder zum Stillstand bringt. Die Tabelle V *A* gibt die in diesem Falle natürlich nicht sehr genauen Epochen der abgelesenen Wendepunkte, nebst der Vergleichung mit den Elementen F:

$$2422029^d + 407^d\,E + 0.165\,E^2;$$

$$v = 8^m.99 \pm 0^m.249\ \text{(m.F.).}$$

Es wurden nun wieder, genau wie bei *T Cassiopeiae* (Proc, **34**, 220) und *T Cephei* (Proc. **34**, 945), drei mittlere Teilkurven gebildet, welche sich, wie aus der Fig. 2 ersichtlich, so gut wie vollständig an einander anschliessen, und zusammen die mittlere Kurve *B* liefern (s. Tabelle VI).

Wird auch bei diesem Stern in der üblichen Weise die Kurve von der Störung befreit, so entstehen die "ungestörten" Maxima, welche

(Tabelle V*B*) mit den einfachen Elementen $2422092^{d} + 407^{d} E$, und auch mit den Elementen *F*:

$$2422084^{d} + 407^{d}\,E + 0.165\,E^{2};$$
$$v = 3^{m}.73 \pm 0^{m}.112 \text{ (m. F.)}$$

verglichen wurden.

TABELLE V.

E	*A* Wendepunkte				*B* Ungestörte Maxima				
	B	*v*	*F*	*B—F*	*B*	*v*	*R*	*B—R*	*B—F*
— 12	^{241}7154	$\overset{\mathrm{m}}{8.6}$	7169	— 15	^{241}7211	$\overset{\mathrm{m}}{2.7}$	7208	+ 3	— 13
— 11	7561	9.1	7572	— 11	7629	3.8	7615	+ 14	+ 2
— 10	7962	9.3	7976	— 14	8027	3.9	8022	+ 5	— 4
— 9	8364	7.7	8379	— 15	8423	2.7	8429	— 6	— 11
— 8	8766	9.9	8784	— 18	8839	3.9	8836	+ 3	0
— 7	9186	7.6	9188	— 2	9249	3.2	9343	+ 6	+ 6
— 6	9596	9.9	9593	+ 3	9652	3.4	9650	+ 2	+ 4
— 5	^{242}0013	9.8	9998	+ 15	^{242}0067	3.8	0057	+ 10	+ 14
— 4	0407	7.3	0404	+ 3	0468	3.5	0464	+ 4	+ 9
— 3	0813	9.3	0810	+ 3	0859	4.1	0871	— 12	— 6
— 2	1229	9.3	1216	+ 13	1272	4.1	1278	— 6	+ 1
— 1	1613	8.1	1622	— 9	1674	3.3	1685	— 11	— 3
0	2020	10.9	2029	— 9	2081	4.4	2092	— 11	— 3
+ 1	2448	9.2	2436	+ 12	2495	4.0	2499	— 4	+ 4
+ 2	2837	11.0	2844	— 7	2904	4.0	2907	— 3	+ 5
+ 3	3240	9.3	3252	— 12	3305	3.5	3313	— 8	— 2
+ 4	3657	8.2	3660	— 3	3714	3.6	3720	— 6	— 1
+ 5	4078	9.3	4068	+ 10	4117	4.9	4127	— 10	— 6
+ 6	4499	5.7	4477	+ 22	4535	3.0	4534	+ 1	+ 3
+ 7	4884	8.1	4886	— 2	4927	4.2	4941	— 14	— 14
+ 8	5312	8.2	5296	+ 16	5353	3.6	5348	+ 5	+ 2
+ 9	5710	9.3	5705	+ 5	5767	3.8	5755	+ 12	+ 7
+ 10	6119	11.7	6116	+ 3	6185	4.8	6162	+ 23	+ 14
+ 11	6528	8.9	6526	+ 2	6577	3.4	6569	+ 8	— 4
		8.99		± 8		3.73			± 6

Die Teilkurve *A* der ungestörten Maxima schliesst sich derjenigen der Minima vollständig an. Für die Schiefe der ungestörten Kurve findet man $\frac{M-m}{P} = 0.386$.

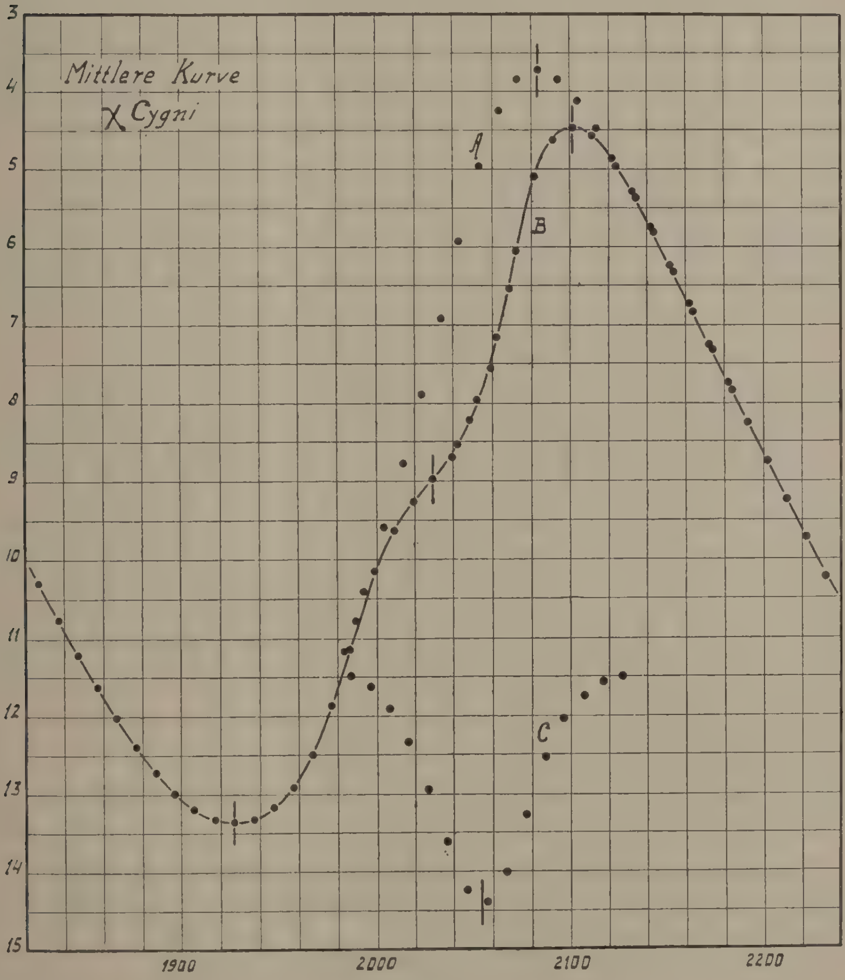

Fig. 2.

Die Differenzkurve $C = A - B$ ist so gut wie genau symmetrisch. Das Minimum, zu $2^m.91$, fällt auf 2422055, also 29 Tage vor dem ungestörten Maximum; die Helligkeit des Veränderlichen erleidet also beim Aufstieg eine Verfinsterung, welche ihn von 93% seines Lichtes beraubt.

TABELLE VI. Die mittlere Kurve.

Phase	v	Phase	v	Phase	v	Phase	v	Phase	v
-100^{d}	$10\overset{m}{.}31$	-20^{d}	$13\overset{m}{.}19$	$+60^{d}$	$11\overset{m}{.}10$	$+140^{d}$	$6\overset{m}{.}66$	$+230$	$6\overset{m}{.}51$
-90	10.77	-10	13.32	$+70$	10.30	$+150$	5.56	$+240$	7.02
-80	11.21	0	13.35	$+80$	9.72	$+160$	4.78	$+250$	7.52
-70	11.63	$+10$	13.31	$+90$	9.34	$+170$	4.50	$+260$	8.03
-60	12.03	$+20$	13.16	$+100$	9.05	$+180$	4.50	$+270$	8.53
-50	12.40	$+30$	12.92	$+110$	8.76	$+190$	4.71	$+280$	9.02
-40	12.73	$+40$	12.50	$+120$	8.32	$+200$	5.09	$+290$	9.50
-30	13.00	$+50$	11.87	$+130$	7.65	$+210$	5.53	$+300$	9.98
						$+220$	6.01	$+310$	10.45

Zusammenfassung.

Aus 962 in den Jahren 1905 bis 1932 (2416836 bis 2426915) angestellten Beobachtungen von χ *Cygni* sind die folgenden Elemente des Lichtwechsels abgeleitet worden:

$$\begin{array}{l} \text{Maximum: } 2421927^{d} \\ \text{Minimum: } 2422102 \end{array} \Big\} + 407^{d}\, E + 0.165\, E^{2}; \quad \begin{array}{r} v = 13^{m}.35 \\ v = \ \ 4\ .48 \\ \hline \text{Amplitude} = \ \ 8\ .87. \end{array}$$

Der Stern scheint beim Aufstieg eine Verdunkelung von $2^{m}.91$ zu erleiden, welche einen vollkommen symmetrischen Verlauf hat, und deren Minimum auf 2422055 fällt.

Utrecht, August 1932.

Chemistry. — *Osmotic systems in which non-diffusing substances may occur also*. I. By F. A. H. SCHREINEMAKERS.

(Communicated at the meeting of October 29, 1932.)

I. *Equilibria*.

We take an osmotic system:

$$L_P \,|\, L'_{P'} \quad \ldots\ldots\ldots\ldots \quad (1)$$

in which on the left side a liquid L under the pressure P and on the right side a liquid L' under the pressure P'. We now assume that there are d diffusing substances, that liquid L still contains n-and liquid L' still n' non-

diffusing substances; in most cases it does not matter here, as will appear later on, whether one or more of these non-diffusing substances occur together or do not occur together in both liquids.

Now when system (1) has come in equilibrium, either the two liquids will contain the d diffusing substances, no matter whether they were originally present on the two sides of the membrane yes or no. Then liquid L will contain: $d+n$ and liquid $L' : d+n'$ substances. We now represent this equilibrium by

$$L\,(d+n)_P \,|\, L'\,(d+n')_{P'} \quad . \; . \; . \; . \; . \; . \; . \; . \quad (2)$$

If W is one of the diffusing substances, then with the aid of the ζ-function we can find an equation, expressing that the total ζ of (2) does not change when a small quantity of W passes from the one liquid towards the other. This equation expresses that the substance W has the same thermodynamical potential in the two liquids, or in other words that both liquids (the one under the pressure P and the other under the pressure P') have the same O.W.A. (Osmotic Water Attraction).

As there are d diffusing substances, consequently also d of these equations exist, expressing that every diffusing substance has the same O.A. on both sides of the membrane. From this follows:

A. when an osmotic system is in equilibrium, then every diffusing substance has the same O.A. on the two sides of the membrane and the reverse.

Let us take as an example the equilibria:

$$L\,(W+\bar{X}+\bar{Y})_P \,|\, L'\,(W+\bar{X}+\bar{Y})_{P'} \quad . \; . \; . \; . \; . \quad (3)$$

$$L\,(W+\bar{X})_P \,|\, L'\,(W+\bar{X}+\bar{Y})_{P'} \quad . \; . \; . \; . \; . \; . \quad (4)$$

$$L\,(W+X)_P \,|\, L'\,(W+X+\bar{Y})_{P'} \quad . \; . \; . \; . \; . \; . \quad (5)$$

in which the dash placed above a substance indicates that this substance does not diffuse.

For the equilibria (3) and (4) it then suffices that the two liquids have the same O.W.A.; in (5), however, the two liquids must have the same O.W.A. and O.X.A.

To enable us to express various results in a simpler way, we shall understand by "state" on the left(right)side of a membrane: the composition and the pressure of the left(right)side liquid.

As liquid L contains $d+n$ substances, its composition is determined by $d+n-1$ concentrations; if besides we add to this the pressure P, then it follows that the state on the left side of the membrane depends upon $d+n$ variables. The state on the right side of the membrane is determined by $d+n'$ variables. The entire system (2) contains, therefore: $2d+n+n'$ variables.

As, however, the system is in equilibrium, d relations will exist between these variables:

$$O.A = (O.A)' \quad \dots\dots\dots \quad (6)$$

expressing that every diffusing substance must have the same O.A. on both sides; so there are only $2d + n + n' - d = d + n + n'$ free variables left. From this it follows:

B. the osmotic equilibrium

$$L\,(d+n)_P \,|\, L'\,(d+n')_{P'} \quad \dots\dots\dots \quad (7)$$

has $d + n + n'$ freedoms.

From this it follows that we may say also:

C. the number of freedoms of an osmotic equilibrium is equal to the number of substances, unless every non-diffusing substance, occurring on both sides of the membrane counts for two.

Now we may say also:

D. the osmotic equilibrium (7) can exist with an ∞ number of states on the left and on the right side of the membrane, having together $d + n + n'$ freedoms.

If we apply *B* or *C* to (3), (4) and (5), then we find that (3) has five freedoms, (4) four and (5) three, although all these equilibria consist of the same substances.

In the special case that the membrane is permeable for all substances, we have an equilibrium

$$L\,(d)_P \,|\, L'\,(d)_{P'} \quad \dots\dots\dots \quad (8)$$

As now $n = 0$ and $n' = 0$, the number of freedoms now will be d.

Each of the states namely, on the left and on the right side of the membrane, has d variables (viz. $d - 1$ concentrations and the pressure).

If we now take a definite state on one of the sides so that d freedoms are left out, then the state on the other side has no freedoms any more. From this it follows: when the state on one of the sides is determined, then the other state is determined also.

If only stable states are considered, then we can deduce with the aid of thermodynamica that we must always have $P = P'$.

If besides only those systems are considered, of which the liquids are mixable in all ratios, then we also find that we must have: $L = L'$.

As we shall here suppose both these conditions present, it follows:

E. when an osmotic system in which a membrane permeable for all substances, is in equilibrium, then the same state will be found on the two sides. Consequently both liquids have the same composition and pressure.

Later on I shall refer to systems in which also dimixtion can occur.

We now take the equilibrium

$$L\,(d)_P \,|\, L'\,(d+\bar{U})_{P'} \quad . \; . \; . \; . \; . \; . \; . \; . \; . \quad (9)$$

in which, besides the d diffusing substances, a non-diffusing substance U is also present in liquid L'. As now $n=0$ and $n'=1$, this equilibrium will have $d+1$ freedoms. Now with the aid of thermodynamica we can deduce that we must always have $P<P'$.

If we now take a definite state on the left side, so that the number of freedoms decreases with d, then the right-side state will have one freedom left. Consequently an ∞ number of states can exist on the right side, but in such a way that a definite composition goes with every definite pressure.

If, however, we take a definite state on the right side, so that the number of freedoms decreases with $d+1$, then the left side will have no freedom left. On the left side, consequently, there will also exist a definite state now, viz. a definite pressure and a definite composition.

From these considerations it follows:

F. the equilibrium

$$L\,(d)_P \,|\, L'\,(d+\bar{U})_{P'} \quad . \; . \; . \; . \; . \; . \; . \; . \; . \quad (10)$$

has $d+1$ freedoms; the pressure P' is always greater than the pressure P; if we have a definite state on the left side, then an ∞ number of states can occur on the right side, having one freedom (viz. an ∞ number of pressures P' and an ∞ number of compositions of the liquid L', but in such a way, that with every definite pressure P' goes also a definite composition of L'). If we have a definite state on the right side, then also on the left side a definite state will exist.

As a special case of (10) we take

$$L\,(Water)_P \,|\, L'\,(Water+\bar{U})_{P'} \quad . \; . \; . \; . \; . \; . \; . \quad (11)$$

in which only one diffusing substance, viz. water; what has been said above in F for equilibrium (10) obtains here also. The difference in pressure $P'-P$ is now the osmotic pressure of liquid L' (namely with respect to water under the pressure P).

We now suppose a definite state in the general equilibrium (2) on the left side of the membrane; as the number of freedoms now decreases with $d+n$, there will still remain

$$d+n+n'-(d+n)=n'. \quad . \; . \; . \; . \; . \; . \; . \quad (12)$$

freedoms; so the right-side state has as many freedoms as it has non-diffusing substances. From this it follows:

G. when in the equilibrium

$$L\,(d+n)_P \,|\, L'\,(d+n')_{P'} \quad . \; . \; . \; . \; . \; . \; . \; . \quad (13)$$

one of the states has been determined, the other state will still have as many freedoms as it has non-diffusing substances.

We see that the rules E and F only form a special case of the general rule G; an application of this rule to other cases is left to the reader.

In discussing equilibrium (7) we have not made any suggestion as to the quantity of each of the substances present and the two pressures P and P'; for this reason we shall call this equilibrium a free equilibrium.

If, however, we have an equilibrium with two definite pressures P and P', we shall call it a definite pressure- or Def. P-equilibrium.

If we take an equilibrium, containing a definite quantity of each of the substances present, we shall call it a definite quantity- or Def. Q-equilibrium.

If we take an equilibrium, having not only two definite pressures but a definite quantity of each of the substances as well, we shall call it a Def. PQ-equilibrium.

In order to illustrate the difference between these different equilibria, we take the equilibrium:

$$m \times L\,(W + X + \bar{Y} + \bar{Z})_P \,|\, m' \times L'\,(W + X + \bar{Y} + \bar{U})_{P'} \quad . \quad (14)$$

in which m quantities of a liquid L with the composition

$$x\,X + y\,Y + z\,Z + (1 - x - y - z)\,W \quad . \quad . \quad . \quad . \quad (15)$$

and m' quantities of a liquid L' with the composition

$$x'\,X + y'\,Y + u'\,U + (1 - x' - y' - u')\,W \quad . \quad . \quad . \quad (16)$$

If besides the two pressures and the six concentrations (x, y, z, x', y' and u') we consider the quantities m and m' of the two liquids as well, then (14) will contain 10 variables.

As (14) is in equilibrium there will always exist between these variables the two relations

$$OWA = (OWA)' \quad \text{and} \quad OXA = (OXA)' \quad . \quad . \quad . \quad (17)$$

expressing that both liquids have the same O.W.A. and the same O.X.A.

If (14) is a free equilibrium, so that it needs only satisfy the two relations (17), it will consequently have $10 - 2 = 8$ freedoms. These two relations, however, do not contain the quantities m and m', so that we may take always them quite arbitrarily; this is indeed obvious, because the being in equilibrium or not in equilibrium of two liquids does not depend upon their quantities.

If, therefore, we only take into consideration the state of the equilibrium (viz. the compositions and pressures of the two liquids), then the quantities m and m' cannot play a part in the free equilibrium. If we omit them because of this, then $8-2=6$ freedoms will still remain. As $d=2$, $n=2$ and $n'=2$, this is also in accordance with (7).

If we now give a definite value to both pressures, then (14) becomes a Def. P-equilibrium, having $6-2=4$ freedoms. It is clear that the quantities m and m' now will not play a part either.

This becomes different, however, when (14) is a Def. Q-equilibrium, so that it contains a definite quantity of each substance. We shall assume namely that in total (viz. on the left and on the right side of the membrane together) there are w_0 and x_0 quantities of the substances W and X. From this follow the two equations

$$\left.\begin{array}{c} m\,(1-x-y-z)+m'\,(1-x'-y'-u')=w_0 \\ m\,x+m'\,x'=x_0 \end{array}\right\} \quad . \quad . \quad (18)$$

Further we assume that on the left side of the membrane y_0 and z_0 quantities of the non-diffusing substances Y and Z occur; from this then follows:

$$m\,y=y_0 \quad \text{and} \quad m\,z=z_0 . \quad . \quad . \quad . \quad . \quad . \quad . \quad (19)$$

Finally we assume besides that on the right side of the membrane y'_0 and u'_0 quantities of the non-diffusing substances Y and U are present; from this then follows also:

$$m'\,y'=y_0' \quad \text{and} \quad m'\,u'=u_0' \quad . \quad . \quad . \quad . \quad . \quad . \quad (20)$$

So, as is apparent from (19) and (20) we have assumed that the non-diffusing substance Y, occurring on both sides of the membrane, is also present on both sides in a definite quantity.

We now shall substitute (18) by

$$\left.\begin{array}{c} m+m'=w_0+x_0+y_0+z_0+y_0'+u_0' \\ m\,x+m'\,x'=x_0 \end{array}\right\} \quad . \quad . \quad . \quad (21)$$

The first of these equations is found by adding up all equations (18)—(20); of course we might also have written down this equation, expressing that $m+m'$ is the total quantity of all substances, at once.

So the 10 variables of (14) now must not only satisfy the 2 equations (17), but also the 6 equations (19)—(21). From this it follows that the Def. Q-equilibrium (14) has $10-8=2$ freedoms.

It appears from the equations (19)—(21) that the quantities m and m' are no longer arbitrary now. At first sight this may perhaps seem a little peculiar, because, as has been said already above, the being in equilibrium or not in equilibrium of two liquids does not depend upon their quantities. It is clear, however, that in a Def. Q-equilibrium we cannot change m and m' without changing the quantities of the substances at the same time.

If in this Def. Q-equilibrium (14) we take two more definite pressures

P and P', so that it becomes a Def. PQ-equilibrium, it will have no freedom left; then the composition and the quantities m and m' of the two liquids will be completely determined.

From this it appears that the state of a Def. PQ-equilibrium is absolutely determined; of course it depends upon the quantities of the substances present, what state will occur. It appears namely from the equations (19)—(21) that the variables m, m', x, y etc. also depend upon the quantities w_0, x_0 etc. Consequently each change in one or more of these quantities results also in a change of the state. Only in the special case that we change w_0, x_0 etc. in the same ratio, m and m' will change only, but the composition of the two liquids will remain the same.

From these considerations it appears among other things also that the state of a Def. PQ-equilibrium is one definite state of the ∞ number the free equilibrium can have.

Now we may also apply these considerations to the general equilibrium

$$m \times L\,(d+n)_P \,|\, m' \times L'\,(d+n')_{P'} \quad . \quad . \quad . \quad . \quad . \quad (22)$$

Instead of the two equations (17) we now have the d equations

$$OA = (OA)' \quad . \quad . \quad . \quad . \quad . \quad . \quad . \quad . \quad . \quad (23)$$

expressing that each of the d diffusing substances has the same O.A. in both liquids.

Instead of the two equations (18) or (21) we now find d equations, instead of the two equations (19), n equations and instead of the two equations (20) now n' equations.

In a similar way as for (14) we now find:

H. The free equilibrium (22) has $d+n+n'+2$ freedoms; the quantities m and m', however, may always be taken arbitrarily. This equilibrium can exist in an ∞ number of states, having $d+n+n'$ freedoms.

I. The Def. P-equilibrium (22) has $d+n+n'$ freedoms; we may always take the quantities m and m' arbitrarily, however. This equilibrium can exist in an ∞ number of states, having $d+n+n'$-2 freedoms. In the special case that there is only one diffusing and one non-diffusing substance, there is only one state too.

K. The Def. Q-equilibrium (22) has two freedoms; the quantities m and m' are determined now. This equilibrium can exist in an ∞ number of states (with 2 freedoms) which are all included in the ∞ number of states of the free equilibrium.

L. The Def. Q-equilibrium (22) has no freedom left; now the quantities m and m' are also determined. This equilibrium only exists in one absolutely determined state, being one of the ∞ number of states of the free equilibrium.

In the special case that an equilibrium contains diffusing substances only, both liquids must have the same pressure and composition (comp. E). Of course this involves that some of the preceding results must be a little altered; this is left to the reader.

We now imagine the m quantities of liquid L closed up in a space with a volume V and the m' quantities of liquid L' in a space with a volume V'. We now represent this by:

$$[m \times L\,(d+n)_P]_V \,|\, [m' \times L'\,(d+n')_{P'}]_{V'} \quad . \quad . \quad . \quad . \quad (24)$$

As we now have two variables V and V' more than in (22), (24) will now contain $2d+n+n'+4$ variables. Between them, however, now always exist the two relations

$$m\,v = V \quad \text{and} \quad m'\,v' = V' \quad . \quad . \quad . \quad . \quad . \quad . \quad (25)$$

in which v and v' represent the volume of one quantity of the liquids L and L'. As $v(v')$ is a function of the pressure $P(P')$ and the composition of liquid $L(L')$, these relations consequently will contain all the variables of (24).

If we do not make a single suggestion as to the variables, we shall call (24) once more a free equilibrium; if we take definite volumina V and V', we may call (24) a Def. V-equilibrium; if we take a definite quantity of each of the substances, then we call (24) a Def. Q-equilibrium; if we take as well definite volumes as definite quantities of the substances, we may call (24) a Def. VQ-equilibrium.

If, besides considering the equations obtaining for equilibrium (22) we take into consideration the two equations (25) as well, then we find results for the equilibrium (24) corresponding to those above in H—L for the equilibrium (22).

Of course there are some differences indeed, as now that m and m', as appears from (25), are also connected with the volumina V and V'.

A closer consideration of these differences is left to the reader, however.

Leiden, Lab. of Inorg. Chemistry.

(To be continued).

Chemistry. — *Osmotic systems with water, NaCl and Na_2CO_3 in which one invariant liquid.* II. By F. A. H. SCHREINEMAKERS and L. J. VAN DER WOLK.

(Communicated at the meeting of October 29, 1932.)

II. *Systems with a binary and with a unary invariant liquid.*

We now take an osmotic system

$$L(z) \,|\, inv.\, L'(W+X) \quad . \quad . \quad . \quad . \quad . \quad . \quad . \quad . \quad (1)$$

in which the invariant liquid consists of the substances X and W only; it is represented in the partially drawn XYW-diagram (fig. 1) by a point i of side WX.

In this special system two paths of the bundle of this point i are known already at the beginning without any further experimental investigations. If namely we take the system

$$L(beg.\, Water) \,|\, inv.\, L'(W+X) \quad . \quad . \quad . \quad . \quad . \quad . \quad (2)$$

in which at the beginning of the osmosis the variable liquid L consists of pure water, this system will contain the substances X and W only; consequently the variable liquid will during the osmosis proceed along the straight line Wi, so that Wi is one of the paths of the bundle.

If we take the osmotic system

$$L(beg.\, u) \,|\, inv.\, L'(W+X) \quad . \quad . \quad . \quad . \quad . \quad . \quad . \quad . \quad (3)$$

then it is clear that the variable liquid will now travel along the straight line ui so that ui and consequently Xi also, is one of the paths of this bundle.

From this follows, what can also be deduced in another way [1]), that side WiX must be one of the two axes of the bundle; the other axis has been represented by line ki, which we can imagine lengthened with a part ik' below side WX. As we have already stated in the preceding communication it depends upon the nature and the composition of the invariant liquid and upon the nature of the membrane, which of these two axes will be the principal and which the secondary axis; they determine the direction of the axis ki and the station of the two diffusing final mixtures d_1 and d_2 as well.

In connection with the osmotic systems, that will be discussed later on and which, just as in the preceding communication will contain the substances.

---

[1]) F. A. H. SCHREINEMAKERS. These Proceedings **34**, 823 (1931).

$$X = NaCl \qquad Y = Na_2CO_3 \qquad \text{and} \qquad W = \text{water}$$

we take *ki* as principal and *WiX* as secondary axis; all paths (except the straight-lined *Wi* and *Xi*) must, therefore, touch line *ki* in point *i*.

The experimental determinations show besides that point d_1 is situated on the undrawn prolongation *ik'* of the principal axis, and point d_2 on the undrawn prolongation of side *XW*, consequently on the left side of point *W*; so the two points d_1 and d_2 are situated outside the triangle *XYW*. If we compare fig. 1 of this communication with fig. 1 of the preceding one, we see that in both figures the situation of the points d_1 and d_2 with respect to point *i* corresponds.

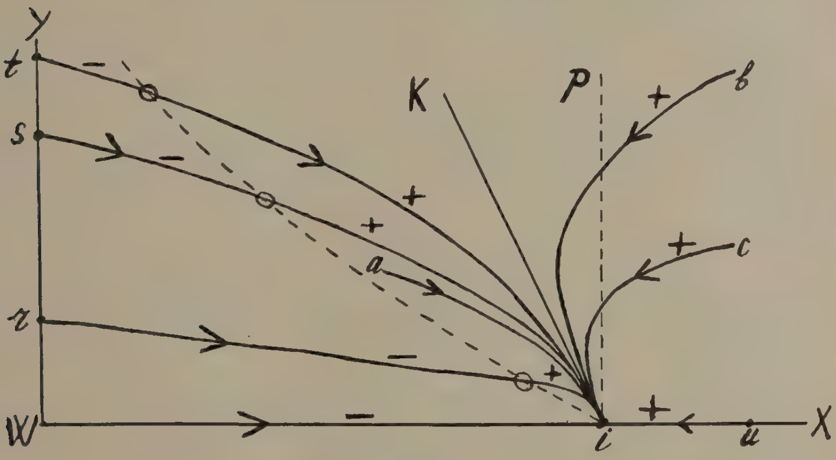

Fig. 1.

From the position of point d_1 it follows that the variable liquids of all paths (except *Wi* and *Xi*) will take in this mixture d_1 towards the end of the osmosis; consequently the quantity of the variable liquid of all these paths will increase towards the end of the osmosis.

From the position of point d_2 it follows that the variable liquid of path *Wi* will give off this mixture towards the end of the osmosis and that the variable liquid of path *ui* will take in this mixture.

In the preceding communication we have seen that a zero-curve runs through point *i*; here this is the case also. From the position of the points d_1 and d_2 it follows that this curve (at least in the vicinity of point *i*) will be situated within the angle *Wik*; in fig. 1 we imagine this curve drawn through the points indicated by the sign o; so, just as in the preceding communication this sign indicates again also the zeropoints of the osmosis-paths, namely the point of the path where the quantity of the variable liquid does not change.

It now appears from the experimental determinations that this zero-curve ends in a point of side *WY* and is situated completely within the angle *Wik*.

Now we are able to divide the paths into three groups, namely

1. paths in which the quantity of the variable liquid increases continuously (e.g. the paths *bi*, *ci* and *ui*).
2. path *Wi* in which the quantity of the variable liquid decreases continuously.
3. paths in which the quantity of the variable liquid first decreases and afterwards increases until the end of the osmosis (e.g. paths *ri*, *si* and *ti*).

Consequently there are no paths in this bundle in which the quantity of the variable liquid first increases and decreases afterwards until the end of the osmosis (in the bundle of fig. 1 of communication I such paths are indeed met with, e.g. path *ri*).

We now take the osmotic system

$$L\,(z)\,|\,inv.\,L'\,(i) \qquad M = pig's\ bladder\ \ldots\ldots \quad (4)$$

in which a membrane of pig's bladder; the invariant liquid has the composition

$$9.325\,\%\ Na\,Cl + 90.675\,\%\ Water$$

which we imagine represented by point *i* in the schematical fig. 1.

At the beginning of the osmosis we took for the variable liquid $L(z)$ the liquids which have been represented in fig. 1 by the points *W*, *r*, *a*, *s*, *t*, *b*, *c* and *u*; the compositions of these liquids are found in table 1.

TABLE I.

Liq.	% Na Cl	% Na_2CO_3	% Water	Path	Table
W	0	0	100	*Wi*	2
r	0	2.018	97.982	*ri*	3
a	5.078	1.999	92.923	*ai*	4
s	0	3.056	96.944	*si*	5
t	0	4.063	95.937	*ti*	6
b	14.213	5.035	80.752	*bi*	7
c	14.111	1.998	83.891	*ci*	8
u	14.129	0	85.871	*ui*	9

The data for these eight parts [1]) are found in the tables 2—9, which have been arranged in the same way as in the preceding communication.

---

[1]) The data for the paths *ai*, *bi* and *ci*, which have been determined in collaboration with H. H. SCHREINEMACHERS are also to be found in a slightly different way in the dissertation of L. J. VAN DER WOLK (Leiden, 1932); the five other paths were not determined until much later.

If we draw these paths, we obtain a diagram like the schematical fig. 1; all paths namely (except *Wi* and *ui*) touch a line *ki*, which consequently forms the principal axis of this bundle.

The direction of this axis also depends upon the nature of the membrane, which, however, is slowly changing during the osmosis. The experimental determination of many bundles has taught us, however, that this change generally has such a small influence, that practically all the paths of a bundle have the same tangent in *i* notwithstanding.

In the system under discussion, however, this is different. In footnote (2) namely we have already pointed out that first the paths *ai*, *bi* and *ci* were determined; the five other paths were not determined until later and besides an other bladder was used, because the first had become unserviceable.

Now, as was indeed to be expected, it appears from an accurate drawing of the paths, that the paths *ai*, *bi* and *ci* have a slightly different tangent in point *i* than the paths *ri*, *si* and *ti*. This difference, however, is so small that we may practically unite all paths into one and the same bundle.

From the last column of the tables 2—9 it appears that the quantity of the variable liquid

of path *Wi* decreases during the entire osmosis (sign — in fig. 1);

of the paths *bi*, *ci* and *ui* it increases during the entire osmosis (sign + in fig. 1);

and of the paths *ri*, *si* and *ti* it first decreases and afterwards increases until the end of the osmosis (signs — O + in fig. 1).

If, with the aid of the tables we draw the approximate position of the zero-points, we see that it approximates a straight line.

TABLE II. Path *Wi*.

N⁰.	t in hours	Composition of the variable liq.		Diffused to the variable liq.		$\triangle m$
		% X	% W	gr. X	gr. W	
1	0	0	100			
2	10	0.899	99.101	+ 2.551	+ 7.903	— 5.352
3	29	2.676	97.324	+ 4.279	— 12.587	— 8.308
4	51	4.576	95.424	+ 3.913	— 11.674	— 7.761
5	72	5.999	94.001	+ 2.615	— 7.915	— 5.300
6	106	7.641	92.359	+ 2.736	— 8.349	— 5.613
7	166	8.881	91.119	+ 1.912	— 5.579	— 3.667

TABLE III. Path *r i*.

N^0.	t in hours	Composition of the variable liq.			Diffused to the variable liq.			Δm
		% X	% Y	% W	gr. X	gr. Y	gr. W	
1	0	0	2.018	97.982				
2	11	1.248	1.889	96.863	+ 3.818	− 0.436	− 5.568	− 2.186
3	17	1.968	1.806	96.226	+ 1.898	− 0.242	− 2.701	− 1.045
4	27	3.182	1.673	95.145	+ 2.876	− 0.347	− 4.042	− 1.513
5	43	4.810	1.463	93.727	+ 3.222	− 0.445	− 4.239	− 1.462
6	63	6.488	1.204	92.308	+ 2.804	− 0.452	− 3.196	− 0.844
7	88	7.180	1.074	91.746	+ 2.271	− 0.430	− 1.959	− 0.118
8	135	8.084	0.848	91.068	+ 2.810	− 0.673	− 1.218	+ 0.919
9	231	8.844	0.528	90.628	+ 2.240	− 0.851	+ 0.848	+ 2.237
10	351	9.152	0.273	90.575	+ 0.884	− 0.538	+ 2.127	+ 2.473

TABLE IV. Path *a i*.

N^0.	t in hours	Composition of the variable liq.			Diffused to the variable liq.			Δm
		% X	% Y	% W	gr. X	gr. Y	gr. W	
1	0	5.078	1.999	92.923				
2	17	6.115	1.745	92.140	+ 4.129	− 0.964	− 1.762	+ 1.403
3	$38^1/_2$	7.136	1.450	91.414	+ 3.755	− 1.010	− 0.569	+ 2.176
4	$64^1/_2$	7.967	1.151	90.882	+ 2.813	− 0.923	+ 0.351	+ 2.241
5	95	8.606	0.820	90.574	+ 2.015	− 0.874	+ 2.040	+ 3.181
6	129	8.994	0.527	90.479	+ 1.117	− 0.653	+ 2.145	+ 2.609
7	$177^1/_2$	9.212	0.232	90.556	+ 0.594	− 0.518	+ 2.184	+ 2.260

If we draw the starting-point *a* of path *ai* (table 4) then we see that this point is situated a little to the right side of the zero-curve (fig. 1) it appears indeed from table 4 that this path has no zero-point; if, however we had taken this starting-point to the left of the zero-curve (as the points *r*, *s* and *t*), we should indeed have found a zero-point.

TABLE V. Path *si*.

N⁰.	t in hours	Composition of the variable liq.			Diffused to the variable liq.			$\triangle m$
		$^0/_0\ X$	$^0/_0\ Y$	$^0/_0\ W$	gr. X	gr. Y	gr. W	
1	0	0	3.056	96.944				
2	14	1.014	2.898	96 088	+ 3.348	— 0.536	— 3.242	— 0.430
3	32	2.270	2.688	95.042	+ 3.761	— 0.641	— 3.448	— 0.328
4	52	3.537	2.463	94.000	+ 3.577	— 0.638	— 3.102	— 0.163
5	76	4.829	2.205	92.966	+ 3.454	— 0.682	— 2.540	+ 0 232
6	112	6.297	1.849	91.854	+ 3 642	— 0.845	— 1.631	+ 1.166
7	163	7.683	1.398	90.919	+ 3.356	— 0.986	+ 0.380	+ 2.750
8	252	8.735	0.834	90.431	+ 2.635	— 1.161	+ 3.065	+ 4.539
9	323	9.057	0.525	90.418	+ 0.923	— 0.587	+ 2.914	+ 3.250
10	419	9.223	0.270	90 507	+ 0.532	— 0.450	+ 2.454	+ 2.536

TABLE VI. Path *ti*.

N⁰.	t in hours	Composition of the variable liq.			Diffused to the variable liq.			$\triangle m$
		$^0/_0\ X$	$^0/_0\ Y$	$^0/_0\ W$	gr. X	gr. Y	gr. W	
1	0	0	4 063	95.937				
2	13	0.979	3.883	95.138	+ 3.128	— 0.592	— 2.931	— 0.395
3	30	2.250	3.623	94.127	+ 3.728	— 0.752	— 2.729	+ 0.247
4	48	3.505	3.366	93.129	+ 3.395	— 0.665	— 1.982	+ 0.748
5	76	5.066	2.909	92.025	+ 4.006	— 1.088	— 1.008	+ 1.910
6	119	6.724	2.339	90.937	+ 4.242	— 1.271	+ 1.056	+ 4 027
7	169	7.788	1.799	90.413	+ 2.794	— 1.134	+ 3.294	+ 4.954
8	252	8.644	1.109	90.247	+ 2.313	— 1.298	+ 6.009	+ 7.024
9	352	9.028	0.598	90.374	+ 1.085	— 0.921	+ 3.968	+ 4.132
10	492	9.213	0.217	90.570	+ 0.660	— 0.616	+ 3.837	+ 3.881

TABLE VII. Path *bi*.

Nº.	t in hours	Composition of the variable liq.			Diffused to the variable liq.			Δm
		$^0/_0\ X$	$^0/_0\ Y$	$^0/_0\ W$	gr. X	gr. Y	gr. W	
1	0	14.213	5.035	80.752				
2	14	12.844	4.529	82.627	− 3.856	− 1.460	+ 20.601	+ 15.285
3	31	11.658	4.009	84.333	− 3.325	− 1.606	+ 18.650	+ 13.719
4	52	10.678	3.442	85.880	− 2.483	− 1.811	+ 17.909	+ 13.615
5	86	9.756	2.707	87.537	− 2.300	− 2.554	+ 19.063	+ 14.209
6	135	9.223	1.900	88.877	− 1.070	− 2.979	+ 15.318	+ 11.269
7	203	9.074	1.127	89.799	+ 0.431	− 2.806	+ 13.336	+ 10.961
8	274	9.146	0.573	90.281	+ 0.537	− 1.899	+ 4.513	+ 3.151
9	359	9.257	0.248	90.495	+ 0.381	− 0.993	+ 1.096	+ 0.484

TABLE VIII. Path *ci*.

Nº.	t in hours	Composition of the variable liq.			Diffused to the variable liq.			Δm
		$^0/_0\ X$	$^0/_0\ Y$	$^0/_0\ W$	gr. X	gr. Y	gr. W	
1	0	14.111	1.998	83.891				
2	16	12.836	1.786	85.378	− 4.160	− 0.722	+ 13.432	+ 8.550
3	39	11.499	1.509	86.992	− 4.166	− 0.943	+ 14.230	+ 9.121
4	63	10.611	1.262	88.127	− 2.570	− 0.826	+ 9.919	+ 6.523
5	$98^1/_2$	9.823	0 932	89.245	− 1.984	− 1.054	+ 10.066	+ 7.028
6	$144^1/_2$	9.392	0.590	90.018	− 0.753	− 1.003	+ 7.659	+ 5.903
7	$183^1/_2$	9.299	0.359	90.342	− 0.014	− 0.577	+ 3.036	+ 2.445
8	274	9.301	0.084	90.615	+ 0.315	− 0.535	+ 3.577	+ 3.357

We now shall first consider the change of the X-amount of the variable liquid.

The paths *bi* and *ci* intersect the vertical axis *ip* and will after this intersection consequently have a point somewhere in which the tangent is vertical. From this it follows: the X-amount of the variable liquid of these paths, which at the beginning of the osmosis is greater than that of the invariant liquid *i*, becomes equal to it at a certain moment of the osmosis, afterwards this X-amount will decrease still further, reaches a minimum and increases afterwards again to that of liquid *i* (comp. column 3 of the tables 7 and 8). It is hardly possible to determine this increase experimentally in case of path *ci*, the minimum of which is situated close to point *i*.

From the tables 7 and 9 and the X-amount of liquid *i* it appears that the substance X diffuses successively according to the symbols:

$$\underset{\rightarrow}{>} \qquad \underset{\rightarrow}{<} \qquad \underset{\leftarrow}{<}$$

so during a certain time there is a negative X-osmosis. It appears besides that the direction of diffusion turns round towards the end of the osmosis.

TABLE IX. Path *u i*.

N⁰.	*t* in hours	Composition of the variable liq.		Diffused to the variable liq.		Δm
		% X	% W	gr. X	gr. W	
1	0	14.129	85.871			
2	18	13.266	86.734	— 2.238	+ 5.903	+ 3.665
3	46	12.092	87.908	— 3.095	+ 7.785	+ 4.690
4	88	10.898	89.102	— 3.239	+ 7.718	+ 4.479
5	161	9.891	90.109	— 2.907	+ 5.198	+ 2.291
6	205	9.658	90.342	— 0.679	+ 1.059	+ 0.380

We see that this phenomenon viz. the occurrence of a minimum X-amount is connected with the position of the axis *ki* within angle *piW*. If this axis had been situated within angle *piX*, then these paths *bi* and *ci* would have had no minimum; the paths *ri*, *ai si* and *ti* on the other hand would have shown a maximum.

In order to consider the change of the W-amount of the variable liquid we imagine a line *iq* in fig. 1, so that $\angle Wiq = 45°$; the points of this line represent liquids with the same W-amount as liquid *i*. As $\angle Wik = \pm 67°$, this line *iq*, which has not been drawn, is situated within $\angle Wik$.

Path *ti* intersects this line *iq* and, therefore, after this intersection will have a point in which the tangent is parallel to *iq*. From this follows: the W-amount of the variable liquid, which at the beginning of the osmosis is greater than that of the invariant liquid *i*, becomes equal to it at a certain moment of the osmosis; afterwards this W-amount will decrease still further, reaches a minimum and afterwards increases again to that of liquid i. From column 5 of table 6 it appears that the minimum is situated in the vicinity of determination N⁰. 8.

From columns 5 and 8 of this table and from the W-amount of liquid i it also appears that the water diffuses successively according to the symbols:

$$\underset{\rightarrow}{>} \qquad \underset{\leftarrow *}{>} \qquad \underset{\leftarrow}{<}$$

from this it appears that during a part of the osmosis the water diffuses negatively and that at a certain moment the direction of the W-diffusion turns round.

Of course all this obtains also for the paths *si*, *ai* and *ri* (tables 5, 4 and 3); from table 3 it appears, however, that this minimum of path *ri* is situated so close to point i, that it was not determined experimentally.

Now we take instead of (4) the system

$$L\,(z) \mid inv.\ L'\,(i_1) \qquad M = pig's\ bladder \quad . \; . \; . \; . \quad (5)$$

in which the invariant liquid i_1 has the composition

$$5.641\,\%\ Na_2CO_3 + 94.359\,\%\ Water$$

So this liquid is no longer represented now by a point of side, WX, but by a point i_1 on side WY of fig. 1, which has not been drawn.

We are able to deduce that side Wi_1Y now must be one of the axes of the bundle. It appeared from the experimental determination of four paths that they all touch side WY in point i_1 so that this side is the principal axis of the bundle.

In the osmotic system

$$L\,(z) \mid inv.\ (Water) \qquad M = pig's\ bladder \quad . \; . \; . \; . \quad (6)$$

the invariant liquid consists of pure water; consequently it is represented by point W (fig. 1). We are able to deduce that the sides WX and WY now must be the axes of the bundle. From the experimental determination of three paths it appeared that they all touch side WY in point W, so that WY is the principal axis and WX the secondary axis of this bundle.

For a closer consideration of these paths of systems (5) and (6), which have also been determined in collaboration with H. H. SCHREINEMACHERS we refer to the dissertation mentioned in note 2.

By the support of the "Bataafsch Genootschap der Proefondervindelijke Wijsbegeerte te Rotterdam" we were enabled to examine the paths *Wi. ri, si, ti* and *ui* (tables 2, 3, 5, 6 and 9) for which we express our thanks to this "Genootschap".

Leiden, Lab. of Inorganic Chemistry.

Chemistry. — *The Exact Measurement of the Specific Heats of Solid Substances at High Temperatures. XI. On the Remarkable Behaviour of Beryllium after preliminary Heating above 420° C.* By F. M. JAEGER and E. ROSENBOHM.

(Communicated at the meeting of October 29, 1932.)

§ 1. In the course of our precision-measurements of the specific heats of metals executed in this laboratory[1]), we were confronted by serious difficulties in the case of *beryllium*, as soon as the metal was heated at temperatures above 420° C. Two very pure samples of the metal were at our disposal: one obtained from SIEMENS and HALSKE in Berlin, the other from the *American Beryllium Company*, — which both possessed about the same degree of purity. Analysis proved, that the metals used contained 99.55 % *Be*, about 0.4 % *Fe* and almost undeterminable traces of aluminium and carbon. Both samples showed *exactly the same* behaviour; there cannot be any doubt whatsoever about the fact, that the phenomena here described are truly characteristic for the *pure* element.

Although several determinations of the specific heat of *beryllium* already have been made[2]), the results obtained by different investigators appear in general strongly deviating from each other. This divergence of the data obtained is, however, by no means restricted to the specific heats alone: quite a number of other physical properties: the thermoelectric and thermoionic behaviour, the electrical resistance, etc. in their dependence on the temperature, — all these properties equally show characteristic irregularities, which mostly were accounted for by assuming some allotropic change in the metal, occurring at various and not quite determinable temperatures[3]). As we soon will see, however, the phenomena manifested by this metal are of a very particular kind; so that up till now it does not seem allowed to explain them exclusively in the way just mentioned, although it is certain, that they are accompanied by such an allotropic change. It must be emphazised, that the discovery of the very curious behaviour of the previously heated metal has only been possible, because of the high perfection of our calorimetrical device now in use, which allows the reproduction of the data obtained within 0.1 % of their values and because of the extreme sensitiveness and reliability of the much improved method of measurement; it is not astonishing therefore, that hitherto the said phenomena evidently have escaped observation.

---

[1]) F. M. JAEGER, and E. ROSENBOHM, Recueil des Trav. chim. Pays-Bas, **47**, (1928), 513; **51**, (1932). 1—46; F. M. JAEGER, E. ROSENBOHM and J. A. BOTTEMA, Proceed. R. Acad. Sciences Amsterdam, **35**, (1932) 347, 763, 772; E. ROSENBOHM, ibid., **35**, (1932) 876; F. M. JAEGER and J. A. BOTTEMA, ibid., **35**, (1932), 352, 916, 929.

[2]) J. EMERSON REYNOLDS, Phil. Mag., (5), **3**, (1877), 38; T. S. HUMPIDGE, Proc. R. Soc. London, **38**, (1885), 188; E. J. LEWIS, Phys. Rev. **34**, (1929) 1577; P. VERNOTTE and A. JEUFROY, Compt. rend. Paris, **192**, (1931), 612; A. MAGNUS and H. HOLZMANN, Ann. der Phys., (5), 3, (1929) 600; etc.

[3]) Conf. e.g.: E. J. LEWIS, Phys. Rev., **34**, (1929), 1577, 1584, 1585.

§ 2. *Beryllium* melts at 1278° ± 5° C. Especially at higher temperatures its investigation is much hampered because of its specific chemical and physical properties: its enormous affinity to oxygen compels the investigator to study it at higher temperatures in a *complete vacuum*, avoiding any contract with reducible substances; the metal is brittle and extremely hard, so that it cannot, or only with great difficulty, be worked with tools; it cannot be brought into the shape of sufficiently thin wires, hardly into that of thin plates; etc. For these reasons the *X*-ray-analysis of this metal at higher temperatures is extremely difficult and the data hitherto obtained are still so contradictory, that we need postpone their publication, till a more complete evidence about their significance will have been obtained. In this preliminary communication we, therefore, will only deal with the *thermal* data and simply will communicate the facts observed, without trying to give a final explanation of them.

§ 3. All measurements of the specific heats were made with lumps of the crystalline metal of pea-size, enclosed in evacuated platinum crucibles of the usual type, each containing 3 to 6 grammes *beryllium*.

In our present calorimeter the increase of the temperature of the metallic block commonly reaches its maximum, with ordinary metals, e.g. *copper*, — after 3 minutes. In the case of not previously heated *beryllium* or of the metal being preserved during a long time, — say one year, — this maximum is reached after about 3—7 minutes, as, for instance, may be seen from the curve I in the following figure: the "old" *beryllium* was heated at 100° C. and then dropped into the calorimeter. The metal behaves in this respect quite normally, so that there is no difficulty of determining its mean specific heats, up to 400° C. in the usual way; the corresponding data will be published later-on. Such a sample of the "old" metal, if brought into liquid air, proves, — exactly like each normal metal, — to have assumed the temperature of the surrounding liquified gas in about 3 minutes, — no heat-development then being any more observed. But all this ceases, as soon as the metal has previously been heated at, for instance, 450° or 490° C. If such a sample, after previous heating at these temperatures is cooled till room-temperature and afterwards again is heated at 100° C., — then, if dropped in the calorimeter, its heat-development, as indicated by the time-temperature-curve II of Figure 1, now appears *to be extended over a very long interval of time*, the maximum temperature of the calorimeter only being reached after 35—42 minutes and the normal course of the instrument being not earlier re-established than after many hours. It is evident, that because of this, *no* reliable measurements of the specific heats can, by means of this method, be any more made, because it is no longer allowed to determine the necessary cooling correction, with any certainty, by the usual extrapolation to the moment τ_0, at which the object was introduced into the calorimeter.

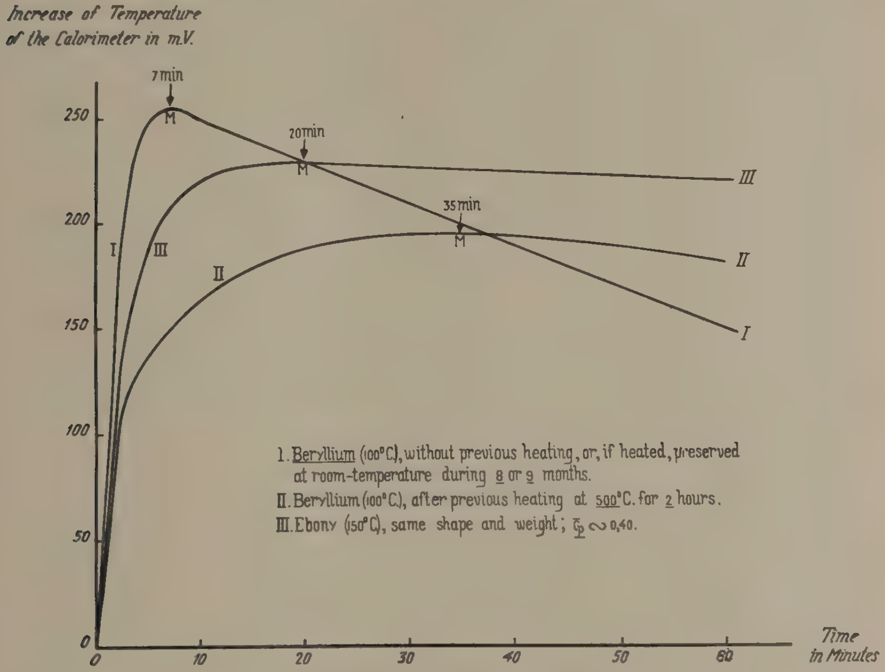

Time-temperature-Curves of the Calorimeter.

Fig. 1.

In those cases, where the crucible was heated at higher temperatures than 500° C., — say at 800°, 900° C., etc., — it even lasted 60 or 90 minutes, before the maximum temperature of the block was reached; subsequently the normal cooling-rate of the instrument then also appeared diminished during several hours.

This fact, which never was observed with ordinary metals¹), clearly indicates, that the metal shows *a strong retardation of the delivery of its heat-content to its surroundings,* after having been brought into its new condition. If such a heated sample of the metal, — say previously heated at 900° C., — be dropped into solid carbondioxide and then in liquid air, it continually seems to develop heat during 40—90 minutes, before it has obtained the temperature of the surrounding liquid. If the sample thus

---

¹) On the contrary: with ordinary metals the maximum temperature of the calorimeter is, in general, reached the sooner, the higher was the temperature of the heated metal itself.

treated be brought at room-temperature, subsequently be heated at 100° C. and then dropped into the calorimeter, it still shows its abnormal behaviour: but the time-interval necessary for reaching the maximum temperature of the block now proves to be somewhat diminished, — for instance, to 25 minutes, while also the cooling-rate of the calorimeter sooner assumes its normal size. A sample of the previously heated metal, after being preserved at room-temperature during several days, still manifests a prolonged heat-development, if brought into liquid air. Even if the sample be preserved during 7 or 8 months, it still shows, when heated at 100° C. and dropped into the calorimeter, a slight abnormality, — the interval of time necessary for reaching the maximum temperature of the block being somewhat greater than in the case of a sample of non-heated *beryllium*; only "old" *beryllium*, i.e. a metal preserved at room-temperature for at least 9 months or one year, proves to behave in a normal way. These facts prove, that the metal surely goes back to its original state, but with an ever more decreasing velocity, so that its *complete* transformation exiges months and months.

§ 4. Now it is a highly remarkable fact, that the total area of the surface bordered by the curves I and II in figure 1, if measured by means of the planimeter, up to the time at which the calorimeter has resumed its normal cooling-rate, — or if it is calculated by means of integration of the heat-effects observed, — proves practically to be *the same* in both cases.

From this evaluation of the areas considered by measuring them or by integral calculation, — the total amount of heat given off can be determined with a fair degree of accuracy: for the heat given off by the *platinum* is exactly known and that corresponding to the cooling of the *beryllium* also, because the mean specific heats of *beryllium* are, up to 400° C., very well measurable. In this way the heat-effect "in excess", — which should correspond to the supposed heat of transformation of the metal, — can easily be found. By these calculations the remarkable result is obtained, that practically *there remains no supplementary heat-effect at all*: it is *zero* or, at least, *unappreciably small.*

This leads to the conclusion, that practically there is *no additional heat-effect* superimposed upon the heat given off by the heated metal, after having been brought into the new state, if compared with the metal in its original state. The whole phenomenon rather makes the impression, as if *beryllium*, — after previously being heated above 420° C., — is brought into a new state, in which its heat-development to its surroundings, — if a temperature-difference between these and the metal be established, — is *enormously retarded*; it seems, as if a certain phenomenon of "thermal hysteresis" there were present. This might be explained, if it could be supposed that the thermal conductivity of the metal, after its change above 420° C., were *very considerably* diminished. In Fig. 1 the curve III represents the behaviour of a lump of *ebony*, — which has about the same specific heat as *beryllium*, but a much smaller thermal conductivity, — after it was brought into exactly the same shape as the platinum crucibles used, heated at 150° C., and then dropped into the calorimeter: here the maximum temperature of the calorimeter-block, indeed, was reached only after 20 minutes and the normal cooling-rate of the instrument also appeared only to be re-established after a rather long time. At first sight, however, it must appear highly improbable, that the metal in its new condition, would have a thermal conductivity even poorer than that of a block of *ebony*. Indeed, the experiment soon proved, that this supposition is completely *inadequate* for explaining the behaviour of the metal: direct *comparitive* measurements of the thermal conductivities between 100° and 0° C. of *copper*, of *ebony*, and of *beryllium* in its original and in its new state [1]), lead to the following results:

a. *Copper* and *beryllium* have perfectly comparable thermal conductivities between 100° and 0° C.

b. The thermal conductivity of *beryllium* previously heated at 500° C. remains, between 100° and 0° C., *the same* as that of "old" *beryllium*.

c. *Ebony* has, in the same interval of temperatures, a thermal conductivity, which is appreciably lower than that of the metals just considered.

There can be no doubt, *that the phenomenon observed cannot be explained by a change of the thermal conductivity of the metal* in its new state; its "thermal hysteresis" can, therefore, neither be caused by this fact, nor by a simple process of transformation, slowly going back, because there is only an apparently *un*appreciably small heat-effect accompanying it.

§ 5. There are, moreover, other particularities which are contradictory to the supposition, that here we would only have to deal with an "ordinary" allotropic change of the metal. Experiments proved, that the prolonged heat-development of the previously heated *beryllium* is *not* appreciably *retarded* by quenching the sample at — 190° C.: evidently it is impossible to "fix" the new state of the metal by such quenching, — for instance after heating at 900° C. and suddenly cooling at — 190° C., — because the velocity of the inverse transformation is, at — 190° C., apparently *not appreciably smaller* than at room-temperature. This fact is completely contradictory to the general experience gathered about the transformation-velocity of allotropic or polymorphous modifications in its dependence on the temperature: the whole method of stabilizing "metastable" modifications by quenching, exactly is founded upon the well-known, generally very rapid decrease of the velocity of transformation with diminishing temperatures.

Special experiments taught us, that also the specific gravities of the original and of the heated and quenched material, remained about the same: although really there are two modifications, their specific volumes evidently can only differ quite unappreciably 1). These experiments on the specific weight under different circumstances were made with samples of *beryllium* enclosed in small evacuated platinum crucibles, which, during a long time, were heated at different constant temperatures, ranging from 0° to 800° C.; then suddenly they were quenched and the crucibles were rapidly opened. The determinations of the specific weights were made by means of the pycnometer at 17° C. and several times repeated after a sufficient lapse of time, with the purpose of stating accidentally occurring gradual changes of d_{4°, as a function of the time elapsed. The experiment after quenching at 800° C. gave: $d_{4^\circ} = 1.903$ at 17° C.; after 2 hours: 1.902; after 3 hours: 1.903; after 14 hours still: 1.903. These values are somewhat greater than those published in the literature; according to FICHTER and JABLEZYNSKI 2) such deviations might be explained by an admixture of some BeO, generated by the contact of the metal with the water of the pycnometer. Using *toluene* in stead of water in the pycnometer, we found, however, the same values; so that the small difference of about 3 % seems to be a real one, — the theoretical value of d_{4° being: 1.837, as calculated from the spectrographical data.

---

[1]) The metal was preliminary heated in a vacuum at 485° C. during many hours and then compared with the original sample.

In all cases, no striking physical differences between the two states of the metal could be found, with the exception of the calorimetric behaviour just described. It may be remarked that these negative results are in agreement with those obtained by LEWIS 3): according to this author, no allotropic change of the metal betrays itself in the temperature-curve of the specific heats between — 190° and + 200° C., nor in that of the thermal conductivity within the same interval of temperature. In this connection we, moreover, can draw attention to the fact, that between — 190° C. and the ordinary temperature, no change of the X-ray-spectrogram of *beryllium* could be stated by us: besides the ordinary diffraction-lines, some faint extra-lines are always present, evidently persisting after a preliminary heating of the metal. HIDNERT and SWEENEY 4) observed no discontinuity in the curve of the linear expansion of the metal, — not even in the vicinity of 420° C. These facts seem to prove, that *a discontinuous and abrupt change in the physical properties of beryllium does not manifest itself*, as would be expected in the case of the occurrence of an enantiotropic,

---

1) F. FICHTER and K. JABLEZYNSKI, Ber. d. d. chem. Ges., **46**, (1913), 1609.

2) Recent experiments have definitely shown that an allotropic change really occurs at higher temperatures, which, on cooling, only partially and slowly goes back; both modifications evidently are simultaneously present at a whole series of temperatures, so that the metal at ordinary temperatures represents a not quite definite, complex system. This is proved by the appearance of new diffraction-lines amongst the ordinary ones in the X-ray-spectrogram, if the metal is heated in a vacuum at 650° C. for several hours, and by the subsequent fainting of these new lines, if the preliminary heated metal is cooled in acetone and solid carbondioxide or in liquid air.

3) E. J. LEWIS, loco cit.

4) P. HIDNERT and W. T. SWEENEY, Bull. Bur. of Stand. Washington, **22**, (1927), 533.

completely reversible allotropic transformation. But, especially from LEWIS' experiments it must, however, be concluded, that a continuous heating of the element at 700° C., undoubtedly causes more or less radical changes in its physical condition. We will return to this question in a later publication, dealing with the spectrographical pecularities of *beryllium* heated at this temperature for a long time. The most remarkable effect of those changes, manifests itself in the thermal behaviour here described, with its gradual disappearance after a sufficiently long interval of time, which, at ordinary temperatures, can be extended over several months.

§ 6. Although the results of the X-ray-analysis, as already mentioned, cannot yet here be considered in detail, finally some general remarks concerning them may, however, be made. In the first place it has become clear during these experiments, that the problem about the true structure of *beryllium* is still *unsettled*. All investigators observed the occurrence of a smaller or greater number of *extra* structure-lines in their spectrograms, even at the ordinary temperature, which hitherto, always were ascribed to the presence of mysterious "impurities" in sufficient quantities. Moreover, neither the relative intensities of these extra lines with respect to each other appear to be quite constant, nor is there a sufficient agreement between the observed and calculated intensities of the *normal* diffraction-lines, — as they follow from the structure of the metal, as indicated by MC KEEHAN [1]) and others. That a certain number of the additional diffraction-lines certainly do *not* correspond to "accidental impurities" or to admixed *beryllium-oxide*, now has become quite clear to us, — although it proved hitherto impossible, completely to determine the special circumstances, under which they are produced. Certainly there exists a second modification of the element, which seems to co-exist with the ordinary from *at all* or, at least, *at a whole series* of temperatures. However, — as already has been said, — even then the curious thermal behaviour of the metal *cannot be explained in this way alone*; but it seems rather to be connected with some other kind of change, — perhaps occurring in the atoms or molecules themselves, — by which the crystalline *beryllium* is built up. For both modifications seem to possess almost the same thermal conductivity; so that even their simultaneous presence in the metal cannot explain its curious thermal behaviour, after being heated at higher temperatures, which more particularly manifests itself in the strange hysteresis of its heat-development. All this, however, must still be thoroughly investigated, before a final decision will be possible. We soon hope to return to these interesting questions in a following publication on this subject.

Groningen, Laboratory for Inorganic and
Physical Chemistry of the University.

---

[1]) L. W. MC KEEHAN, Proceed. Nat. Acad. Sciences Washington, **8**, (1922), 270. An analogous disagreement between the calculated and observed intensities of the diffraction-lines is present in the case of *magnesium*.

Physics. — *The* "VAN LEEUWENHOEK *Microscope" in possession of the University of Utrecht.* By Dr. P. H. VAN CITTERT. (Communicated by Prof. L. S. ORNSTEIN.)

(Communicated at the meeting of October 29, 1932.)

In his book: "ANTONY VAN LEEUWENHOEK and his little animals" (Amsterdam 1932) C. DOBELL remarks in a footnote (page 324): "The lens examined by HARTING was in a microscope preserved at that date in the physical collection at Utrecht. The instrument now in the zoological collection of the same University is greatly inferior, its lens having a focal length of about $^1/_4$ in. (fid MAYALL 1886)". On page 327, in the text itself DOBELL remarks: "Most of the recent descriptions and pictures of "LEEUWENHOEK's microscope" are based on the rather poor specimen now preserved in the Zoological Laboratory at Utrecht".

As it was generally believed in Utrecht that the microscope now in possession of the Utrecht University was identical with the specimen examined by HARTING, the above mentioned remarks urged me to compare it with HARTING's description (Het Microscoop, III, page 43—44, Utrecht, 1850). Its dimensions proved to be in accordance with the dimensions given by HARTING (4.5×2.5 cm^2), the length of the focussing screw is 1 cm, the number of threads on the screw amounts to 11. The lens is biconvex and has a focal length slightly less than 1 mm, which is in fair accordance with the magnification of 270 diameters, measured by HARTING. The magnification was measured directly by viewing an ABBE testplate having a line distance of $^1/_{20}$ mm through the microscope. Five lines of this testplate were seen in a field of view, which was aequivalent to a circle of 7 cm diameter at a distance of 25 cm. This gives a magnification of 280 diameters. Furthermore, the microscope examined by HARTING, was capable of resolving the 3rd group of lines on a NOBERT testplate, and with good illumination, also the 4th group (distance of the lines 0.0014 mm). Now the physical institute in Utrecht is in possession of such a NOBERT testplate, probably the same as used by HARTING, and it was possible to resolve the 4th group of lines. *Consequently there is no doubt that the microscope now in possession of the University of Utrecht is identical with the specimen examined by* HARTING, *and that, far from being an inferior and a rather poor specimen, it probably is as* HARTING *concluded, the best specimen known.*

In fig. 1 is reproduced a microphotograph of the ABBE testplate, i.e. a plate covered with a silver layer, wherein lines have been scratched $^1/_{20}$ mm apart. The magnification is about 180 diameters. The lack of sharpness at

P. H. VAN CITTERT: THE "VAN LEEUWENHOEK MICROSCOPE" IN POSSESSION OF THE UNIVERSITY OF UTRECHT.

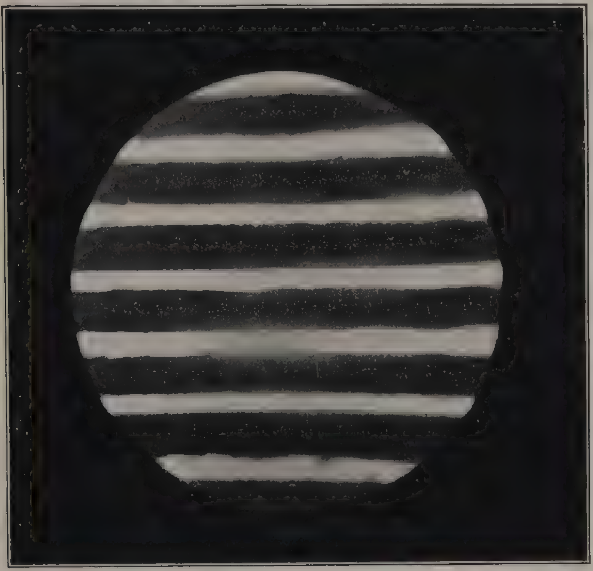

Fig. 1.

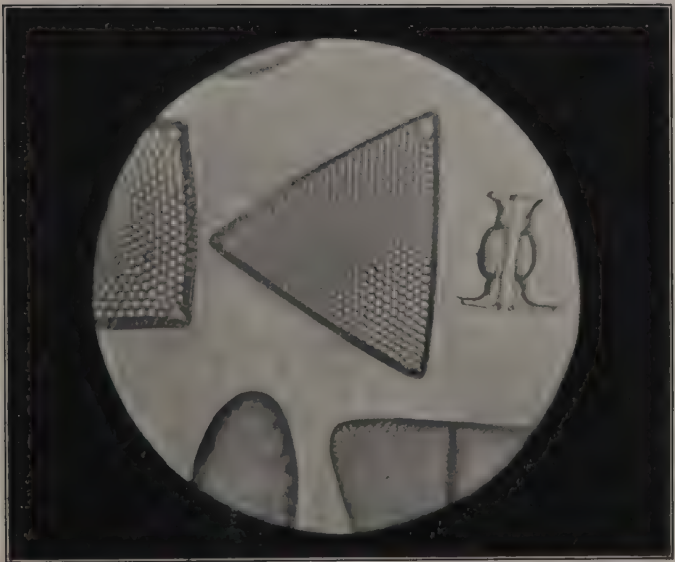

Fig. 2.

the borders of the photograph is mainly due to chromatic aberration. The irregularities in the borders of the lines show that the resolving power of the lens is fairly good and that structures of about $^1/_{500}$ mm can be easily resolved. Fig. 2 shows a photograph of some diatomees. The magnification is slightly more than 200, the length of the sides of the triangle being 0.18 mm. The slight indistinctness in the centre of the field of view is partly due to some scratches on the top of the very highly curved lens, partly to the fact that the image does not lie in a plane, but on a curved surface. It is astonishing that a lens with a free aperture of less than half a millimeter can give such a large image without showing a greater curvature than is observed.

Chemistry. — *The Thermal decomposition of Paraffin wax in the Presence and in the Absence of Hydrogen of High Pressure.* By H. I. WATERMAN, A. J. TULLENERS, and J. DOOREN. (Communicated by Prof. J. BÖESEKEN).

(Communicated at the meeting of September 24, 1932.)

In previous communications a comparative examination was made of the gaseous and low boiling products (gasoline), obtained in the thermal decomposition of paraffin wax by berginization (high pressure hydrogen) and by cracking (without addition of hydrogen) [1]. A comparative examination of the higher fractions, which gave analogous results, was described n 1929 [2].

In PERQUIN's Thesis the results of these investigations were summarized as follows:

1. The quantities of the products boiling up to 150° are about the same for berginization and for cracking (32—34$^0/_0$ of the paraffin wax after 90 minutes at 450° C.).

2. In both products the presence of considerable quantities of paraffin-hydrocarbons has been detected with great certainty.

3 The products obtained by cracking are considerably less saturate.

4. Besides the higher degree of unsaturation of these cracking-products they differ qualitatively more from the products obtained by berginization, as their boiling-points become higher.

---

[1] H. I. WATERMAN and A. F. H. BLAAUW, Rec. trav. chim. 45, 284 (1926); H. I. WATERMAN and J. N. J. PERQUIN, ibid 46, 813, (1927); Comptes rendus du 7me congrès de chimie industrielle, octobre 1927, Chimie et industrie, numéro spécial, April 1928, p. 244. The same subject is discussed more in detail in J. N. J. PERQUIN's Thesis: Bijdrage tot de kennis van het BERGIUS-proces, Delft 1929.

[2] H. I. WATERMAN, T. W. TE NUYL and J. N. J. PERQUIN, Journal of the Institution of Petroleum Technologists 15, 369—371 (1929).

5. From the higher indices of refraction and specific weights together with the lower aniline-point of the cracking-products after saturation with hydrogen, we may conclude to a more cyclic character of these hydrocarbons.

6. The residues boiling above 150° C. differ greatly in character, the berginized product is solid and resembles paraffin wax, the cracked product is a very mobile liquid.

7. The gasoline-fractions obtained by cracking are less stable than the bergin-products, which manifests itself in the increase of the refraction and the specific weight and in the deposition of a viscid, insoluble residue ("gum").

8. In the C-fractions benzol and toluol were detected in small quantities with certainty.

Now the investigation was taken in hand again, and this chiefly, because it had become possible, to learn more about the nature of the hydrocarbon mixtures by a new method of investigation, and this without being obliged to isolate the separate hydrocarbons ¹). Besides more attention could be given to the examination of the higher boiling fractions, because the greatest differences were to be expected here.

We had at our disposal products freed from the lower boiling gasoline. First they were distilled under atmospheric pressure to about 240° C.; then the residue was distilled under a vacuum of 8—10 mm. pressure (vapour temperature from 120—130° to about 210° C.), while the residue of this vacuum distillation was further distilled in cathode light vacuum with internal condensation C. V. D. I. C. ²). The liquid-temperature in this last distillation was from 100° to 225° for the cracking product and from 107° to 178° for the berginization product. In this last distillation the residue that was subjected to C. V. D. I. C., was already solid, therefore cooling with cold water was impossible.

A survey of the distillation is found in the following schemes.

The symbol C means cracking and B berginization; A. D. means distillation under atmospheric pressure; L. V. D. distillation under low vacuum (8—10 mm. pressure), the cathode vacuum-distillation being denoted by C. V. D. I. C. (see above).

Of the fractions obtained we have determined the following constants: $n_D^{t^\circ}$, $d_4^{t^\circ}$, $\frac{n^2-1}{n^2+2}\frac{1}{d}$, aniline point, bromine number, and molecular weight. This last by the lowering of the point of solidification of benzol for

---

¹) J. C. VLUGTER, H. I. WATERMAN and H. A. VAN WESTEN, Improved methods of examining mineral oils, especially the high boiling components of non aromatic character, Journal Institution of Petroleum Technologists **18**, 735, (1932); Chemisch Weekblad **29**, 226 (1932).

²) Method of H. I. WATERMAN and E. B. ELSBACH, Chem. Weekbl. **26**, 469 (1929) and H. I. WATERMAN and J. N. J. PERQUIN, Technische analysen, 4th edition, Dordrecht. Ed. G. VAN HERWIJNEN.

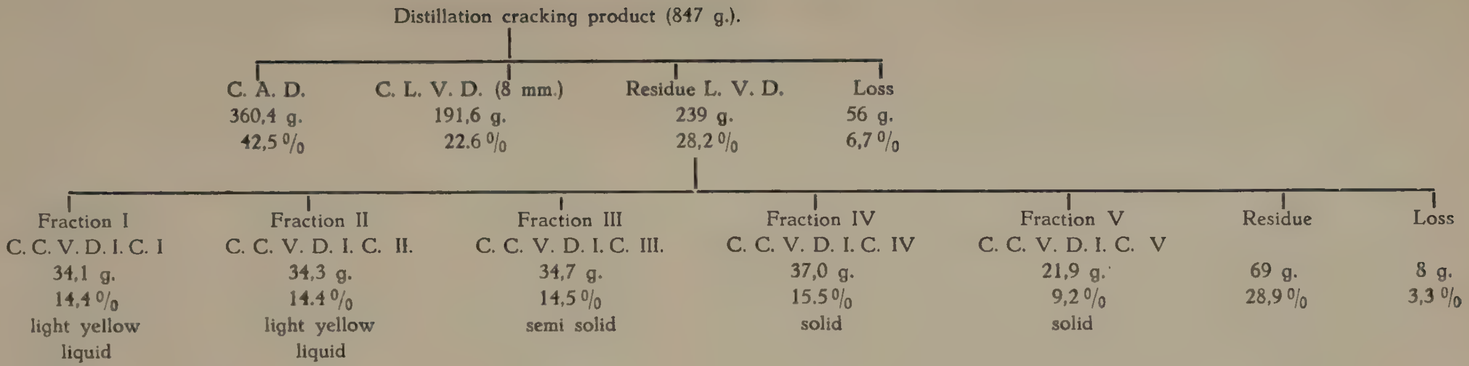
Distillation cracking product (847 g.).
C. A. D.
360,4 g.
42,5 %
C. L. V. D. (8 mm.)
191,6 g.
22.6 %
Residue L. V. D.
239 g.
28,2 %
Loss
56 g.
6,7 %
Fraction I
C. C. V. D. I. C. I
34,1 g.
14,4 %
light yellow liquid
Fraction II
C. C. V. D. I. C. II.
34,3 g.
14.4 %
light yellow liquid
Fraction III
C. C. V. D. I. C. III.
34,7 g.
14,5 %
semi solid
Fraction IV
C. C. V. D. I. C. IV
37,0 g.
15.5 %
solid
Fraction V
C. C. V. D. I. C. V
21,9 g.
9,2 %
solid
Residue
69 g.
28,9 %
Loss
8 g.
3,3 %

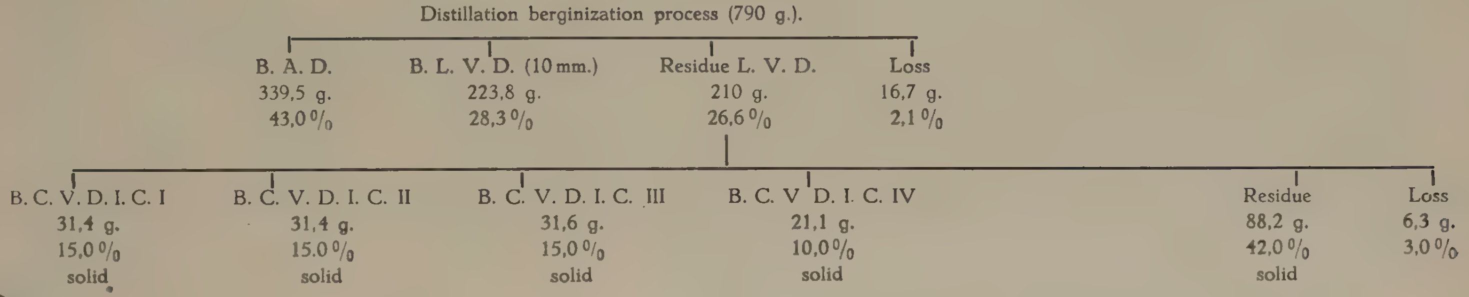
Distillation berginization process (790 g.).
B. A. D.
339,5 g.
43,0 %
B. L. V. D. (10 mm.)
223,8 g.
28,3 %
Residue L. V. D.
210 g.
26,6 %
Loss
16,7 g.
2,1 %
B. C. V. D. I. C. I
31,4 g.
15,0 %
solid
B. C. V. D. I. C. II
31,4 g.
15.0 %
solid
B. C. V. D. I. C. III
31,6 g.
15,0 %
solid
B. C. V D. I. C. IV
21,1 g.
10,0 %
solid
Residue
88,2 g.
42,0 %
solid
Loss
6,3 g.
3,0 %

the lower fractions, for the higher fractions by the lowering of the point of solidification of naphthalene.

Then the C. V. D. I. C.-fractions were hydrogenated at 225° under high hydrogen pressure (some hundreds of kg/cm^2) with nickel on guhr as catalyst, after which all the constants mentioned were determined once more. After the hydrogenation the bromine-number was practically nihil; sometimes feebly negative values were found. With a few exceptions the hydrogenated products were free from aromates. The aniline point predicted (for products free from aromates and olefines) from specific refraction and mean molecular weight was in accordance with the value determined save for a single exception, viz. the hydrogenated C. C. V. D. I. C. V; evidently this fraction was not completely hydrogenated, the calculated aniline point was considerably lower (92.2° instead of 105°) The other observations differed for the completely hydrogenated C. C. V. D. I. C. I—IV inclusive 4° maximally; for the completely hydrogenated B. C. V. D. I. C. I—IV inclusive almost 5° maximally. It appeared from the values for the specific dispersion of B. C. V. D. I. C. III and IV $\frac{n_{G'}-n_c}{d} \cdot 10^4$, that a considerable percentage of aromates could no more be present. For C. C. V. D. I. C. IV the specific dispersion was higher (about 166) after complete hydrogenation. Accordingly for C. C. V. D. I. C. I—III inclusive and for B. C. V. D. I. C. I—IV inclusive the mean formula after complete hydrogenation was derived, and also the mean number of rings per molecule of these products:

Completely hydrogenated products.

Calculated *elementary formula* and *number of rings per molecule.*

Formula	Mol. Weight	Mean number of rings per molecule
C. C. V. D. I. C. I $C_nH_{2n-1,2}$	259	1.6
II $C_nH_{2n-1.3}$	278	1.65
III $C_nH_{2n-1,0}$	298	1.5
IV $C_nH_{2n-1,2}$	315	[1.6] $^{1)}$
B. C. V. D. I. C. I $C_nH_{2n+1.5}$	311	0.25
II $C_nH_{2n+1.4}$	315	0.3
III $C_nH_{2n+1,6}$	338	0.2
IV $C_nH_{2n+1,5}$	351	0.25

---

1) In this case this calculation is not entirely permissible, because, as appears from the specific dispersion, which was too high, the product could not be considered as free from aromates. The error made will, probably not be great in this case.

	C. A. D.	C. L. V. D.	C. C. V. D. I. C. I		C. C. V. D. I. C. II		C. C. V. D. I. C. III		C. C. V. D. I. C. IV		C. C. V. D. I. C. V		B. A. D.	B. L. V. D.	B. C. V. D. I. C. I		B. C. V. D. I. C. II		B. C. V. D. I. C. III		B. C. V. D. I. C. IV	
t	20°	20°	before 20°	after 20°	before 20°	after 20°	before 40°	after 40°	before 40°	after 40°	before 40°	after 40°	20°	20°	before 40°	after 40°	before 40°	after 40°	before 70°	after 70°	before 70°	after hydrogenation 70° C.
n_D^t	1.4466	1.4730	1.4920	1.4682	1.4929	1.4700	1.4920	1.4669	1.5012	1.4740	1.5133	1.4845	1.4236	1.4416	1.4429	1.4402	1.4431	1.4415	1.4333	1.4321	1.4344	1.4333
d_4^t	0.7988	0.8453	0.8753	0.8536	0.8778	0.8567	0.8694	0.8491	0.8829	0.8611	0.9000	0.8832	0.7565	0.7903	0.7928	0.7919	0.7938	0.7943	0.7788	0.7789	0.7812	0.7819
$\frac{n^2-1}{n^2+2}\cdot\frac{1}{d}$	0.3342	0.3319	0.3315	0.3258	0.3310	0.3257	0.3337	0.3267	0.3338	0.3264	0.3341	0.3242	0.3370	0.3345	0.3343	0.3329	0.3340	0.3325	0.3339	0.3331	0.3336	0.3326
Aniline point determined	54.7°	65.8°	66.5°	87.2°	73.7°	90.8°	76.6°	94.5°	79.6°	97.2°	82.0°	92.2°	73.0°	89.2°	99.9°	106.8°	102.7°	108.7°	107.5°	111.7°	110.7°	115.8°
Aniline point read in °C	—	—	—	90	—	93	—	98	—	101	—	105	—	—	—	111.5	—	112	—	116	—	117
Bromine value [1]	16.6	11.6	10.7	0	8.5	0	8.2	0	7.5	0	6.1	0	10.3	6.8	6.1	0	5.4	0	5.1	0	4.7	0
Molecular weight [2]	163 (*b*)	216 (*b*)	259 (*b*)	259 (*b*)	278 (*b*)	278 (*b*)	301 (*b*)	298 (*b*)	316 (*b*) 322 (*n*)	315 (*b*)	390 (*b*) 386 (*n*)	379 (*b*)	153 (*b*)	229 (*b*)	312 (*b*)	311 (*b*)	319 (*b*) 314 (*n*)	315 (*b*)	334 (*n*)	338 (*b*)	351 (*n*)	351 (*b*)
$n_C^{70^\circ}$	—	—	—	1.4658 (20°)	—	1.4681 (20°)	—	1.4534	—	1.4602	—	1.4714	—	—	—	—	—	—	1.4307	1.4298	1.4320	1.4310
$n_D^{70^\circ}$	—	—	—	1.4682 (20°)	—	1.4705 (20°)	—	1.4559	—	1.4629	—	1.4742	—	—	—	—	—	—	1.4332	1.4321	1.4344	1.4333
$n_F^{70^\circ}$	—	—	—	1.4741 (20°)	—	1.4767 (20°)	—	1.4618	—	1.4688	—	1.4810	—	—	—	—	—	—	1.4385	1.4374	1.4398	1.4386
$n_{G'}^{70^\circ}$	—	—	—	1.4790 (20°)	—	1.4817 (20°)	—	1.4665	—	1.4741	—	—	—	—	—	—	—	—	—	1.4416	—	1.44295
$\frac{n_{G'}-n_C}{d^{70}/_4}\cdot 10^4$	—	—	—	155 $\left[\frac{(n_{G'}-n_C)}{d^{20}/_4}\cdot 10^4\right]$	—	159 $\left[\frac{(n_{G'}-n_C)}{d^{20}/_4}\cdot 10^4\right]$	—	158	—	166	—	—	—	—	—	—	—	—	—	151 à 152	—	153

---

[1] The bromine values of the products after complete hydrogenation were very small or in some cases feebly negative; practically they might be put equal to zero.

[2] *b*: benzol solvent.
n: naphthalene solvent.

The molecular weights have been determined only for one single concentration, and not calculated by extrapolation at infinite dilution. This was sufficient for our purpose. For the products hydrogenated with nickel the determination was afterwards repeated by G. J. F. BREEDVELD. His observations follow below. They differ fairly much from the values given, but practically they do not affect the conclusions drawn.

C. C. V. D. I. C.	I (*b*)	II (*b*)	III (*b*)	IV (*b*)	V (*b*)	B. C. V. D. I. C.	I (*b*)	II (*b*)	III (*b*)	IV (*n*)
Δ	1.290°; 1.690°	1.102°; 1.490°	1.075°; 1.126°	1.063°; 1.240°	0.747°		1.180; 1.098	1.135; 1.005	1.159; 1.074	1.46; 1.13
Molecular weight . . .	274; 278	289; 310	329; 320	353; 365	384		315; 315	333; 321	364; 348	388; 374

In this it was assumed that $K_{benzol} = 50.0$ and $K_{naphthalene} = 69.0$

For the rest we point out that the lowering in specific refraction is large with the hydrogenation of the cracking-products, smaller with the berginization-fractions, where the change in *n* and *d* is also small.

From this investigation it appears clearly how in berginization the formation of cyclic compounds is hindered.

It should be remembered that both series of experiments were performed at 450° C., an initial pressure of 110 kg/cm^2 at about 15° C. in the Bergin-series, and an initial pressure of 1 kg/cm^2 or vacuum in the Cracking-series. The duration of the experiments was 90 minutes at 450° C. In the berginization experiments the maximum pressure was on an average 280—290 kg/cm^2 at 450° C., and the final pressure on an average 80 kg/cm^2 at about 15°; in the cracking experiments the maximum pressure was on an average 100—110 kg/cm^2 at 450° C. and the final pressure on an average 15—18 kg/cm^2 at about 15°.

By the presence of hydrogen in the berginization, which caused a hydrogen consumption of 1.4°/₀, the ring-formation is reduced to one seventh of that in the cracking.

By following this method of analysis we have succeeded for the first time in measuring the cyclisation in the cracking quantitatively and in establishing the inhibitory influence of high pressure hydrogen on this cyclisation quantitatively.

Laboratory for Chemical
Delft, July 1932. *Technology of the Technical University.*

Physics. — *On the Directional Effect of the Single Hot Wire Anemometer.*

By M. ZIEGLER (Mededeeling N⁰. 25 uit het Laboratorium voor Aero- en Hydrodynamica der Technische Hoogeschool te Delft). (Communicated by Prof. J. M. BURGERS).

(Communicated at the meeting of October 29, 1932.)

1. *Introduction.*

In hot wire work still little attention has been given to the fact that exact measurements with a single wire anemometer are only possible in a two dimensional field of flow, provided the position of the wire is perpendicular to the plane of the motion. The indications of the wire, calibrated in the so-called normal position, that is perpendicular to the direction of flow, then give the absolute value of the velocity for an arbitrary direction of the velocity vector in that plane. However, as soon as a third component of the velocity, i.e. a component parallel to the wire is present, then neither the absolute value of the velocity, nor the resultant of the two components perpendicular to the wire can be determined if no other indications are available.

It is well known that the cooling of the wire by an air current is a function of the angle between the wire and the velocity vector. This function, the value of which for the normal position (angle of incidence = 90°) is given by KING's formula [1]), presents a sharp minimum in the "zero position" (wire parallel to the flow, angle of incidence = 0°). A few measurements concerning the dependence of the cooling effect on the angle of incidence have been published by SIMMONS and BAILEY [2]) and by BURGERS [3]), which clearly show the presence of this minimum.

If a three dimensional field of flow is to be investigated, then for the case of a stationary motion it is yet possible to determine the true value of the air speed at a given point of the field with a single wire, provided it can be turned in all directions in order to find out the position of minimum cooling. In this position the wire has the direction of the flow and the true velocity then follows at once, provided a calibration curve relating to the zero position is available. SIMMONS and BAILEY in their publication point out the practical inconveniences of this method, and give a description of three and four wire "speed and direction" meters which can be kept in a fixed position and work satisfactorily. For reliable experiments all such instruments of course must satisfy the condition of being so small, that the streamlines may be considered as being straight and parallel over the region occupied by the wire system.

As, however, the range of directions for which such instruments can be used is limited, there is always the possibility that in cases of heavy turbulence the velocity vector at a given point varies so strongly both with regard to magnitude and to direction, that a more complicated instrument than the single hot wire has little utility for the determination of the instantaneous velocity.

If f.i. the flow in the turbulent boundary layer is to be investigated, the question thus arises what errors can be caused in the indications of a single wire anemometer, by the presence of a velocity component parallel to the wire. At the same time it can be asked if it would be possible to obtain an estimate of the magnitude of the "cross" component in the boundary layer, by comparing the indications of a single wire which is turned into various positions at the same point of the field.

The purpose of the present publication is to describe the results of some experiments on the directional effect of the wires used by us and to give an empirical formula for this effect.

---

[1]) L. V. KING, On the convection of heat from small cylinders in a stream of fluid; determination of the convection constants of small platinum wires with applications to hot-wire anemometry, Phil. Trans. A **214**, 373—432, 1914.

[2]) L. F. G. SIMMONS and A. BAILEY, Rep. & Mem. N⁰. 1019 of the Aeron. Research Committee (England).

[3]) J. M. BURGERS, Hitzdrahtmessungen § 6 (Handbuch der Experimentalphysik. Band 4, 1. Teil). The curves published are due to VAN DER HEGGE ZIJNEN in Delft.

2. *Experimental method.*

In the smaller windchannel of the laboratory, the flow of which is very steady, a hot wire was mounted in such a way that it could be turned, in a horizontal plane, through all angular positions between 0° and 360° with regard to the direction of the air current, which also is horizontal. The wire was moved from the outside; the angle could be read accurately on a dial divided into degrees. The zero position of the wire was determined experimentally as the position of least cooling, with an accuracy of about 0.5 degree. For various air speeds and various angles of incidence the indication of the anemometer arrangement was observed. For each velocity the mean value of readings for equivalent angular positions was taken.

The experiments have been made with hot wires as described in "Mededeeling 21" and "23" of this laboratory[1]). As being the most convenient one, that method was used in which the current through the galvanometer is observed, the electrical tension between the terminals of the Wheatstone bridge arrangement being kept constant. The arrangement of fig. 1, used for the experiments of July 1932, may be given as an example.

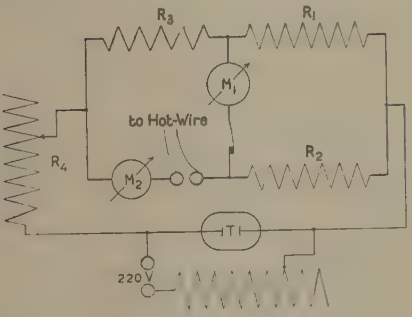

Fig. 1.

Electrical part of the single hot wire anemometer arrangement used for the experiments on the directional effect.

$R_1 = R_2 = 1000\ \Omega$

R_3 = Hot wire resistance (adjusted for air velocity = 0).

R_4 = Variable resistance for adjusting the heating current at the desired value.

M_1 = Milliammeter the deviation of which is observed.

M_2 = Heating current meter.

T = Gas valve which maintains a constant tension of about 78V between its electrodes independently of input tension variations during the experiment. (Lorenz Stabilisator TRT 10).

The accurate and rapid measurement of very low air speeds in the wind channel gave some difficulty; therefore the channel was narrowed considerably (in the ratio 1 : 20) at some point downward from the space of measurement. The difference between the static pressure in this throat and that at the place of the wire could be taken as a measure of the velocity.

---

[1]) M. ZIEGLER, these Proceedings, **34**, p. 663, 1931: A complete arrangement for the investigation, the measurement and the recording of rapid air speed fluctuations with very thin and short wires; and these Proceedings, **35**, p. 419, 1932: Oscillographic records of the turbulent motion developing in a boundary layer from a sheet of discontinuity.

3. *Apparent velocity.*

The measurements again showed that the rate of heat loss presents a sharp minimum for the position of the wire parallel to the flow. As to the rate of cooling at other positions the following may be remarked:

We call φ the angle between the wire and the velocity vector and consider an anemometer calibrated for the normal position of the wire; thus for $\varphi = 90°$ the indication of the anemometer arrangement as a function of the velocity is known. Now let V_t be the true velocity of the air which may make an arbitrary angle with the wire. Then we define the apparent velocity V_a as the velocity which, on the normal calibration curve, would correspond to the indication of the instrument. For $\varphi = 90°$, $V_a = V_t$; for $\varphi \neq 90°$, $V_a < V_t$. Taking especially $\varphi = 0$ we shall write $V^a = \alpha_0 V_t$, where α_0 is a coefficient smaller than unity. The value of α_0 depends on the velocity, and will be considered as a function of V_t.

Now it might be supposed that for an arbitrary angle of incidence the apparent velocity would not differ very much from the value given by the expression

$$V_a = \sqrt{V_n^2 + \alpha_0 V_p^2} \quad . \quad . \quad . \quad . \quad . \quad . \quad . \quad . \quad (1)$$

where V_n is the component of the true velocity perpendicular to the wire and V_p the component parallel to it. This expression may also be written:

$$V_a = V_t \sqrt{\sin^2 \varphi + \alpha_0^2 \cos^2 \varphi} \quad . \quad . \quad . \quad . \quad . \quad . \quad (1a)$$

It has been found that this formula is in satisfactory agreement with the behaviour of the wire, as may be seen e.g. from the results of the following

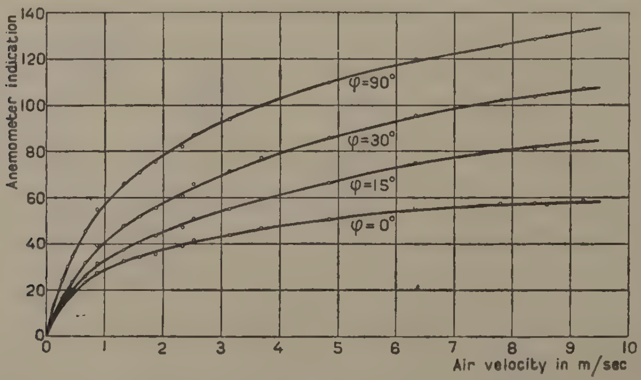

Fig. 2

Calibration curves of the hot wire arrangement for four angular positions of the wire.

experiments (July 1932). The electrical arrangement was that of fig. 1. Platinum hot-wire, diameter 0.005 mm, length 2 mm. For $V=0$: heating current $=$ 32 mA; resistance of the wire $=$ ca. 60 Ω. The bridge was balanced for $V=0$.

The curves of fig. 2 for $\varphi=90°$, 30°, 15° and 0° give the anemometer indication as a function of the velocity (calibration curves), while those of fig. 3 show the variation of the apparent velocity with the angle of incidence for the air velocities of 8.60, 4.85 and 1.60 m/sec.

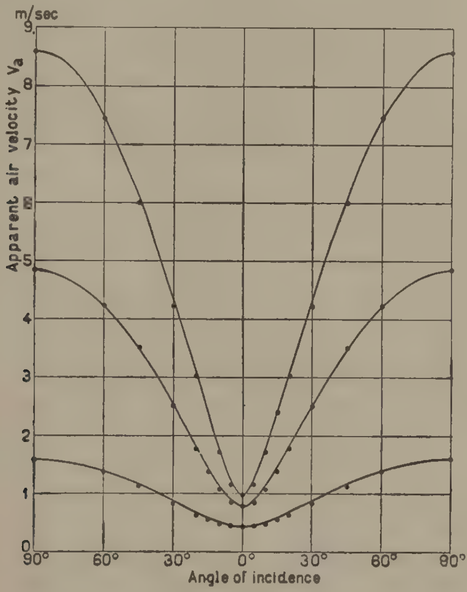

Fig. 3.

Variation of the apparent velocity V_a with the inclination of the wire to the wind direction for true wind speeds V_t resp. equal to 8,60, 4,85 and 1,60 m/sec. The full drawn curves have been deduced from the formula; the small circles represent the values deduced from the measurement.

The values of a_0 which belong to these velocities can be obtained from fig. 2; they are respectively:

$$\frac{0.97}{8.60}=0.113 \qquad \frac{0.78}{4.85}=0.161 \qquad \frac{0.44}{1.60}=0.275.$$

For an arbitrary angle of incidence the apparent velocity is given by formula (1*a*).

The following table gives the course of the calculation for the three velocities mentioned (corresponding respectively to column I, II, III) and for various angles:

φ	$\alpha=\sqrt{\sin^2\varphi+\alpha_0^2\cos^2\varphi}$			V_a calculated $= V_t \times \alpha$			Anemometer Indication			V_a observed		
	I	II	III	I	II	III	I	II	III	I	II	III
0°	0.113	0.161	0.275	0.97	0.78	0.44	56.7	50.3	34.1	0.97	0.78	0.44
5°	0.146	0.186	0.289	1.26	0.90	0.46	61.5	52.5	34.7	1.15	0.85	0.45
10°	0.207	0.236	0.323	1.78	1.14	0.52	71.4	58.9	36.9	1.71	1.07	0.49
15°	0.281	0.302	0.371	2.42	1.46	0.59	82.2	66.4	40.3	2.40	1.38	0.56
20°	0.358	0.374	0.429	3.08	1.81	0.69	91.4	74.1	44.1	3.02	1.78	0.64
30°	0.509	0.519	0.554	4.38	2.52	0.89	104.6	86.1	51.8	4.22	2.50	0.83
45°	0.711	0.716	0.734	6.12	3.47	1.17	117.1	97.9	60.6	6.00	3.51	1.13
60°	0.868	0.870	0.876	7.47	4.21	1.40	124.5	104.9	66.5	7.47	4.23	1.38
90°	1.000	1.000	1.000	8.60	4.85	1.60	129.7	109.9	70.9	8.60	4.85	1.60

It will be seen from fig. 3 that the values of V_a deduced from the observation are very close to the calculated curve. Other experiments performed (January 1932) with hot wires of the same type agree equally well with the formula.

It is possible also to check the formula on results of other investigators. SIMMONS and BAILY in the publication mentioned above describe experiments performed with a wire of 3.07″ = 78 mm length and 0.00105″ = 0.027 mm diameter. Fig. II 1) of their paper gives the measured wire resistance in ohms, for a heating current of 0.215 A and an air velocity of 40 ft/sec, as a function of the angle with the direction of stream.

For the same wire two empirical formulae are given expressing the amount of energy carried off by the wind:

1°. for the case the wire is perpendicular to the air flow:

$$H = 6{,}68 \, . \, 10^{-5} \, V^{1/2} + 9{,}60 \, . \, 10^{-5} \quad . \quad . \quad , \quad . \quad . \quad . \quad (2)$$

2°. for the case the wire is parallel to the flow:

$$H = 1.673 \, . \, 10^{-6} \, V + (1.0 \, . \, 10^{-4} + 7.5 \, . \, 10^{-8} \, t) \quad . \quad . \quad . \quad (3)$$

where $H = \dfrac{0.24 \, i^2 R}{(t - t_0) \, l}$ is the rate of heat loss in calories, per unit of length of the wire 2), and per 1° C difference of temperature with the air (t being the temperature of the wire, t_0 that of the air).

---

1) To avoid confusion figures of SIMMONS and BAILEY's paper wil be indicated here by Roman numerals.

2) The authors indicate "per foot". It appears from comparison with values read off from the graphs that the length of the wire has to be taken in cm and not in feet.

From the graphs of fig. II we read:

for $\varphi = 90°$: .... $R = 19.33\ \Omega$
for $\varphi = 0°$: .... $R = 29.20\ \Omega$

Inserting the first value of R into equation (2), V being equal to 40 ft/sec, the temperature difference $t - t_0$ is found to be 53.1° C (fig. I gives $t - t_0 = 54.5°$, which differs not exaggeratedly from the calculated value in view of the inexactitude inherent to the readings).

Inserting the second value for R into equation (3), taking t_0 equal to 22° C as indicated in fig. I, gives $t - t_0 = 224.2°$ C (fig. I gives 225°). V_{a0} now can be calculated easily by substituting into (2): $R = 29.20\ \Omega$; $t - t_0 = 224.2°$ C. We get $V_{a0} = 1.8$ ft/sec, and thus finally $\alpha_0 = V_{a0}/V_t = 1.8/40 = 0.045$.

With the value of α_0 thus obtained the apparent velocity V_a can be calculated for various positions of the wire. In the expression for H instead of $t - t_0$ we write $(R - R_0)\,\beta$; for β we find easily 17.34 degree/ohm, while $R_0 = 16.26\ \Omega$. Equation (2) now assumes the form:

$$\frac{0{,}24\, i^2 R}{17{,}34\,(R - R_0)\, l} = 6{,}68\,.\,10^{-5} \sqrt{V_a} + 9{,}60\,.\,10^{-5} \quad . \quad . \quad . \quad (2a)$$

from which the value of R corresponding to any value of V_a can be found.

The following table shows the course of the calculation. The last column gives the values which can be read directly from fig. II.

φ	$\alpha = \sqrt{\sin^2\varphi + \alpha_0^2 \cos^2\varphi}$	$V_a = \alpha\, V_t$ in ft/sec	R calculated	R observed
0°	0.045	1.80	29.2	29.2
5°	0.104	4.15	25.2	25.0
10°	0.179	7.17	23.2	23.0
20°	0.345	13.78	21.3	21.3
30°	0.501	20.06	20.5	20.6
45°	0.709	28.31	19.9	19.8
60°	0.866	34.64	19.6	19.6
90°	1.000	40.00	19.3	19.3

We see that here again the agreement is very satisfactory.

It is of importance to investigate whether the relation between V_a and V_t, defined by eq. (1), is independent of the particular arrangement of the anemometer circuit. For any particular arrangement, equality of the indication of the anemometer, be it the position of the bridge galvanometer, or the current through the wire, ensures equality of temperature of the latter. Hence eq. (1) expresses that for a particular value of the temperature (the same in both cases), the cooling effect of the true air current V_t acting under the angle φ and that of the air current V_a acting under 90° are equal. This equality, however, will also hold for other temperatures of the wire as long as we can neglect radiation effects and the influences of the temperature upon the heat conductivity and the viscosity of the air, for then the cooling effect of the air current as well as that of the supports of the wire, can be assumed to be proportional to the temperature difference between wire and air. Under these circumstances the value of α_0 will depend uniquely on V_t, and will be the same function of V_t for all kinds of circuits.

4. *Variation of the coefficient α_0 with V_t.*

It has already been mentioned that the value of α_0 depends on the velocity of the air in which the wire is placed. From the calibration curves for the normal and the zero position of the wire, we can obtain this coefficient as the quotient of the velocities corresponding to the same indication of the anemometer. The curves A and B from fig. 4 show its dependence on the true velocity (V_t) as deduced respectively from experiments of January and of July 1932 (for the latter, see fig. 2).

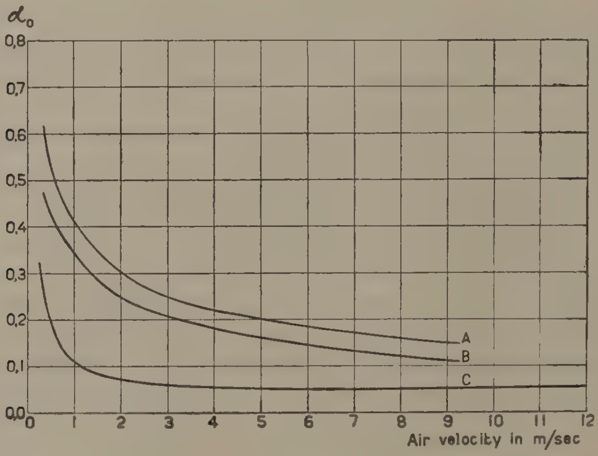

Fig. 4.

Variation of the factor α_0 with the true velocity V_t:

A = For a wire of 1,2 mm length (diam. 0,005 mm).
B = For a wire of 2,0 mm length (diam. 0,005 mm).
C = As deduced from Simmons and Bailey's results for a wire of 78 mm length (diam. 0,026 mm).

The same diagram also shows the α_0 curve calculated from SIMMONS and

BAILEY's results for a wire of 78 mm length (curve C). As, according to what has been said in the foregoing section, the same indication of the anemometer means the same heat loss per degree of temperature difference between wire and air, and thus equal values of H in equation (2) and (3), the relation between V_a and V_t is given by:

$$H_{(eq.\ 2)} = H_{(eq.\ 3)}$$

or

$$6{,}68 \, . \, 10^{-5} \, V_a^{1/2} + 9{,}60 \, . \, 10^{-5} = 1{,}673 \, . \, 10^{-6} \, V_t + 10^{-4} + 7{,}5 \, . \, 10^{-8} \, t.$$

For a_0 we obtain:

$$a_0 = \frac{V_a}{V_t} = \frac{(0{,}1673 \, V_t + 0{,}40 + 7{,}5 \, . \, 10^{-3} \, t)^2}{6{,}68^2 \, V_t}.$$

It must be remarked that this formula cannot be applied to very low velocities (a_0 would grow indefinitely); this can be explained by the fact that the formulae upon which the calculation is based, have but a limited range of validity. For the calculation of curve C in fig. 4 a temperature of 400° C has been chosen; V_t is in ft/sec.

We see that the general character of this curve is the same as that of curves A and B. Most typical is the rapid increase of a_0 with decreasing velocities. It is not possible to determine experimentally which limiting value will be reached if V decreases infinitely to zero; it may be that in that case a_0 is equal to unity, as it might be supposed that for very low velocities the rate of heat loss does not depend on the angular position of the wire with regard to the velocity vector.

The value of a_0 calculated from the equation given by SIMMONS and BAILEY reaches a minimum for $V = 6.19$ m/sec and then increases again indefinitely. The minimum occurs in the range of velocities investigated by the authors and thus must exist in reality. We have not further given attention to this point as it was of little interest for our work; besides experiments are complicated by the circumstance that vortices are formed behind the needles between which the wire is stretched if the REYNOLDS' number is higher than about 50. A calibration curve for the hot wire of 2 mm length used for the experiments in July, in zero position and for high velocities, indeed shows a fairly sharp bend in upward direction at $V = 21$ m/sec.

There must also be an important effect of the length of the wire on its cooling if placed in the zero position. With increasing length the temperature of the air at the end of the wire will assume a higher value, and thus the mean rate of heat transfer per unit of length of the wire will decrease. This must cause a decrease of a_0 with increasing length of the wire. It can also be expected that the shorter the wire is, the sooner a_0 will increase to unity with decreasing velocities. These relations are clearly confirmed by experiment (see fig. 4).

5. *Discussion of results.*

From the results of the preceding pages can be deduced that the errors which were signalized in the first section of this communication readily may be neglected in ordinary hot wire work. If the length of the wire is not below 1 cm and the velocities which have to be measured do not decrease below a few meters per second, the presence of a velocity component parallel to the wire will not sensibly affect the indication of the anemometer. In fact under these conditions we may assume that α_0 will be at most 0.1 (comp. fig. 4). From the formula for V_a etc. it follows that the component of the velocity parallel to the wire may increase to 1.42 times the normal component, before an error of 1 % in the indication of the normal component will be introduced. This means a rotation of the velocity vector over 55°, its absolute value being in the ratio 1.75/1 to the normal component. We thus may safely say that the single hot wire anemometer within a large range is only sensitive for the value of the air speed component perpendicular to the wire.

The case is different with short wires if low velocities are to be measured. The value of α_0 then may rise e.g. to 0.4; in this case an error of 1 % in the value of the normal component would be obtained with a parallel component equal to 0.35 times the normal one, corresponding to an angle of deviation of 19°. These values are mentioned only in order to show the order of magnitude of the errors to be expected; the formula is only an approximation and the actual differences may be either smaller or greater.

In regions of the turbulent boundary layer near to the wall where the mean value of the velocity component in the general direction of flow is very low, it may happen (as the fluctuations in x, y and z direction are not necessarily in phase), that a maximum of the cross component coincides with a minimum of the other components and thus of their resultant ¹)[1]. Assuming the wire to be parallel to the wall and normal to the general flow, this means that at certain moments the component parallel to the wire may obtain a value greater than that of the component perpendicular to the wire. In that case the recorded value will differ both from the velocity in a plane normal to the wire and from the absolute value of the velocity in space. The greatest percentage differences always will be found near the wall; however, compared to the value of the velocity in the free stream, the errors will appear not very important. Oscillograms of the velocity fluctuations recorded with short wires in regions near to the

---

¹) In a work of A. FAGE and H. C. H. TOWNEND, An examination of turbulent flow with an ultra-microscope Proc. Roy. Soc. A. Vol. 135, p. 656 1932, some experimental data are given on the distribution of turbulent velocities near a wall. The fact that the cross component of the velocity fluctuations attains a higher value than the other components is in agreement with our own observations with hot wires. It must be remarked that in some cases the magnitude of the velocity fluctuations observed by us was still greater than the values given by these authors for turbulent flow in a square pipe.

wall thus still may be considered as representative of the fluctuations of the air speed in the plane perpendicular to the wire[1].

At the same time it can be remarked that the use of a wire mounted parallel to the direction of the general flow may give valuable information concerning the magnitude of the cross component. We hope to come back to this in a future paper.

The investigation of the directional properties of the single hot wire has not been extended further for the present, as it was considered that the data obtained were sufficient for a general discussion of its behaviour, while on the other hand the inaccuracies inherent to experimental work with thin wires, especially with the short ones, as yet do not allow the deduction of a more accurate relation.

---

[1] Such oscillograms have been reproduced in Mededeeling 23 (these Proceedings, 35, p. 419, 1932).

Mathematics. — *Ueber die henkelfreien Kontinua.* Von Dr. W. HUREWICZ.

(Communicated by Prof. L. E. J. BROUWER.)

(Communicated at the meeting of October 29, 1932.)

Ein kompaktes Kontinuum C heisst *henkelfrei* („unicoherent"), wenn bei jeder Zerlegung von C in zwei Teilkontinua ihr Durchschnitt zusammenhängend ist. Der Begriff der Henkelfreiheit und seine Verallgemeinerungen spielen eine bedeutende Rolle in den topologischen Untersuchungen der letzten Jahre[1]. Im Falle eines *lokal zusammenhängenden Kontinuums* C bedeutet nach KURATOWSKI[2] die Henkelfreiheit, dass in C der klassische BROUWER-PHRAGMEN'sche Satz gilt, d.h. für jedes Teilkontinuum M von C sämtliche Komponenten der offenen Menge C-M zusammenhängende Begrenzungen[3] haben. Wir wollen daher lokal zusammenhängende henkelfreie Kontinua kurz als BROUWER*'sche Kontinua* bezeichnen.

Wir beweisen nun: *Für* $n \geq 3$ *ist jeder n-dimensionale* (separable und metrisierbare) *Raum* R *mit einer Teilmenge eines n-dimensionalen* BROUWER*'schen Kontinuums homöomorph.*

Beim Beweis können wir R als kompakt voraussetzen, da doch jeder Raum R in einen kompakten Raum von derselben Dimension topologisch einbettbar ist[4]. Wir stützen uns auf das folgende Ergebnis des Verfassers: Jeder kompakte Raum R kann durch oberhalb-stetige Zerlegung einer abgeschlossenen beschränkten Menge des Euklidischen E_3 in *zusammenhängende Teilmengen* erzeugt werden [1]. Diese Zerlegung lässt sich offenbar zu einer oberhalb-stetigen Zerlegung einer M enthaltenden dreidimensionalen Kugel K erweitern, indem man als die noch fehlenden Bestandteile der Zerlegung die einzelnen Punkte der Menge K-M hinzunimmt. Der durch die erweiterte Zerlegung erzeugte Raum R^* ist eine topologische Erweiterung von R. Nun ist bekanntlich die Kugel K henkelfrei, anderseits bekommt man durch oberhalb-stetige Zerlegung eines henkelfreien Raumes in zusammenhängende Teilmengen stets wieder einen henkelfreien Raum [2]. Folglich ist R^* henkelfrei, ferner ist der Raum R^* als stetiges Bild von K natürlich lokal-zusammenhängend, also ein BROUWERscher Raum. Schliesslich ist, falls R n-dimensional $(n \geqq 3)$, auch R^* n-dimensional. Nach der Konstruktion von R^* ist nämlich die Menge R^*-R mit K-M homöomorph, also dreidimensional. In der Zerlegung $R^* = R + (R^*\text{-}R)$ sind beide Summanden höchstens dimensional und der erste ist überdies kompakt und somit in R^* abgeschlossen. Nun ist aber nach einem bekannten Satz der Dimensionstheorie die Summe zweier höchstens n-dimensionaler Mengen, von denen eine abgeschlossen ist, selbst höchstens n-dimensional. Damit ist alles bewiesen.

---

[1] Vgl. u.a. KNASTER, C. R. du Premier Congrés des Mathématiciens des Pays Slaves, p. 287. Der Ausdruck „henkelfrei" stammt von VIETORIS (diese Proceedings 29 (1926) S. 440).

[2] Vgl. Fund. Math. 8, S. 148.

[3] Selbstverständlich handelt es sich hier um Begrenzungen in Bezug auf C *als* Raum.

[4] Vgl. meine Arbeit in den Monatsheften f. Math. u. Phys., 37, S. 199.

Für $n = 1$ ist der Satz sicher falsch, denn unter den eindimensionalen Kontinua stimmen die BROUWER'schen mit den sog. Baumkurven überein [3] und jedes Teilkontinuum einer Baumkurve ist wieder eine Baumkurve. Daraus folgt, dass sich beispielweise die Kreislinie in kein eindimensionales BROUWER'sches Kontinuum einbetten lässt.

Fragen:

1⁰. Gilt das obige Ergebnis für $n = 2$ [4] (oder ist etwa die Torusfläche ein Gegenbeispiel)?

2⁰. Ist jedes BROUWERsche Kontinuum durch eine oberhalb-stetige Zerlegung der dreidimensionalen Kugel in zusammenhängende Teilmengen darstellbar?

---

[1] Fund. Math. **14**, S. 57.

[2] Vgl. VIETORIS, diese Proceedings, **29**, (1926), S. 440.

[3] VIETORIS, a.a.O., S. 446.

[4] Jedenfals kann man den oben durchgeführten Beweis nicht auf den Fall $n = 2$ übertragen, denn es lässt sich beweisen, dass man durch oberhalb-stetige Zerlegungen von ebenen abgeschlossenen Mengen in zusammenhängende Teile *nicht alle* zweidimensionale konpakte Räume erhalten kann. Vgl. KURATOWSKI, Fund. Math. **14**, S. 143.

Mathematics. — *Asymptotische Entwicklungen von* BESSEL*schen*, HANKEL*schen und verwandten Funktionen*. IV [1]). Von C. S. MEIJER. (Communicated by Prof. J. G. VAN DER CORPUT).

(Communicated at the meeting of October 29, 1932.)

§ 3. Beweis der Sätze 1—6.

Beweis von Satz 1. Ist x reell, $\Re(\nu) = \alpha$ und $\Im(\nu) = \gamma$, dann hat man

$$|\cosh \nu x| = \tfrac{1}{2}\,|e^{(\alpha+i\gamma)x} + e^{-(\alpha+i\gamma)x}| \leqq \tfrac{1}{2}\,(e^{\alpha x} + e^{-\alpha x}) = \cosh \alpha x. \tag{101}$$

Ist $\zeta e^{-\frac{i\mu}{2}} \geqq 0$, x reell, $w \neq 0$, $-\pi < \arg w < 2\pi$ und

$$\mathrm{Max}\left(-\frac{\pi}{2}, -\frac{3\pi}{2} + \arg w\right) < \mu < \mathrm{Min}\left(\frac{\pi}{2}, \frac{\pi}{2} + \arg w\right), \quad . \tag{66}$$

dann können wir in Hilfssatz 15

$$r = 2\,|w|\cosh^2\frac{x}{2}, \; d = |\zeta|^2 \;, \; e^{\beta i} = -\,i e^{-\mu i}\,\frac{w}{|w|}$$

setzen, sodass $\beta = \arg w - \dfrac{\pi}{2} - \mu$ ist. Wir erhalten dann

$$\left.\begin{aligned} \left|\frac{2iw\cosh^2\frac{x}{2}}{2iw\cosh^2\frac{x}{2} - \zeta^2}\right| &= \left|\frac{-2ie^{-\mu i}\,w\cosh^2\frac{x}{2}}{-2ie^{-\mu i}\,w\cosh^2\frac{x}{2} + |\zeta|^2}\right| \\ &\leqq \frac{1}{\left|\sin\left(\arg w - \frac{\pi}{2} - \mu\right)\right|} \end{aligned}\right\} \tag{102}$$

und sogar

$$\left|\frac{2iw\cosh^2\frac{x}{2}}{2iw\cosh^2\frac{x}{2} - \zeta^2}\right| \leqq 1, \text{ falls } -\frac{\pi}{2} \leqq \arg w - \frac{\pi}{2} - \mu \leqq \frac{\pi}{2} \text{ ist.} \tag{103}$$

---

[1]) Erste, zweite und dritte Mitteilung: These Proceedings, Vol. **35** (1932), S. 656—667, S. 852—866 und S. 948—958.

Es werde gesetzt:

$$A = 1, \text{ falls } -\frac{\pi}{2} \leqq \arg w - \frac{\pi}{2} - \mu \leqq \frac{\pi}{2} \text{ ist,}$$

und

$$A = \left| \sin\left(\arg w - \frac{\pi}{2} - \mu\right) \right|, \left\{ \begin{array}{l} \text{falls} -\pi < \arg w - \frac{\pi}{2} - \mu < -\frac{\pi}{2} \text{ und} \\ \text{falls } \frac{\pi}{2} < \arg w - \frac{\pi}{2} - \mu < \pi \text{ ist.} \end{array} \right.$$

Wegen

$$\int_0^{\infty e^{\frac{i\mu}{2}}} e^{-|\zeta|^2 \cos\mu} |\zeta|^{2N} |d\zeta| = \int_0^{\infty} e^{-t^2 \cos\mu}\, t^{2N}\, dt = \frac{1}{(\cos\mu)^{N+1/2}} \int_0^{\infty} e^{-\zeta^2} \zeta^{2N}\, d\zeta$$

folgt also aus (101), (102) und (103) für jedes ganze rationale $N > |\alpha| - \frac{1}{2}$ [1])

$$\left| \int_0^{\infty e^{\frac{i\mu}{2}}} e^{-\zeta^2} \zeta^{2N}\, d\zeta \int_{-\infty}^{\infty} \frac{2iw \cosh^2\frac{x}{2} \cosh \nu x\, dx}{\left(\cosh\frac{x}{2}\right)^{2N+1} \left(2iw\cosh^2\frac{x}{2} - \zeta^2\right)} \right| <$$

$$\frac{1}{A} \int_0^{\infty e^{\frac{i\mu}{2}}} e^{-|\zeta|^2 \cos\mu} |\zeta|^{2N} |d\zeta| \int_{-\infty}^{\infty} \frac{\cosh \alpha x\, dx}{\left(\cosh\frac{x}{2}\right)^{2N+1}} =$$

$$\frac{1}{A\,.\,(\cos\mu)^{N+1/2}} \int_0^{\infty} e^{-\zeta^2} \zeta^{2N}\, d\zeta \int_{-\infty}^{\infty} \frac{\cosh \alpha x\, dx}{\left(\cosh\frac{x}{2}\right)^{2N+1}}.$$

Hieraus und aus (67) von Hilfssatz 13 und (56) und (57) von Hilfssatz 9 folgt, falls $\alpha + \frac{1}{2}$ nicht ganz rational ist,

$$H_\nu^{(1)}(w) = \sqrt{\frac{2}{\pi}} \frac{e^{i\left(w - 1/2\,\nu\pi - \frac{\pi}{4}\right)}}{w^{1/2}} \left\{ \begin{array}{l} \displaystyle\sum_{l=0}^{N-1} \frac{(i)^l \prod_{h=0}^{l-1} (4\nu^2 - (2h+1)^2)}{l!\,(8w)^l} + \\ \displaystyle\frac{\varrho}{A\,.\,(\cos\mu)^{N+1/2}} \frac{\cos\nu\pi}{\cos\alpha\pi} \frac{(i)^N \prod_{h=0}^{N-1} (4\alpha^2 - (2h+1)^2)}{N!\,(8w)^N} \end{array} \right\}. \qquad (104)$$

---

[1]) In (102) und (103) gilt nicht für jedes ζ mit $\zeta e^{-\frac{i\mu}{2}} \geqq 0$ das Gleichheitszeichen.

und, falls $|\alpha| = k + \frac{1}{2}$ (k ganz rational) ist,

$$H_\nu^{(1)}(w) = \sqrt{\frac{2}{\pi}}\, \frac{e^{i\left(w - \frac{1}{2}\nu\pi - \frac{\pi}{4}\right)}}{w^{1/2}} \left\{ \sum_{l=0}^{N-1} \frac{(i)^l \prod\limits_{h=0}^{l-1} (4\nu^2 - (2h+1)^2)}{l!\,(8w)^l} + \right. \\ \left. \frac{\varrho\,(-1)^{k+1}\,(i)^N (8k+4) \cos\nu\pi}{A\,.\,(\cos\mu)^{N+1/2}\,\pi\, N!\,(8w)^N} \prod_{\substack{h=0 \\ h \neq k}}^{N-1} (4\alpha^2 - (2h+1)^2) \right\}, \quad . \quad . \quad (105)$$

worin $|\varrho| < 1$ ist.

Wenden wir jetzt Hilfssatz 17 mit $\varkappa = N + \frac{1}{2}$ und $\sigma = \arg w - \frac{\pi}{2}$ an, dann finden wir, wenn

$$M = \underset{Max\left(-\frac{\pi}{2},\, -\frac{3\pi}{2} + \arg w\right) < \mu < Min\left(\frac{\pi}{2},\, \frac{\pi}{2} + \arg w\right)}{Max} A\,.\,(\cos\mu)^{N+1/2}$$

gesetzt wird:

Falls $0 \leqq \arg w \leqq \pi$ ist, ist $M = 1$.

Falls $-\pi < \arg w < 0$ ist, ist

$$M = \cos(\mu_1 - \arg w)\,(\cos\mu_1)^{N+1/2};$$

hierin ist μ_1 der durch [1]

$$\sin(\arg w - 2\mu_1) = \frac{2N-1}{2N+3} \sin\arg w$$

eindeutig bestimmte, im Falle $-\pi < \arg w \leqq -\frac{\pi}{2}$ zwischen $-\frac{\pi}{2}$ und $\frac{\pi}{2} + \arg w$ und im Falle $-\frac{\pi}{2} < \arg w < 0$ zwischen $\arg w$ und 0 liegende Winkel.

Falls $\pi < \arg w < 2\pi$ ist, ist

$$M = -\cos(\mu_2 - \arg w)\,(\cos\mu_2)^{N+1/2};$$

hierin ist μ_2 der durch

$$\sin(\arg w - 2\mu_2) = \frac{2N-1}{2N+3} \sin\arg w$$

eindeutig bestimmte, im Falle $\frac{3\pi}{2} \leqq \arg w < 2\pi$ zwischen $-\frac{3\pi}{2} + \arg w$ und $\frac{\pi}{2}$ und im Falle $\pi < \arg w < \frac{3\pi}{2}$ zwischen 0 und $\arg w - \pi$ liegende Winkel.

---

[1] In Formel (16) liese man $\frac{2N-1}{2N+3}$ statt $\frac{2N-1}{2N+1}$.

In (104) und in (105) bezeichnet μ einen beliebigen Punkt des Intervalles (66). Wir dürfen also in (104) und in (105) $A \,.\, (\cos\mu)^{N+1/_2}$ durch seinen (oben gegebenen) grössten Wert ersetzen und finden dann, falls $\alpha + \frac{1}{2}$ nicht ganz rational ist,

$$\left.\begin{aligned} H_\nu^{(1)}(w) = \sqrt{\frac{2}{\pi}}\, \frac{e^{i\left(w - 1/_2 \nu\pi - \frac{\pi}{4}\right)}}{w^{1/_2}} \Bigg\{ \sum_{l=0}^{N-1} \frac{(i)^l \prod\limits_{h=0}^{l-1} (4\nu^2 - (2h+1)^2)}{l!\,(8w)^l} + \\ \theta_1 \frac{\cos\nu\pi}{\cos\alpha\pi} \frac{(i)^N \prod\limits_{h=0}^{N-1} (4\alpha^2 - (2h+1)^2)}{N!\,(8w)^N} \Bigg\}. \end{aligned}\right\} \quad . \quad (106)$$

und, falls $|\alpha| = k + \frac{1}{2}$ (k ganz rational) ist,

$$\left.\begin{aligned} H_\nu^{(1)}(w) = \sqrt{\frac{2}{\pi}}\, \frac{e^{i\left(w - 1/_2 \nu\pi - \frac{\pi}{4}\right)}}{w^{1/_2}} \Bigg\{ \sum_{l=0}^{N-1} \frac{(i)^l \prod\limits_{h=0}^{l-1} (4\nu^2 - (2h+1)^2)}{l!\,(8w)^l} + \\ \theta_1 \frac{(-1)^{k+1}\,(i)^N\,(8k+4)\cos\nu\pi}{\pi\, N!\,.(8w)^N} \prod_{\substack{h=0 \\ h \neq k}}^{N-1} (4\alpha^2 - (2h+1)^2) \Bigg\}, \end{aligned}\right\} \quad . \quad (107)$$

worin

$$|\theta_1| < 1, \text{ falls } 0 \leqq \arg w \leqq \pi \text{ ist,}$$

$$|\theta_1| < \frac{1}{\cos(\mu_1 - \arg w)\,(\cos\mu_1)^{N+1/_2}}, \text{ falls } -\pi < \arg w < 0 \text{ ist,}$$

$$|\theta_1| < \frac{-1}{\cos(\mu_2 - \arg w)\,(\cos\mu_2)^{N+1/_2}}, \text{ falls } \pi < \arg w < 2\pi \text{ ist.}$$

Hiermit sind die Beziehungen (14), (15) und (17) der ersten Behauptung und ausserdem die zweite Behauptung von Satz 1 bewiesen.

Der Beweis der Relationen (19) und (20) geht folgendermassen:

Ist

$$\zeta \geqq 0,\, x \text{ reell},\ w \neq 0 \quad \text{und} \quad -\frac{\pi}{2} < \arg w < \frac{3\pi}{2},$$

dann können wir in Hilfssatz 16

$$r = 2|w|\cosh^2\frac{x}{2},\, d = \zeta^2,\, e^{\beta i} = -i\frac{w}{|w|};\ \text{also } \beta = \arg w - \frac{\pi}{2},$$

setzen. Wegen

$$\frac{2iw\cosh^2\frac{x}{2}}{2iw\cosh^2\frac{x}{2} - \zeta^2} = \frac{-2iw\cosh^2\frac{x}{2}}{-2iw\cosh^2\frac{x}{2} + \zeta^2}$$

erhalten wir dann

$$0 \leqq \arg \left(\frac{2\,i\,w \cosh^2 \frac{x}{2}}{2\,i\,w \cosh^2 \frac{x}{2} - \zeta^2} \right) \leqq \arg w - \frac{\pi}{2}\,, \text{ falls } \frac{\pi}{2} \leqq \arg w < \frac{3\pi}{2} \text{ ist,}$$

und

$$\arg w - \frac{\pi}{2} \leqq \arg \left(\frac{2\,i\,w \cosh^2 \frac{x}{2}}{2\,i\,w \cosh^2 \frac{x}{2} - \zeta^2} \right) \leqq 0, \text{ falls } -\frac{\pi}{2} < \arg w \leqq \frac{\pi}{2} \text{ ist.}$$

Ist $\mathfrak{I}(\nu) = 0$, also $\nu = \alpha$, dann folgt hieraus

$$\left.\begin{aligned} &\int_0^\infty e^{-\zeta^2} \zeta^{2N}\, d\zeta \int_{-\infty}^{\infty} \frac{2\,i\,w \cosh^2 \frac{x}{2} \cosh \nu x\, dx}{\left(\cosh \frac{x}{2}\right)^{2N+1} \left(2\,i\,w \cosh^2 \frac{x}{2} - \zeta^2\right)} = \\ &\lambda \int_0^\infty e^{-\zeta^2} \zeta^{2N}\, d\zeta \int_{-\infty}^{\infty} \frac{\cosh \alpha x\, dx}{\left(\cosh \frac{x}{2}\right)^{2N+1}}, \end{aligned}\right\}. \qquad (108)$$

worin

$$0 \leqq \arg \lambda \leqq \arg w - \frac{\pi}{2}, \text{ falls } \frac{\pi}{2} \leqq \arg w < \frac{3\pi}{2} \text{ ist,}$$

und

$$\arg w - \frac{\pi}{2} \leqq \arg \lambda \leqq 0, \text{ falls } -\frac{\pi}{2} < \arg w \leqq \frac{\pi}{2} \text{ ist.}$$

Ist $-\frac{\pi}{2} < \arg w < \frac{3\pi}{2}$, so dürfen wir in Hilfssatz 13 $\mu = 0$ setzen. Aus (67) mit $\mu = 0$, (108) und (56) folgt jetzt, dass in (106)

$$0 \leqq \arg \theta_1 \leqq \arg w - \frac{\pi}{2} \text{ ist, falls } \nu = \alpha \text{ und } \frac{\pi}{2} \leqq \arg w < \frac{3\pi}{2} \text{ ist,}$$

und

$$\arg w - \frac{\pi}{2} \leqq \arg \theta_1 \leqq 0 \text{ ist, falls } \nu = \alpha \text{ und } -\frac{\pi}{2} < \arg w \leqq \frac{\pi}{2} \text{ ist.}$$

Hiermit ist auch die erste Behauptung von Satz 1 vollständig bewiesen.

Ist ν reell und $|\nu| = k + \frac{1}{2}$ (k ganz rational), dann ist $\cos \nu\pi = 0$ und $\prod\limits_{h=0}^{l-1} (4\nu^2 - (2h+1)^2) = 0$ für jedes ganze $l > k$. Hieraus folgt mit Rücksicht auf (107) die dritte Behauptung von Satz 1.

Beweis von Satz 2. Der Beweis dieses Satzes ist dem Beweis von Satz 1 analog; man braucht dabei nur (68) statt (67) von Hilfssatz 13 und Hilfssatz 10 statt 9 anzuwenden.

Beweis von Satz 3. Ist $u e^{-i\mu} \geqq 0$, x reell, $w \neq 0$, $-\pi < \arg w < \pi$ und

$$Max\left(-\frac{\pi}{2}, -\frac{\pi}{2} + \arg w\right) < \mu < Min\left(\frac{\pi}{2}, \frac{\pi}{2} + \arg w\right), \tag{76}$$

dann können wir in Hilfssatz 15

$$r = |w|^2 \cosh^2 x \quad , \quad d = |u|^2 \quad , \quad e^{\beta i} = e^{-2\mu i} \frac{w^2}{|w|^2}$$

setzen, sodass $\beta = 2 \arg w - 2\mu$ ist. Wir finden dann

$$\left| \frac{w^2 \cosh^2 x}{w^2 \cosh^2 x + u^2} \right| = \left| \frac{e^{-2\mu i} w^2 \cosh^2 x}{e^{-2\mu i} w^2 \cosh^2 x + |u|^2} \right| \leqq \frac{1}{|\sin(2 \arg w - 2\mu)|} \tag{109}$$

und sogar

$$\left| \frac{w^2 \cosh^2 x}{w^2 \cosh^2 x + u^2} \right| \leqq 1, \text{ falls } -\frac{\pi}{2} \leqq 2 \arg w - 2\mu \leqq \frac{\pi}{2} \text{ ist.} \tag{110}$$

Ist $\Re(\nu) = a$ und x reell, dann ist (man vergleiche (101))

$$|\cosh \nu x| \leqq \cosh a x \quad . \quad . \quad . \quad . \quad . \quad . \quad . \quad . \tag{111}$$

Es werde gesetzt:

$$B = 1, \text{ falls } -\frac{\pi}{2} \leqq 2 \arg w - 2\mu \leqq \frac{\pi}{2} \text{ ist,}$$

und

$$B = |\sin(2 \arg w - 2\mu)|, \begin{cases} \text{falls } -\pi < 2 \arg w - 2\mu < -\dfrac{\pi}{2} \text{ und} \\ \text{falls } \dfrac{\pi}{2} < 2 \arg w - 2\mu < \pi \text{ ist.} \end{cases}$$

Wegen

$$\int_0^{\infty e^{i\mu}} e^{-|u|\cos\mu} |u|^{2N} |du| = \int_0^\infty e^{-t\cos\mu} t^{2N} dt = \frac{1}{(\cos\mu)^{2N+1}} \int_0^\infty e^{-u} u^{2N} du$$

folgt also aus (109), (110) und (111) für jedes ganze rationale $N > \frac{1}{2}|\alpha| - \frac{1}{2}$

$$\left| \int_0^{\infty e^{i\mu}} e^{-u} u^{2N} du \int_{-\infty}^{\infty} \frac{w^2 \cosh^2 x \cosh \nu x \, dx}{(\cosh x)^{2N+1} (w^2 \cosh^2 x + u^2)} \right| <$$

$$\frac{1}{B} \int_0^{\infty e^{i\mu}} e^{-|u|\cos\mu} |u|^{2N} |du| \int_{-\infty}^{\infty} \frac{\cosh \alpha x \, dx}{(\cosh x)^{2N+1}} =$$

$$\frac{1}{B\,.\,(\cos\mu)^{2N+1}} \int_0^\infty e^{-u} u^{2N} du \int_{-\infty}^{\infty} \frac{\cosh \alpha x \, dx}{(\cosh x)^{2N+1}}.$$

Hieraus und aus (77) von Hilfssatz 14 und (61) und (62) von Hilfssatz 11 folgt, falls α keine ungerade ganze Zahl ist,

$$\left.\begin{aligned} A_\nu(w) = \sum_{l=0}^{N-1} \frac{1}{w^{2l+1}} \prod_{h=0}^{l-1} (\nu^2 - (2h+1)^2) + \\ \frac{\tau}{B\,.\,(\cos\mu)^{2N+1}} \frac{\cos\frac{\nu\pi}{2}}{\cos\frac{\alpha\pi}{2}} \frac{1}{w^{2N+1}} \prod_{h=0}^{N-1} (\alpha^2 - (2h+1)^2) \end{aligned}\right\} \quad . \; . \; . \quad (112)$$

und, falls $|\alpha| = 2k+1$ (k ganz rational) ist,

$$\left.\begin{aligned} A_\nu(w) = \sum_{l=0}^{N-1} \frac{1}{w^{2l+1}} \prod_{h=0}^{l-1} (\nu^2 - (2h+1)^2) + \\ \frac{\tau(-1)^{k+1}(8k+4)\cos\frac{\nu\pi}{2}}{B\,.\,(\cos\mu)^{2N+1}\,\pi\, w^{2N+1}} \prod_{\substack{h=0 \\ h \neq k}}^{N-1} (\alpha^2 - (2h+1)^2), \end{aligned}\right\} \quad . \; . \; . \quad (113)$$

worin $|\tau| < 1$ ist.

Wenden wir jetzt Hilfssatz 18 mit $\varkappa = 2N+1$ und $\sigma = 2 \arg w$ an, dann finden wir, wenn

$$M^* = \underset{Max\left(-\frac{\pi}{2},\, -\frac{\pi}{2} + \arg w\right) < \mu < Min\left(\frac{\pi}{2},\, \frac{\pi}{2} + \arg w\right)}{Max} B . (\cos \mu)^{2N+1}$$

gesetzt wird:

Falls $-\frac{\pi}{4} \leqq \arg w \leqq \frac{\pi}{4}$ ist, ist $M^* = 1$.

Falls $-\pi < \arg w < -\frac{\pi}{4}$ ist, ist

$$M^* = \sin (2 \mu_3 - 2 \arg w) (\cos \mu_3)^{2N+1};$$

hierin ist μ_3 der durch

$$(2N+3) \cos (3 \mu_3 - 2 \arg w) = (2N-1) \cos (\mu_3 - 2 \arg w)$$

eindeutig bestimmte, im Falle $-\pi < \arg w \leqq -\frac{3\pi}{4}$ zwischen $-\frac{\pi}{2}$ und $\frac{\pi}{2} + \arg w$, im Falle $-\frac{3\pi}{4} < \arg w \leqq -\frac{\pi}{2}$ zwischen [1] $\frac{\pi}{4} + \arg w$ und $\frac{\pi}{2} + \arg w$ und im Falle $-\frac{\pi}{2} < \arg w < -\frac{\pi}{4}$ zwischen $\frac{\pi}{4} + \arg w$ und 0 liegende Winkel.

Falls $\frac{\pi}{4} < \arg w < \pi$ ist, ist

$$M^* = \sin (2 \arg w - 2 \mu_4) (\cos \mu_4)^{2N+1};$$

hierin ist μ_4 der durch

$$(2N+3) \cos (3 \mu_4 - 2 \arg w) = (2N-1) \cos (\mu_4 - 2 \arg w)$$

eindeutig bestimmte, im Falle $\frac{3\pi}{4} \leqq \arg w < \pi$ zwischen $-\frac{\pi}{2} + \arg w$ und $\frac{\pi}{2}$, im Falle $\frac{\pi}{2} \leqq \arg w < \frac{3\pi}{4}$ zwischen $-\frac{\pi}{2} + \arg w$ und $-\frac{\pi}{4} + \arg w$ und im Falle $\frac{\pi}{4} < \arg w < \frac{\pi}{2}$ zwischen 0 und $-\frac{\pi}{4} + \arg w$ liegende Winkel.

Da in (112) und in (113) μ einen beliebigen Punkt des Intervalles (76) bezeichnet, dürfen wir in (112) und in (113) $B . (\cos \mu)^{2N+1}$ durch seinen (oben gegebenen) grössten Wert ersetzen und finden dann, falls a keine ungerade ganze Zahl ist,

---

[1] In der ersten Mitteilung, S. 661, Z. 1 v. u. liese man $\frac{\pi}{4} + \arg w$ statt $-\frac{\pi}{4} + \arg w$.

$$\left.\begin{array}{l} A_\nu(w) = \displaystyle\sum_{l=0}^{N-1} \frac{1}{w^{2l+1}} \prod_{h=0}^{l-1} (\nu^2-(2h+1)^2) + \\[2ex] \theta_3 \dfrac{\cos\dfrac{\nu\pi}{2}}{\cos\dfrac{\alpha\pi}{2}}\, \dfrac{1}{w^{2N+1}} \displaystyle\prod_{h=0}^{N-1}(\alpha^2-(2h+1)^2) \end{array}\right\} \quad . \;\; . \;\; . \quad (114)$$

und, falls $|\alpha| = 2k+1$ (k ganz rational) ist,

$$A_\nu(w) = \sum_{l=0}^{N-1} \frac{1}{w^{2l+1}} \prod_{h=0}^{l-1} (\nu^2-(2h+1)^2) +$$

$$\theta_3 \frac{(-1)^{k+1}(8k+4)\cos\dfrac{\nu\pi}{2}}{\pi\, w^{2N+1}} \prod_{\substack{h=0 \\ h\neq k}}^{N-1} (\alpha^2-(2h+1)^2),$$

worin

$$|\theta_3| < 1, \text{ falls } -\frac{\pi}{4} \leqq \arg w \leqq \frac{\pi}{4} \text{ ist,}$$

$$|\theta_3| < \frac{1}{\sin(2\mu_3 - 2\arg w)(\cos\mu_3)^{2N+1}}, \text{ falls } -\pi < \arg w < -\frac{\pi}{4} \text{ ist,}$$

$$|\theta_3| < \frac{1}{\sin(2\arg w - 2\mu_4)(\cos\mu_4)^{2N+1}}, \text{ falls } \frac{\pi}{4} < \arg w < \pi \text{ ist.}$$

Hiermit sind die Beziehungen (21), (22) und (24) der ersten Behauptung und ausserdem die zweite Behauptung von Satz 3 bewiesen.

Der Beweis der Relationen (26) und (27)[1]) geht folgendermassen: Ist

$$u \geqq 0,\ x \text{ reell},\ w \neq 0 \quad \text{und} \quad -\frac{\pi}{2} < \arg w < \frac{\pi}{2},$$

dann können wir in Hilfssatz 16

$$r = |w|^2 \cosh^2 x,\ d = u^2,\ e^{\beta i} = \frac{w^2}{|w|^2}, \text{ also } \beta = 2\arg w,$$

setzen. Wir erhalten dann

$$0 \leqq \arg\left(\frac{w^2\cosh^2 x}{w^2\cosh^2 x + u^2}\right) \leqq 2\arg w, \text{ falls } 0 \leqq \arg w < \frac{\pi}{2} \text{ ist,}$$

---

[1]) In Beziehung (27) liese man $\arg\theta_3$ statt θ_3.

und

$$2 \arg w \leqq \arg \left(\frac{w^2 \cosh^2 x}{w^2 \cosh^2 x + u^2} \right) \leqq 0, \text{ falls } -\frac{\pi}{2} < \arg w \leqq 0 \text{ ist.}$$

Ist $\Im(\nu) = 0$, also $\nu = \alpha$, dann folgt hieraus

$$\left. \begin{aligned} &\int_0^\infty e^{-u} u^{2N} du \int_{-\infty}^\infty \frac{w^2 \cosh^2 x \cosh \nu x \, dx}{(\cosh x)^{2N+1} (w^2 \cosh^2 x + u^2)} = \\ &\eta \int_0^\infty e^{-u} u^{2N} du \int_{-\infty}^\infty \frac{\cosh \alpha x \, dx}{(\cosh x)^{2N+1}}, \end{aligned} \right\} \quad . \quad . \quad (115)$$

worin

$$0 \leqq \arg \eta \leqq 2 \arg w, \text{ falls } 0 \leqq \arg w < \frac{\pi}{2} \text{ ist,}$$

und

$$2 \arg w \leqq \arg \eta \leqq 0, \text{ falls } -\frac{\pi}{2} < \arg w \leqq 0 \text{ ist.}$$

Aus (77) mit $\mu = 0$ [1]), (115) und (61) ergibt sich nun, dass in (114)

$$0 \leqq \arg \theta_3 \leqq 2 \arg w \text{ ist, falls } \nu = \alpha \text{ und } 0 \leqq \arg w < \frac{\pi}{2} \text{ ist,}$$

und

$$2 \arg w \leqq \arg \theta_3 \leqq 0 \text{ ist, falls } \nu = \alpha \text{ und } -\frac{\pi}{2} < \arg w \leqq 0 \text{ ist.}$$

Hiermit ist die erste Behauptung von Satz 3 vollständig bewiesen.
Der Beweis der dritten Behauptung ist dem Beweis der dritten Behauptung von Satz 1 analog.

Beweis von Satz 4. Der Beweis dieses Satzes ist dem Beweis von Satz 3 analog; man braucht dabei nur (78) statt (77) und Hilfssatz 12 statt 11 anzuwenden.

Beweis der Sätze 5 und 6. Ist

$w \neq 0, -2\pi < \arg w < \pi$, $\arg w^{1/2} = \frac{1}{2} \arg w$, N ganz rational $> |\Re(\nu)| - \frac{1}{2}$,

$$Max\left(-\frac{\pi}{2}, -\frac{\pi}{2} + \arg w\right) < \mu < Min\left(\frac{\pi}{2}, \frac{3\pi}{2} + \arg w\right).$$

---

[1]) Ist $-\frac{\pi}{2} < \arg w < \frac{\pi}{2}$, so dürfen wir in Hilfssatz 14 $\mu = 0$ setzen.

dann folgt aus (67) und (32) 1)

$$H_\nu^{(2)}(w) = \sqrt{\frac{2}{\pi}}\, \frac{e^{-i\left(w - {}^1\!/_2 \nu\pi - \frac{\pi}{4}\right)}}{w^{1/2}} \left\{ \sum_{l=0}^{N-1} \frac{(-i)^l \prod\limits_{h=0}^{l-1} (4\nu^2 - (2h+1)^2)}{l!\,(8w)^l} + \right. \\ \left. \frac{(i)^N \cos\nu\pi}{\pi\sqrt{\pi}(2w)^N} \int_0^{\infty e^{\frac{i\mu}{2}}} e^{-\zeta^2} \zeta^{2N}\, d\zeta \int_{-\infty}^{\infty} \frac{2iw \cosh^2 \frac{x}{2} \cosh \nu x\, dx}{\left(\cosh\frac{x}{2}\right)^{2N+1} \left(2iw\cosh^2\frac{x}{2} + \zeta^2\right)} \right\}. \tag{116}$$

Aus (5) und (6) ergibt sich

$$P_\nu(w) = J_\nu(w) \cos\left(w - \tfrac{1}{2}\nu\pi - \frac{\pi}{4}\right) + Y_\nu(w) \sin\left(w - \tfrac{1}{2}\nu\pi - \frac{\pi}{4}\right),$$

$$Q_\nu(w) = J_\nu(w) \sin\left(w - \tfrac{1}{2}\nu\pi - \frac{\pi}{4}\right) - Y_\nu(w) \cos\left(w - \tfrac{1}{2}\nu\pi - \frac{\pi}{4}\right),$$

also wegen (3) und (4)

$$P_\nu(w) = \tfrac{1}{2}\left(e^{-i\left(w - {}^1\!/_2\nu\pi - \frac{\pi}{4}\right)} H_\nu^{(1)}(w) + e^{i\left(w - {}^1\!/_2\nu\pi - \frac{\pi}{4}\right)} H_\nu^{(2)}(w)\right), \tag{117}$$

$$Q_\nu(w) = -\frac{1}{2i}\left(e^{-i\left(w - {}^1\!/_2\nu\pi - \frac{\pi}{4}\right)} H_\nu^{(1)}(w) - e^{i\left(w - {}^1\!/_2\nu\pi - \frac{\pi}{4}\right)} H_\nu^{(2)}(w)\right). \tag{118}$$

Ist

$$w \neq 0,\ -\pi < \arg w < \pi,\ \arg w^{1/2} = \tfrac{1}{2}\arg w,$$

$$\operatorname{Max}\left(-\frac{\pi}{2}, -\frac{\pi}{2} + \arg w\right) < \mu < \operatorname{Min}\left(\frac{\pi}{2}, \frac{\pi}{2} + \arg w\right),$$

dann folgt aus (67) und (116), mit $N = 2m$ angewendet (m ist ganz rational $> \frac{1}{2}|\mathfrak{R}(\nu)| - \frac{1}{4}$), und (117)

$$P_\nu(w) = \sqrt{\frac{2}{\pi}}\, \frac{1}{w^{1/2}} \left\{ \sum_{j=0}^{m-1} \frac{(-1)^j \prod\limits_{h=0}^{2j-1} (4\nu^2 - (2h+1)^2)}{(2j)!\,(8w)^{2j}} + \right. \\ \left. \frac{(-1)^m \cos\nu\pi}{\pi\sqrt{\pi}(2w)^{2m}} \int_0^{\infty e^{\frac{i\mu}{2}}} e^{-\zeta^4} \zeta^{4m}\, d\zeta \int_{-\infty}^{\infty} \frac{4w^2 \cosh^4 \frac{x}{2} \cosh \nu x\, dx}{\left(\cosh\frac{x}{2}\right)^{4m+1} \left(4w^2\cosh^4\frac{x}{2} + \zeta^4\right)} \right\}. \tag{119}$$

---

1) In Formel (32) liese man $H_{-\nu}^{(1)}(w e^{\pi i})$ statt $H_\nu^{(1)}(w e^{\pi i})$.

Aus (67) und (116), mit $N=2m+1$ angewendet (m ist ganz rational $>\frac{1}{2}|\Re(\nu)|-\frac{3}{4}$), und (118) geht hervor

$$Q_\nu(w)=\sqrt{\frac{2}{\pi}}\,\frac{1}{w^{1/2}}\left\{\begin{aligned}&\sum_{j=0}^{m-1}\frac{(-1)^{j+1}\prod\limits_{h=0}^{2j}\left(4\nu^2-(2h+1)^2\right)}{(2j+1)!\,(8w)^{2j+1}}+\\&\frac{(-1)^m\cos\nu\pi}{\pi\sqrt{\pi}\,(2w)^{2m+1}}\int\limits_0^{\infty e^{\frac{i\mu}{2}}}e^{-\zeta^2}\zeta^{4m+2}\,d\zeta\int\limits_{-\infty}^{\infty}\frac{4w^2\cosh^4\frac{x}{2}\cosh\nu x\,dx}{\left(\cosh\frac{x}{2}\right)^{4m+3}\left(4w^2\cosh^4\frac{x}{2}+\zeta^4\right)}\end{aligned}\right\}. \tag{120}$$

Der Beweis der Sätze 5 und 6 ist weiter dem Beweis von Satz 3 anolog. Im Beweis von Satz 5 braucht man nur (119) statt (77) und Hilfssatz 9 mit $N=2m$ statt Hilfssatz 11 anzuwenden; im Beweis von Satz 6 braucht man nur (120) statt (77) und Hilfssatz 9 mit $N=2m+1$ statt Hilfssatz 11 anzuwenden.

BERICHTIGUNG

zu der ersten Mitteilung (These Proceedings, Vol. **35** (1932), S. 656—667).

S. 659, Formel (16): *lies* $\frac{2N-1}{2N+3}$ *statt* $\frac{2N-1}{2N+1}$.

S. 661, Z. 1 v. u.: *lies* $\frac{\pi}{4}+\arg w$ *statt* $-\frac{\pi}{4}+\arg w$.

S. 662, Formel (27): *lies* $\arg\theta_3$ *statt* θ_3.

S. 666, Formel (32): *lies* $H^{(1)}_{-\nu}(w\,e^{\pi i})$ *statt* $H^{(1)}_{\nu}(w\,e^{\pi i})$.

Geology. — *The interference of meridional and transversal stress in the southeastern part of Borneo*. By G. L. SMIT SIBINGA. (Communicated by Prof. H. A. BROUWER.)

(Communicated at the meeting of October 29, 1932.)

Several geologists who worked in the tertiary strata of the southeastern part of Borneo have noticed the interference of two different main trends, caused by interfering compressional stress. I.e. a transversal main trend, parallel to the pretertiary nucleus of the island interferes with a meridional main trend, parallel to the eastcoast. Predominating meridional stress results in a transversal main trend, predominating transversal stress in a meridional one, whilst balanced meridional and transversal stresses result in an intermediate main trend. In detail, matters are much more complicated, as the individual strikes are always changing according to the local predominance of the interfering forces.

The writer during his two years' stay on Borneo has equally been struck over and again by this remarkable phenomenon. Though he is not able to give particulars about his observations and therefore cannot enter into details, some general outlines will be dealt with, which may contribute to a right understanding of the phenomenon of interference. Besides, some other noticeable characteristics of the tertiary geosyncline at the eastern border of the Sundaland, which are closely connected with it, will be discussed.

The Sunda-geosyncline.

The major stratigraphic features of the eastern portion of the marginal Sunda-geosyncline show a great principal conformity with those of its southern portion, next to several points of gradual difference. Both parts of the geosyncline are bounded on the one side by the relatively stable, tertiary Sundaland, on the other side by unstable, moving geanticlines: on the South by the Sunda-geanticline, on the East by the Western Celebes-geanticline.

The southern portion of the geosyncline, already wholly filled up by sedimentation is completely, or nearly completely folded. The eastern portion however did not yet reach this stage of evolution. Being but partly filled up with sediments, its central part (Makassar Straits) still finds itself in the geosynclinal stage of sedimentation. The eastern part of the geosynclinal basin is only affected by marginal folding at its continental and geanticlinal borders, thus representing a less developed stage of evolution compared with its southern part.

Considering the stratigraphical relations, we therefore have to compare the continental-side parts and the geanticlinal-side parts i.e. the northern part of the Java-Sumatra geosyncline with Eastern Borneo, its southern part with Western Celebes. Now it is a wellknown fact, still confirmed by recent investigations, that the continental-side younger tertiary deposits of Java and Eastern Borneo bear much resemblance, especially in the early stages of geosynclinal evolution. The continental-side lower Neogene of continental-litoral facies is characterised by much klastic material, originating from the tertiary Sundaland and limestones with intercalated coal measures. The central zone of marine facies mainly consists of marls, well developed on Java, partly developed in the coast region of Eastern Borneo and for the greater part still below sealevel. The tertiary deposits at the geanticlinal side on Java and Western Celebes are on the other hand characterised by their riches in volcanic material.

During the younger stages of geosynclinal evolution, in consequence of the narrowing, aggradation and folding of the geosyncline, the continental-litoral and the volcanic facies in the southern part of the geosyncline have been alternated and mixed, in the eastern part of the geosyncline however they remained still separated by a central submarine zone (Makassar Straits).

In detail of course these general features are complicated by many accessory circumstances, causing a secundary change of facies. In the southeastern coast region of Borneo e.g. pretertiary consolidated rocks formed islands and shallows within the geosynclinal basin like the Meratus mountainranges, the Kukusan- and Senakin-mountains, P. Laut and P. Sebuku. These islands furnished terrigeneous deposits, which effected a change of facies at short distance.

The tertiary tectonic plans of both parts of the geosyncline are totally different. Instead of the plan of branching trend lines, on the geanticlinal side on Java-Sumatra, all trends are parallel or nearly parallel to the geanticlinal axis on Western Celebes. On the continental side (Sundaland) in the southern part transversal stress acted, in the eastern part meridional stress interfered with transversal stress. in the northeastern part single transversal stress again acted.

The eastern border of the Sundaland.

Recent investigations [1]) on Borneo allow us to trace the eastern boundary of the tertiary Sundaland for the greater part, as indicated on the accompanying sketchmap. W. of the Meratus mountainrange the boundary between the relatively stable Sundaland and the geosynclinal basin is still uncertain. Young tertiary deposits have been found as far as Southwestern Borneo, but it is still uncertain whether all these neogene sediments bear a geosynclinal character. Most probably they are partly subcontinental shelfdeposits, partly real geosynclinal sediments. The tertiary Sundaland possessed, as it still does at present, submerged continental shelves as e.g. in the region of the Middle Mahakkamriver, where tertiary strata of small thickness, but slightly folded or in nearly horizontal position have been deposited upon a continental substratum. The typical geosynclinal tertiary deposits however on Borneo have great thickness (up to 10.000 m.) and usually are strongly folded. In the eastern part of the geosynclinal coast-region they form broad belts of folds ; in the southeastern part more stable obstacula like the Meratus mountainrange, etc., mentioned above, have prevented that.

The pretertiary massives.

Tertiary orogenesis did not affect these mountains in a high degree, which were already strongly folded and solidified in pretertiary times. But it is worthy of note how the pretertiary massives affected the surrounding plastic tertiary strata.

Generally speaking stiff nuclei within a plastic medium, exposed to compressional stress, will partly transmit the primary pressure, causing a secundary one, partly will carry a passive resistance. The rate of compression of the plastic medium round about the nucleus will prove its rate of activity or passivity.

---

[1]) Kwartaalverslagen v. d. Dienst v. d. Mijnbouw in Ned. Indië.

West of the Kukusanmassif e.g. the tertiary layers are lying flat and are but gently folded, East of it however they are intensively folded and turned-up against the massif (l.c.). This proves that the Kukusanmassif carried a passive resistance to a westward directed pressure (action), causing a "pressure-shadow" on its lee-side (W.-side). An eastward directed action would have caused a stronger folding at the W.-side than at the E.-side.

As a second instance, of great interest may be the part acted by the two northern offshoots of the Meratus mountainrange. East of the N.E.-offshoot (riverbasins of S. Telakai and S. Riko) the Tertiary is strongly folded in several anticlines with vertical layers. The tertiary Meliatbasin between both offshoots likewise is intensively folded, showing synclines, which are closed and inverted to the W. The tertiary strata however W. of the Meratus-range are less intensively folded in the Uja-Uwie-basin and but gently folded or not folded worth mentioning in the Barito-basin West of the N.W.-offshoot of the Meratus-range (l.c.).

This tectonic plan can only be explained in the same way by a westward directed action, partly transmitted by the N.E.-offshoot of the Meratus mountainrange and further braked by the passive resistance of the western one. An eastward directed action would have caused the strongest folding at the W.-side of the Meratus mountainrange and a decrease of action towards the East.

The tertiary tectonic plan.

Two belts of folds can be distinguished in the eastern coastregion, separated by the most northern offshoot of the Meratus-mountainrange and the dividing ridge between the Kedang Rantau (a left tributary of the Mahakkam) and Makassar Straits.

The first bundle of folds begins in the upper Barito-riverbasin and crosses the S. Tewe and K. Pahu (right tributaries of the Mahakkam). In the riverbasin of the K. Pahu W.S.W.-E.N.E. up to W.-E. trends interfere with S.-N. up to S.S.W.-N.N.E. trends [1]). The first mentioned direction of trend is also developed in the Tertiary of the Murung river, both main directions are developed in the upper Barito basin. In the Bungan-riverbasin the main trend is about W.-E., in the upper Bungan already bending to a S.W.-N.E. trend. Crossing the Mahakkam the transversal main trend is gradually changing into a meridional main trend due to the predominance of transversal stress and continuing northward up to the region E. of the Telen river. At the Sendowan river S.S.W.-N.N.E. trends have been observed, while the main trend of the ranges of hills in the Sanbentulung riverbasin likewise is S.S.W.-N.N.E. and S.-N. (l.c.).

---

[1]) H Witkamp. Een tocht naar den G. Ketam. De Sabentoeloeng, Sedoelang en Menamang, zijrivieren der Kedang Rantau. Tijdschr. Kon. Ned. Aardr. Gen. Dl. 45, 1928.

The second bundle of folds runs nearly parallel to the present shoreline from Cape Selatan up to the Sangkulirangbay. In this belt of folds transversal and meridional strikes interfere again and again, under predominance of a meridional main trend.

In the peninsula of Mangkalihat, north of the Sangkulirangbay interference of trend still can be observed. North of the peninsula however interfering trends are lacking and all anticlines have the same N.W.-S.E. main trend.

This remarkable transition from a complicated interfering folding plan to a normal, simple plan takes place on the peninsula of Mangkalihat, i.e. just opposite the sharp bendingpoint of the Western Celebes geanticline. N. of Mangkalihat the character of the geosyncline suddenly changes. Its geanticlinal border being bent off to the E. (Northern Celebes), only the continental half continues along the eastern border of the Sundaland.

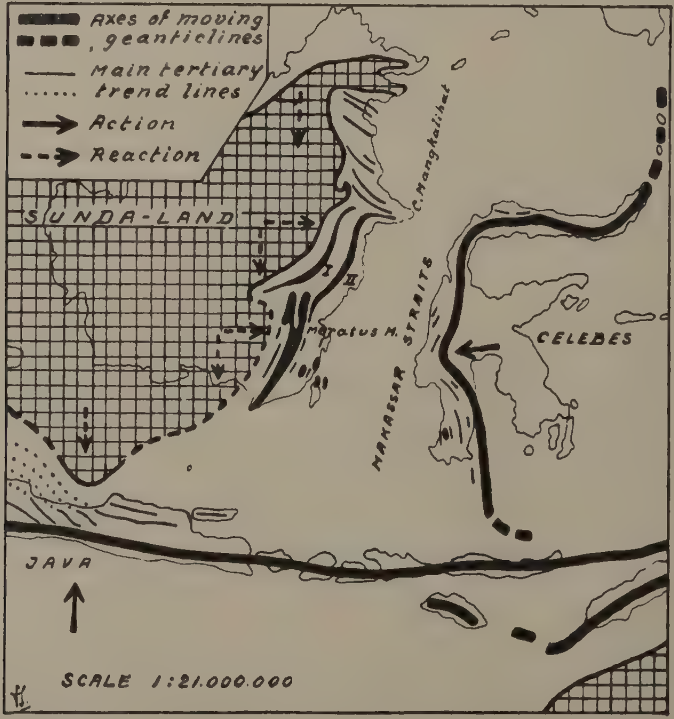

Thus interfering trends have a widespread occurrence in the southeastern part of Borneo and extend even outside the geosynclinal area into the continental shelfregions of central Borneo. However, they only have been observed in the geosyncline and adjoining shelves, which are situated *opposite the Western Celebes geanticline*. This fact is of the utmost importance.

It is obvious that the transversal and meridional trends have been caused by meridional and transversal stress. Where both trends interfere, both directions of stress interfere, where they do not interfere and but one trend exists, only the corresponding stress has acted. We already know, that the meridional stress originates with the moving Sunda-geanticline approaching the Sundaland from the South [1]). If we realise now that the meridional stress only interferes with the transversal stress opposite the Western Celebes-geanticline and that the intensity of folding on both sides of e.g. the Kukusan- and Meratus mountains only could be explained by a westward directed action, it cannot but be this moving geanticline which caused the transversal stress and corresponding meridional trends.

The transversal stress thus originates with striking analogy to the meridional stress with a moving geanticline, situated opposite the Sundaland and approaching it by folding the interjacent geosyncline.

Thus stating the origin of both directions of action a look on the accompanying sketchmap will elucidate several features of the tertiary folding plan. It is obvious now e.g.

a. Why on the geanticlinal side of the geosyncline (Western Celebes) all anticlines run parallel or nearly parallel to the geanticlinal axis, as only transverse stress was acting here.

b. Why transverse stress and consequently meridional trends still predominate in the coastregion opposite Celebes.

c. Why meridional stress predominates North of the Meratus mountainrange and transversal stress West of it as well as in the Meliatbasin between the two northern offshoots of the Meratus range, originating with the approaching geanticlines and transmitted by this already solidified pretertiary range.

d. In short why interference of stress only occurs within their mutual sphere of action.

CONCLUSIONS.

1. Opposite the southern and eastern border of the tertiary Sundaland moving geanticlines are situated, which approaching the Sundaland folded the interlying tertiary geosyncline.

2. The geosynclinal part at the southern border of the Sundaland being already wholly filled up by sedimentation is nearly entirely folded. The geosynclinal part at the eastern border of the Sundaland being but partly filled up by sedimentation, its central portion (Makassar Straits) finding

---

[1]) G. L. SMIT SIBINGA. The tertiary virgations on Java and Sumatra, their relation and origin. These Proceedings XXXV, 1932.

itself still in the geosynclinal stage of sedimentation is only affected by marginal folding, thus representing a less developed stage of evolution compared with its southern part.

3. The tertiary main trend lines at the geanticlinal sides of the geosyncline are all running parallel or nearly parallel to the geanticlinal axes, the phenomenon of virgation in the southern part being a secundary one, caused by the sharp bending of the geanticlinal Sunda-axis (l.c.).

4. The tertiary main trend lines at the continental sides of the geosyncline show where they are lying within the mutual sphere of action of both approaching geanticlines, the interference of transversal and meridional trends, caused by two interfering directions of stress, originating with the approaching geanticlines.

5. During the tertiary process of folding the Meratus mountainranges, the Kukusan- and Senakin-mountains, P. Laut and P. Sebuku acted as pretertiary consolidated nuclei within a plastic medium and are to be considered as tectonical analoga of e.g. the Tigapuluh- and Duablas-mountains in the southern part of the geosyncline.

Geology. — *Über Fossilien aus dem Altmiozän von Rembang (Nord Java).* Von U. HAANSTRA und E. SPIKER. (Communicated by Prof. L. RUTTEN).

(Communicated at the meeting of October 29, 1932.)

Das Geologisch-Mineralogische Institut in Utrecht besitzt eine Sammlung neogener Mollusken, von Dr. J. TH. ERB geschenkt und von ihm gesammelt während geologischen Aufnahmen in der Residenz Rembang auf Java. Diese Fossilien stammen von der Nordseite des Lodan-Sattels und zwar vom Oberlauf des linken Seitenastes eines Flüsschens, das die Nordflanke des Lodanhügels entwässert und auf seinem Wege zum Meere das Dorf Lodan durchfliesst. Die Fossil-führenden Schichten bestehen aus grauen und braungrauen Tonen, die mit *Lepidocyclinen*-Kalksteinen, Mergeln und Quarzsanden wechsellagern. Sie gehören den „Ngrajong-Schichten" an (Unt. Miozän, siehe W. LEUPOLD u. I. M. VAN DER VLERK, Tabelle zu „Tertiary" in: Feestbundel Prof. Dr. K. MARTIN 1931, p. 648). Die folgenden, schon bekannten Arten konnten bestimmt werden

Terebra jenkinsi Mart. *
Terebra butaciana Mart.
Conus hardi Mart.
Conus ?pamotanensis Mart.
Drillia aff. molengraaffi Mart.
Pleurotoma carinata Gray.
Ancilla rembangensis Mart.
Olivancillaria subulata Lam. *

Marginella quinqueplicata Lam. *prior minor* Mart.
Mitra rembangensis Mart.
Mitra granatinaeformis Mart.
Mitra sedanensis Mart.
Turricula gembacana Mart.
Columbella njalindungensis Mart.
Persona djunggranganensis Mart.
Ranella pamotanensis Mart.
Ranella bitubercularis Lam.
Cypraea sondeiana Mart.
Cypraea (Trivia) smithi Mart.
Rostellaria verbeeki Mart.
Strombus sedanensis Mart.
Tenagodes obtusiformis Mart.
Vermetus javanus Mart.
Turritella subulata prior sedanensis Mart.
Turritella ?javana Mart.
Melania woodwardi Mart. *
Natica ?pellis-tigrina Chemn. *
Natica vitellus Linn.
Natica powisiana Recluz.
Niso aff. denticulata Mart. *
Turbo pamotanensis Mart.
Amussium ?hulshofi Mart.
Arca hulshofi Mart.
Arca debilis Mart.
Pectunculus (Axinaea) angsanana Mart.
Chama aff. ovalis Mart.
Dosinia longilunata Reeve. *
Meretrix jonkeri Mart.
?Meretrix ?problematica Mart.
Venus listeri Gray.
Corbula socialis Mart.

In der obigen Liste sind die, für das Alt-Miozän neuen Formen mit einem Sternchen angedeutet worden.

Die nachfolgenden neuen Arten wurden gefunden:

Terebra erbi n. sp.
Conus erbi n. sp.
Pleurotoma (? Drillia) sedanensis n. sp.
Solarium martini n. sp.
Nucula sedanensis n. sp.
Chama sedanensis n.sp.

Neben den genannten, spezifisch bestimmbaren Arten wurden noch gefunden nicht weiter bestimmbare Vertreter der Genera *Terebra, Conus, Voluta, Rimella* (2 spec.), *Cerithium, Niso, Spondylus, ?Avicula, Arca, Cardium, ?Dosinia* und *Tellina.*

Von den 47 Arten sind 8 oder etwa 17 % rezent, welche Zahl mit der von MARTIN für die „Rembangschichten" gefundenen gut übereinstimmt.

Wir haben unsere Objekte verglichen mit den Originalen der Martinschen Sammlungen in Leiden und mit rezenten Mollusken im Leidener naturhistorischen Reichsmuseum. Eine Angabe der benutzten Literatur findet man am Ende dieses Aufsatzes.

Die Fossilien geben zu den folgenden Bemerkungen Anlass.

Terebra erbi n. sp. (Taf. fig. 1, 2, 3, 4).

Ein einziges spitzes, turmförmiges Gehäuse von 15 mm. Länge und 4 mm. grösstem Durchmesser. Die Hinterseite ist weniger spitz als die Vorderseite, wodurch die Profillinie des Ganzen etwas gebogen ist.

Die Embryonalwindungen, welche glatt und etwas kugelförmig sind, umfassen 1½ Umgang; dann folgen 8½ Mittelwindungen und die Schlusswinding. Anfangs ist nur eine Querskulptur zu bemerken, später tritt auch die Spiralskulptur auf. In der Durchkreuzung der beiden Skulpturen entstehen Knötchen. Auf den jüngeren Mittelwindungen, wo die Skulptur vollkommen ausgebildet ist, ist sie in folgender Weise entwickelt: die Hinterseite der Windungen wird eingenommen von einem breiten Band, welches von der Vorderseite durch eine deutliche falsche Naht abgetrennt ist. Dieses Band trägt eine schmale Reihe scharf ausgeprägte Knötchen. Die Vorderseite der Windingen ist bezetzt mit drei scharfen Spiralleisten, welche anfangs breiter, später gleich breit bis schmäler sind wie ihre Zwischenräume. Auf der jüngsten Mittelwindung schaltet sich zwischen der vorderen und der nach hinten folgenden Spiralleiste eine vierte, schwach entwickelte Leiste ein. Die Querskulptur ist auf dem abgeschnürten Band konkav nach hinten und auf dem vorderen Abschnitt gerade bis schwach konkav nach vorne. Die Schlusswindung zählt ausser den obengenannten Spiralleisten nach vorne deren noch vier, wóvon die vordere schwach ausgebildet ist.

Innenlippe kaum anwesend. Die Spindel ist gedreht und trägt, ausser dem umgeschlagenen Spindelrand, nach innen noch eine scharfe Falte. Die Mundöffnung ist nahezu oval und endet in einem kurzen Ausguss. Die Form gleicht etwas der *Terebra tjilonganensis* Mart. (K. MARTIN. Foss. v. Java, p. 283. T. XLII. fig. 679.). Sie ist jedoch kleiner; die Anzahl der Falten auf der Spindel stimmt nicht und auch die Skulptur ist bei den beiden Formen nicht ganz gleich.

Conus erbi n. sp. (Taf. fig. 5, 6, 7).

Eine einzige doppelt-kegelförmige Schale, deren Stirnabschnitt abgebrochen ist, wodurch die Länge sich nicht genau feststellen lässt. Möglich hatte das Exemplar eine Länge von 35—40 mm. Der grösste Durchmesser ist 13 mm; die Höhe des Gewindes, dessen Winkel etwa 70° misst, ist 8 mm. Die Anzahl der Embryonalwindungen lässt sich nicht gut bestimmen, da der Protokonch ein wenig verletzt ist. Wahrscheinlich gab es deren 2½—3. Auf dem Embryonalabschnitt folgen 8 Mittelwindungen und die Schlusswindung. Anfangs sind die Mittelwindungen auf ihrem Spiralwinkel stark gekörnelt; bei jüngeren Windungen hört die Körnelung auf; statt dieser aber bleibt ein seilförmiges Band auf dem Spiralwinkel. Dieses Band ist Ursache dass die Profillinie des Gewindes, welche im Übrigen schwach konkav ist, etwas treppenartig erscheint, Die Spiralskulptur besteht auf den jüngeren Windungen, wo sie vollkommen ist, aus vier Bändern. Das zweite Band, von hinten gezählt, ist etwas breiter, das vordere etwas schmäler als die zwei übrigen. Auf der Schlusswindung befindet sich vor den vier Hauptbändern noch ein sehr schmales Band. Auf dieser Spiralskulptur folgt am Spiralwinkel noch das obenerwähnte, breitere, seilförmige Band. Die Anwachsstreifung ist konkav nach vorne gekrümmt und setzt sich auf dem, vor dem Spiralwinkel gelegenen. Teil der Schlusswindung stark S-förmig fort. Dieser vordere Abschnitt der Schlusswindung ist glatt, abgesehen von der, nicht stark ausgeprägten, Anwachsstreifung und von einigen, weitauseinander stehenden, mehr oder weniger zarten, Spiralfurchen auf dem vorderen Teil des Exemplares, welche sich auf dem Stirnabschnitt wahrscheinlich in ähnlicher Weise fortgesetzt haben. Ihre Profillinie ist nahezu gerade bis schwach

U. HAANSTRA und E. SPIKER: ÜBER FOSSILIEN AUS DEM ALTMIOZÄN VON REMBANG (NORD JAVA).

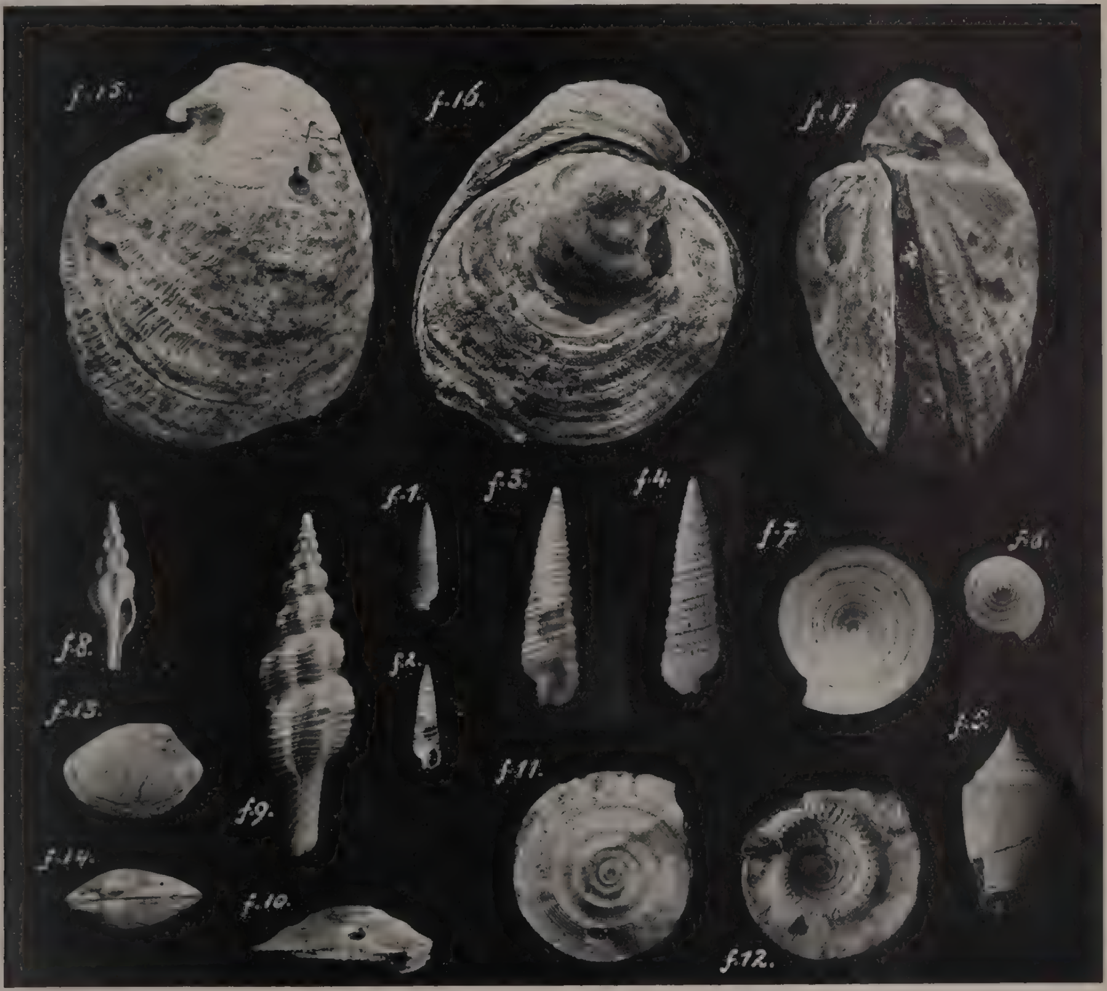

FIGUREN-ERKLÄRUNG.

Fig. 1, 2, 3, 4. *Terebra erbi* n.s. 1, 2 Nat. Gr., 3, 4 ×2.
Fig. 5, 6, 7. *Conus erbi* n.s. 5, 6 Nat. Gr., 7 ungefähr ×2.
Fig. 8, 9. *Pleurotoma (?Drillia) sedanensis* n.s. 8 Nat. Gr., 9 ×2.
Fig. 10, 11, 12. *Solarium martini* n.s. Nat. Gr.
Fig. 13, 14. *Nucula sedanensis* n.s. Nat. Gr.
Fig. 15, 16, 17. *Chama sedanensis* n.s. Nat. Gr.

konvex. Es ist möglich, dass das Exemplar am (abgebrochenen) Ende etwas eingeschnürt war. Der jüngere Teil der Schlusswindung ist nicht erhalten, sodass von der Form der Mundöffnung nichts zu sagen ist.

Diese Art stimmt mit keinen Indischen *Conus* überein. Habituell gleicht sie einigermaassen *C. sinensis* Sow. prior. (K. MARTIN, Foss. v. Java, p. 13, T. I. fig. 13—15; P. TESCH, Pal. v. Timor, Lief. V. p. 18. T. LXXIII, fig. 9—11.), von dem sie u.m. aber verschieden ist durch relativ geringere Höhe des Gewindes und durch das Fehlen der Spiralskulptur auf dem, vor dem Spiralwinkel gelegenen Teil der Schlusswindung. *Conus protofusus* Noetling (Mem. Geol. Surv. India. New. Ser. I. p. 365. Pl. XXIII. fig. 25—26.) sieht auch ähnlich aus, aber bei genauer Betrachtung sind doch viele Unterschiede zu erkennen. *C. protofusus* hat u.m. einen spitzeren Winkel des Gewindes, während die Skulptur auf den Umgängen und auf dem Stirnabschnitt ganz verschieden ist.

Conus ?pamotanensis Mart.

K. MARTIN. Foss. v. Java, p. 288. T. XLII. f. 689.
K. MARTIN. Alt-Mioc. Fauna d. West Progogeb. p. 226.

Es liegt nur ein Exemplar vor; der vordere Abschnitt ist nicht erhalten. Im Allgemeinen stimmt es mit dem Original gut überein. Der ältere Teil des Gewindes ist aber bei unserem Exemplar mehr ausgezogen und seine rekonstruirte Länge ist nur etwa 18—20 mm.; möglich ist es eine Jugendform.

Drillia aff. molengraaffi Mart.

K. MARTIN. Alt-mioc. Fauna des West Progogeb. p. 230. T. I. fig. 14.
K. MARTIN. Leidsche Geol. Med. III. 2. p. 121.

Ein Exemplar, das im Allgemeinen mit *Drillia molengraaffi* gut übereinstimmt, aber etwas schlankere Form besitzt, und grössere Dimension bei mehr Windungen hat. Die Länge ist mehr als 28 mm.; die Anzahl Mittelwindungen grösser als 9.

Pleurotoma (?Drillia) sedanensis n. sp. (Taf. fig. 8, 9).

Ein eindiges sehr schlankes Gehäuse. Die unvollständig erhaltene Mündung ist kürzer als die halbe Schalenlänge. Von den embryonalen Windungen ist nur eine erhalten. Auf dieser folgen 9 Windungen, welche alle stark konvex und mit breiten Querrippen, deren Zahl pro Windung 7 ist, versehen sind. An der hinteren Sutur befindet sich ein schmales Band, das infolge der starken Querrippung wellenartig verläuft. Auf dieses Band folgt eine Depression mit Anwachslinien, welche hier nach hinten gekrümmt sind. und mit schwachen, bis zu 5 zählenden Längsleisten. An der ältesten Mittelwindung ist auf dem vorderen Abschnitt anfangs wenig von Spiralstreifung zu bemerken. An der zweiten Mittelwindung fängt sie an mit drei primären Spiralen, deren Zahl auf den jüngeren Windungen bis zu 7 anwachsen kann. Abgesehen von den ältesten Windungen schiebt sich schon bald zwischen je zwei primären Spiralen eine sekundäre und auf der letzten Mittelwindung und der Schlusswindung zwischen den primären und sekundären tertiäre Spiralen. Die stark zusammengeschnürte Stirn der Schlusswindung ist von vielen Spiralen versehen.

Diese Art ist verwandt mit *Drillia tjemoroënsis* Mart. (K. MARTIN. Foss. v. Java. p. 295. T. XLIII. fig. 705.), aber durch stärkere Wölbung der Windungen und mehr Skulpturdifferentiation verschieden.

Marginella quinqueplicata Lam. *prior minor* Mart.

K. MARTIN. Tertiärschichten. p. 24. T. V. fig. 2.
K. MARTIN. Samml. Leiden. (1). III. p. 94.
K. MARTIN. Foss. v. Java. p. 70. T. X. fig. 156—160.
K. MARTIN. Dienst. Mijnbouw. Ned. Ind. Wet. Med. 4. 1926. p. 13.

Die vorhandenen Schalen stimmen genau überein mit einem Teil der Leidener Exemplaren, nämlich mit jenen Formen, deren Gewinde nicht eingesunken, sondern etwas über der Schlusswindung erhoben ist. Sie ähneln den Individuen, welche bei Tjikeusik in Bantam auf Java gefunden sind (Foss. v. Java. T. X. fig. 160 und 160*a*.).

Drei vollständige und drei unvollständige Exemplare, nebst einigen Bruchstücken.

Mitra granatinaeformis Mart.

K. MARTIN. Samml. Leiden (I), III. p. 86. T. V. fig. 87.

Von den zwei unvollständigen Exemplaren zeigt das eine nur vier Mittelwindungen und Schlusswindung während das zweite neun Mittelwindungen hat. Das von MARTIN beschriebene Exemplar von Ngembak auf Java ist kleiner und hat nur sechs Mittelwindungen. Die Skulptur und Form ist aber so genau übereinstimmend, dass unsere Fossilien sich bestimmen lassen als ältere Individuen. Die Skulptur, welche anfangs aus fünf Spiralleisten besteht, zwischen denen schmale Furchen mit Querleisten, ändert sich auf den jüngeren Mittelwindungen, wo die Spiralleisten breiter werden, getrennt durch schwache Furchen ohne Querskulptur, um auf der Schlusswindung ganz zu verschwinden. Auf der vorletzten Mittelwindung geht bei einer der Exemplare die erste Spiralleiste über in ein abgeschnürtes Band, welches von einer feinen Furche in zwei geteilt wird. Die Spindel trägt bei dem beinah vollständigen Individuum drei Falten, während das zerbrochene Exemplar deutlich vier hat.

Columbella njalindungensis Mart.

K. MARTIN. Foss. v. Java. p. 464. T. LIX. fig. 47 u. 48.
K. MARTIN. Leidsche Geol. Med. Deel. III. Afl. 2. p. 123.

Die drei vorliegenden Exemplare weichen von den Originalen unbedeutend ab durch das Vorkommen von äusserst feinen Spiralfurchen in wechselnder Anzahl auf dem hinteren Teil der jüngsten Hälfte der Schlusswindung. Unsere Exemplare kommen *Columbella simplex* Mart. (Foss. v. Java. T. XVIII. fig. 276.) auch sehr nahe. Diese ist aber verschieden durch das Vorkommen von Anwachsstreifen auf den Mittelwindungen und durch kleinere Mündung.

Ranella bitubercularis Lam.

R. biturbercularis Lam: H. ICKE u. K. MARTIN. Samml. Leiden. (1). VIII. p. 237.
K. MARTIN. Foss. v. Java. p. 149. T. XXIII. fig. 349—351.
P. TESCH. Pal. v. Timor. Lief. VIII. p. 43. T. CXXIX. fig. 155.
E. VREDENBURG. Mem. Geol. Surv. India. 50. p. 255.
R. raninoides. Mart: K. MARTIN. Samml. Leiden. (1). I. p. 203. T. IX. fig. 6.

Das einzige Exemplar ist einem Teil der in Leiden anwesenden Formen ganz ähnlich. Es gleicht denjenigen Formen, bei denen auf dem jüngeren Abschnitt des Gewindes zwischen zwei Varices, zwei knotenartige Querrippen schärfer ausgeprägt sind als die anderen.

Cypraea (*Trivia*) *smithi* Mart.

K. MARTIN. Samml. Leiden. (1). III. p. 141. T. VIII. fig. 141.
F. NOETLING. Mem. Geol. Surv. India. 27. part I. p. 26. pl. V. fig. 13.
F. NOETLING. Mem. Geol. Surv. India. N. S. vol. I. p. 293. pl. XIX. fig. 13.

Das kleine Exemplar, dessen Abmessungen 4½ × 6 mm. sind, hat nur eine schwache Andeutung von der feinen Querstreifung, welche in den Abbildungen bei MARTIN deutlich sichtbar ist. Es muss aber bemerkt werden, dass auch an MARTIN's Originalexemplar diese Querstreifung viel weniger deutlich ist als auf der Abbildung. Die Anzahl der Rippen ist etwas schwankend; sie ist etwas verschieden bei MARTIN's Original, bei dem von NOETLING abgebildeten und bei unserem Exemplar.

Rostellaria verbeeki Mart.

K. MARTIN. Foss. v. Java. p. 189. T. XXX. fig. 438—440.

Die zwei Bruchstücke, welche uns vorliegen haben keine Embryonalwindungen, während die Schlusswindung verletzt ist.

Die Spiralskulptur vorne auf der Schlusswinding ist die gleiche wie bei *R. verbeeki* Mart.; die anwesenden Umgänge sind aber flächer.

Die letzte Mittelwindung hat bei dem einen Exemplar eine Andeutung, dass die Rinne, welche von der Mundöffnung nach hinten läuft, weniger rückwärts gekrümmt ist als bei *R. verbeeki* und fast bis an die Sutur zwischen letzter und vorletzter Mittelwindung reicht. Das zweite Bruchstück zeigt nichts von einer Rinne.

Die Objekte zeigen auch Übereinstimmung mit *Rostellaria delicatula* Nevil. von Timor (P. TESCH. Pal. v. Timor. Lief. VIII. p. 50. T. CXXX. fig. 169.), aber sind durch das Fehlen von Spiralfurchen in der Nähe der hinteren Sutur von dieser verschieden.

Turritella subulata Mart. *prior sedanensis* Mart.

T. subulata Mart.: K. MARTIN. Samml. Leiden. (1). III. p. 173. T. IX. fig. 168.
K. MARTIN. Alt-Mioc. Fauna des West Propogeb. p. 255. T. III. fig. 71.
T. sedanensis Mart.: K. MARTIN. Foss. v. Java. p. 234. T. XXXV. fig. 554. u. 554*a*.

Drei unvollständige, etwas abgeriebene Exemplare, welche der Form *T. sedanensis* Mart., die früher von MARTIN von *T. subulata* geschieden war, sehr nahe stehen. Sie sind am Vorderende der Windungen auch etwas aufgewölbt und die Anzahl der Spirallinien ist dieselbe. Einige kleine Unterschiede lassen sich feststellen, welche jedoch nicht Ursache einer Abtrennung sein dürfen. Bei einem der grösseren Exemplare sind die zwei vorderen Spirallinien nicht, wie bei *T. subulata* mehr zu einander genähert als die übrigen, sondern etwas weiter von einander entfernt. Das zweite grosse Exemplar hat obengenannte Abweichung nicht, aber hier ist der Unterschied, dass zwischen je zwei Spirallinien sich eine sekundäre, äusserst schwache Linie einschaltet, im Gegensatz mit dem Exemplar, in „Foss v. Java." beschrieben, welches nur zwischen den hinteren eine zweite schwächere Spirallinie aufweist. Das dritte, kleine Exemplar lässt Vergleichung zu, speziell mit denjenigen Formen, die beschrieben sind in „Fauna des West Progogebirges". Es finden sich hier auch einige sekundäre Spiralen auf der Hinterseite der Windung, welche mehr hervortreten und fast ebenso ausgesprochen sind wie die Hauptspiralen. Ein Unterschied ist, dass die Querskulptur, wo sie die Spiralskulptur durchkreuzt, hierauf eine sehr schwache Körnelung entstehen lässt.

Melania woodwardi Mart.

M. woodwardi Mart.: K. MARTIN. Foss. v. Java. p. 239. T. XXXVI. fig. 567—570.
M. aff. woodwardi Mart.: P. TESCH. Pal. v. Timor. Lief. VIII. p. 60. T. CXXXI. fig. 186.

4 Exemplare, von denen zwei weniger gut erhalten. Die Skulptur auf der Stirn besteht aus einer Anzahl sehr feiner Spiralen. Bei den Originalen kommen hier nur drei breite Bänder vor. Die Form und Skulptur der Originale ist aber sehr variabel und unsere Exemplare werden am besten zu dieser Art gebracht.

Solarium martini n. sp. (Taf. fig. 10, 11, 12).

Eine Schale, aus sechs Umgängen bestehend, von 26 mm. Durchmesser, mit einem Gehäusewinkel von etwa 125°. Der Embryonalabschnitt ist nicht anwesend, ebenso wenig wie der letzte ¼ Teil der Schlusswindung, aber im Übrigen ist das Exemplar ziemlich gut erhalten. Die Windungen sind ausgehöhlt, sodass die Naht gelegen ist auf einer Erhöhung zwischen je zwei Aushöhlungen. Sie tragen 10 Haupt-spiralbänder, welche nicht sehr scharf ausgeprägt sind. Die fünf hinteren Bänder, wovon das hintere sogleich an der Naht grenzt, sind etwas breiter als die vorderen und mit Knötchen besetzt. Zwischen dem vierten und fünften Band, von hinten gezählt, schaltet sich eine zarte, sekundäre Linie ein, während auf der Schlusswindung zwischen dem dritten und vierten Band eine noch schwächere Linie zu bemerken ist. Die Körnelung auf den Bändern verschwindet nach vorne fast ganz, ausser dem letzten (10en) Band, das etwas breiter und wieder mit Körnchen besetzt ist. Es bildet die Hintergrenze der Naht. Zwischen je zwei der vorderen 5 Bändern befindet sich ein sekundäres, wovon dasjenige zwischen dem fünften und sechsten Band fast so stark entwickelt ist wie die Hauptspiralbänder. Auf der Schlusswindung ist noch eine sehr zarte „tertiäre" Skulptur zu bemerken (nur u. d. L. zu sehen). Die Anwachsstreifung, insofern sichtbar, ist etwas S-förmig gebogen.

Der tiefe, weite Nabel wird von einem Kiel umschlossen, welcher besetzt ist mit zwei Reihen länglicher, radiärstehender Zähnchen, die von einer Spiralfurche getrennt sind. Die Unterseite der Schlusswindung ist auch wieder ausgehöhlt. Dem Kiel schliessen sich nach aussen eine grosse Anzahl dichtgedrängter, schmaler, nicht scharf ausgeprägter Spiralleisten an. Die zwei inneren sind etwas breiter als die übrigen, während nach der Aussenkante die Linien auch, aber allmählig, breiter werden. Es ist hier wieder zu unterscheiden zwischen primären und sekundären Linien.

Diese Art zeigt einige Ähnlichkeit mit *Solarium incisum* Mart. aus dem Ober-Eocän von Nanggulan, welche in „Dienst Mijnbouw. Ned. Ind. Wet. Med. 18. 1931 (p. 42. T. VI. fig. 6. u. 6a.)" beschrieben ist. Sie besitzt ebenfalls die ausgehöhlten Windungen. Der Gehäusewinkel ist aber weniger spitz und auch die Skulptur ist anders.

Niso aff. denticulata Mart.

K. MARTIN. Die Fauna des Obereocäns von Nanggulan. p. 175. T. VI. fig. 168 u. 169.

Die zwei 1 cm. langen, nicht ganz erhaltenen Schalen stimmen mit einer, zu Niso denticulata Mart. gehörenden Schale im Leidener Museum ziemlich gut überein. Obwohl an einer der Schalen der älteste Teil fast ganz erhalten ist, ist von einem Protoconch nichts zu erkennen.

Die Skulptur des Nabels ist weniger stark als in der Abbild. 168*b* T. VI. Ausserdem fehlen unseren Fossilien die zarten Anwachsstreifen, die bei Niso denticulata Mart. vorkommen; man sieht nur die durch die frühere Lage der Aussenlippe entstandenen Furchen.

Das Vorkommen von einer, mit N. denticulata eng verwandten Art ist bemerkenswert, weil N. denticulata nur aus dem Eozän von Java bekannt ist.

Niso spec.

Ein 12 mm. langes Exemplar, nicht ganz erhalten. Die Windungen sind stärker gewölbt als bei *Niso denticulata* Mart. und die Schlusswindung ist ganz abgerundet. Die Furchen von früheren Lagen der Aussenlippen auf den Windungen treten deutlich hervor; sonst ist die Oberfläche glänzend polirt.

Im Allgemeinen haben wir die nicht-spezifisch bestimmbaren Fossilien bei unseren Beschreibungen nicht weiter berücksichtigt. Für *Niso* sp. machen wir eine Ausnahme, weil nur eine einzige Art aus dem indischen Tertiär bekannt ist.

Turbo pamotanensis Mart.

K. MARTIN. Foss. v. Java. p. 275. T. XLI. fig. 665.
K. MARTIN. Wet. Med. Dienst v. d. Mijnb. in Ned. Indië. N⁰. 10. 1928. p. 14.

Diese *Turbo* stimmt am meisten überein mit *Turbo pamotanensis* Mart. Die Skulptur ist aber etwas verschieden. MARTIN hat schon bemerkt, dass ein Exemplar von *T. pamotanensis* aus dem Neogen von Atjeh stärker gekörnelt ist als das altmiozäne

Original von Java. Unser Exemplar hat statt 2 sekundärer Spiralleisten 3; es schiebt sich nämlich zwischen der letzten gekörnelten Spiral und der ersten ungekörnelten Spiral noch eine feine Leiste ein. Die Furchen zwischen den ungekörnelten Spiralen sind relativ breiter als an den Leidener Exemplaren. Nach vorne folgen auf 5 ungekörnelte Spiralen wieder eine schwache gekörnelte Spiral, dann eine breitere, fast ungekörnelte und von dieser, bis an den Anfang der Stirne noch 5 Spiralen, versehen mit quadratischen bis rundlichen Körnern. Die Spiralentrennenden Furchen sind breiter als an den Leidener Exemplaren.

Pectunculus (*Axinaea*) *angsanana* Mart.

K. MARTIN. Foss. v. Java. p. 484. T. LXI. fig. 104.

Es ist eine Anzahl Schalen vorhanden, die mit *P. angsanana* gut übereinstimmen. Nur treten an unseren Exemplaren eine oder zwei Radiärrippen mehr auf als das Maximum, von *A. angsanana* angegeben, beträgt.

13 Schalenhälften und einige Bruchstücke.

Nucula sedanensis n. sp. (Taf. fig. 13, 14).

Aus Indien sind wenig *Nucula*-Arten bekannt, und von Java hat MARTIN nur zwei Spezies beschrieben. Die acht uns vorliegenden Exemplare haben verschiedene Grösse; die Länge wechselt von 16 bis 23 mm., die Höhe von 12 bis 16 mm., und die Dicke von 6 bis 9 mm. Die Fossilien sind alle etwas abgeblättert, aber lassen noch gut sehen dass sie keine Skulptur haben. Nur eine seichte Anwachsstreifung ist anwesend. Das Vorderende ist etwas schnabelförmig ausgezogen und der gerundete Bauchrand hat in der Nähe dieser Verlängerung eine seichte Einbuchtung. Die Lunula ist etwas eingesenkt, während sich auf dem ziemlich stark gebogenen Rücken eine undeutliche Area befindet.

Länge abgeb. Exemplar 20 mm., Höhe 14 mm., Dicke 8½ mm.

Durch die schnabelförmige Verlängerung an der Vorderseite und den gänzlichen Mangel an Skulptur ist diese neue Art genügend gekennzeichnet.

Chama sedanensis n. sp. (Taf. fig. 15, 16, 17).

Ein vollständiges Exemplar. Das Gehäuse ist ungefähr eiförmig. Der Wirbel der linken Klappe ist stark nach vorne gerichtet, ein wenig eingerollt und die Wirbelspitze ist in Folge der starken Krümmung nach hinten gerichtet. Die Ligamentgrube, welche hinten ziemlich breit ist, wird nach dem Wirbel zu schmäler und reicht bis an die Wirbelkrümmung. An der rechten Klappe ist sie bis an die Wirbelspitze zu verfolgen. Der Leistenförmige Zahn der linken Klappe, welcher parallel der Ligamentgrube verläuft, ist etwas abgebrochen. Der zweite Zahn ist wenig dick und demnach die mit diesem übereinstimmende Grube der rechten Klappe wenig tief. Die Oberfläche der linken Schale hat ausser konzentrischen Runzeln auch Radialstreifung, welche letztere auf der rechten Klappe weniger deutlich ist.

Länge des Exemplares 4½ cm., Höhe 5½ cm., und Dicke 3½ cm.

Wahrscheinlich gehört ein Fragment einer linken Klappe mit besser erhaltenem Schloss und deutlichem vorderen Muskeleindruck zu derselben Art.

LITERATUR.

Für die benutzte Literatur können wir im Allgemeinen auf die Literaturliste in: „I. M. VAN DER VLERK, Caenozoic Amphineura, Gastropoda, Lamellibranchiata,

Scaphopoda" in „Leidsche Geol. Meded. V. 1931 (Feestbundel K. MARTIN)", p. 292 ff. hinweisen. Ausserdem wurden benutzt:

G. DE P. COTTER. The Lamellibranchiata of the Eocene of Burma. Mem. Geol. Surv. India. Pal. Indica. N. S. Vol. VII, 2, 1923.
——— The Pegu-Eocene Succession in the Minbu District near Ngape. Records Geol. Survey of India. Vol. XLI. part 4. 1912.
P. FISCHER. Manuel de Conchyliologie, etc. 1887.
E. J. KOPERBERG. Jungtertiäre und Quartäre Mollusken von Timor. Jaarboek Mijnwezen 1930. Verh. 1e Ged.
F. NOETLING. On some marine fossils from the Miocene of Upper-Burma. Mem. Geol. Survey of India. Vol. XXVII, part 1.
——— Fauna of the Miocene Beds of Burma. Mem. Geol. Survey of India. Pal. Indica. N. S. Vol. 1. 1901.
E. VREDENBURG. Description of Mollusca from the posteocene tertiary formation of North-Western India. Mem. Geol. Survey of India. Vol. 50. part 1.
——— Diagnoses of fossil Terebridae. Rec. Geol. Survey of India. Vol. 51. part 4.
——— Classification of the recent and fossil Cypraeidae. Rec. Geol. Survey of India. Vol. 51. part. 2.
——— Noetling's Tertiary Fauna of Burma. Records Geol. Survey of India. Vol. 51. part 3.
——— Marine Fossils of the Garo Hills. Records Geol. Survey of India. Vol. 51. part 3.

Botany. — *On the Mechanism of the Transport of Organic Materials in Plants.* By T. H. VAN DEN HONERT ¹). (Communicated by Prof. F. A. F. C. WENT).

(Communicated at the meeting of October 29, 1932.)

In recent years our knowledge about the transport of organic substances in plants has made considerable progress. The valuable researches of MASON and MASKELL (9) not only proved conclusively, that in the cotton plant the transport of sugars takes place in the bark, probably through the sieve-tubes, but also that the direction and velocity of the movement is determined by a difference in concentration. In this respect, the rules governing this process are similar to the laws of diffusion; both are determined by forces which tend to equalize a concentration-difference. However, the rate of transport of sucrose was found to be 20600 to 38450 times greater than could be expected in the case of a transport by diffusion through the sieve-tubes. MASON and MASKELL state this as follows:

---

¹) By correspondence about the first results of my experiments with Prof. Dr. F. A. F. C. WENT I recently learned from him that, independently, Prof. Dr. F. KÖGL had come to a conception on the transport of his "auxine" (F. KÖGL and A. J. HAAGEN SMIT, these Proceedings Vol. XXXIV N⁰. 10, 1931, p. 1411), similar to the ideas developed in this paper.

"The very slow rate of diffusion of sugar molecules in water is of course in a large manner due to the tremendous resistance offered by the water molecules to their movement ...... The sugars appear to move in the sieve-tube under unit gradient at about the same rate as they would diffuse in air if they existed in the gaseous state. The question, therefore, arises whether any mechanism in the sieve-tube can be visualized which would reduce the resistance offered by the medium to diffusion. It is tempting to postulate the existence in the sieve-tubes of some special organization of capillary structure which enormously reduces the resistance to diffusion. We are, however, as yet ignorant as to the possibility of this".

The intention of this paper is to point out that it is indeed possible to visualize such a mechanism.

Further experiments of the same authors gave evidence, that nitrogenous substances (8) and some mineral elements (10) are transported in the same way.

Some remarkable experiments with *Tropaeolum majus* enabled SCHUMACHER (14) to show that of all parts of the phloem the sieve-tubes are the only elements along which nitrogenous organic substances are transported through the leaf-stalk.

These authors have therefore confirmed the most current conceptions on the channels of transport of organic matter, formerly concluded from the results of numerous convincing experiments. As to the mechanism of transport they give us no clue. As a mere diffusion-process entirely fails to explain the rapid translocation of matter, two possible explanations seem thusfar to be left. The first is that originally given by DE VRIES (17), who was of opinion that the protoplasmic streaming is the transporting agent. This opinion is still held by some authors (a.o. CURTIS (2)). However it could not yet conclusively be proved that the protoplasmic streaming is essential in the normal transport through the sieve-tubes.

Another explanation has been given by MÜNCH (11, 12), who developed a new and suggestive theory which drew considerable attention. According to this theory the transport through the sieve-tubes should proceed as a current of solution in the direction from higher to lower turgor pressure. The energy required should be produced in the assimilating leaf cells; like the xylem vessels in the water transport, the sieve-tubes should have only a passive function, serving as semipermeable tubes and being mere channels of transport.

This theory seems to be of high value as a working hypothesis. It will have to be demonstrated whether, under natural conditions, such a rapid movement of water takes place through the sieve-tubes. This may be well within the experimental possibilities.

Some experiments of WEEVERS and WESTENBERG (19) did not confirm some of MÜNCH's experimental results. SCHUMACHER's (14) observation, that nitrogenous substances are rapidly transported out of wilted petals, also seems not to agree with MÜNCH's views.

For a more detailed discussion I refer to comprehensive treatises on this subject (see a.o. Weevers (19) ; Kruseman (5)).

As this question seems still far from settled, it may not be superfluous to suggest another possible explanation, which thusfar seems to be overlooked.

When a drop of a liquid, insoluble in water, the molecules of which contain an electropolar group, is placed on a water surface, it will tend to spread rapidly over this surface. This spreading takes place in the direction from lower to higher surface tension and will not stop, until the surface tensions are equalized. This condition will be reached when the layer of the liquid added has become monomolecular. Taking advantage of this phenomenon Langmuir (7) in his well-known experiments measured the length and thickness of a number of molecules. The many interesting experiments, since then made on these "two-dimensional" systems have recently been reviewed by Heymann (3).

So it is clear that along the surface of water a rapid displacement of matter may take place, originating from surface-active forces. Not only the surface of water against air, but, no doubt, also the interfacial surface between water and another liquid may constitute such a channel of transport.

In order to demonstrate this in a clearly visible way an apparatus was constructed, which, after several trials, is shown in its final shape in figure 1.

Two small glass bulbs *a* and *b* with a volume of about 7.5 cc each are

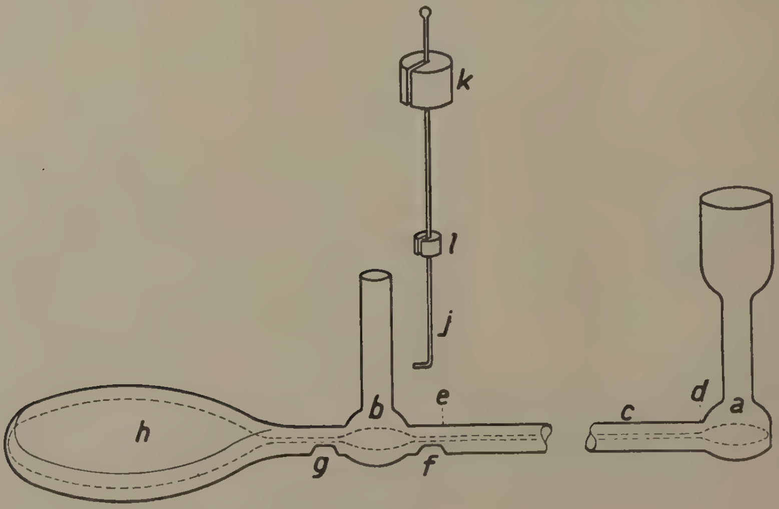

Fig. 1.

connected with a tube *c*. This tube has an inner diameter of 1 cm. The distance between the centres of the bulbs is 1 m. Bulb *a* is provided with a funnel. To the other side of bulb *b* another similar tube is fused, connecting it with the receptacle *h*. This receptacle is of a flat elliptical shape, with the dimensions of $1\frac{1}{2} \times 10 \times 8\frac{1}{2}$ cm.

At both sides of bulb *b* the bottom of the glass tubes *f* and *g* has been elevated over a distance of 1 cm, in such a way that the inner side of the glass bottom nearly reaches the middle of the tubes.

In bulb *b* a small stirrer *j* can be inserted consisting of a tiny glass rod, 1 mm thick and bent at right angles at the lower end. It is inserted in two pierced corks *k* and *l*, which are provided with a slit. Cork *k* is to be fixed in the clamp of a stative, whilst the small cork *l* is inserted in *b*. By rotating between the fingers the head of *l* contents of *b* may be stirred without shaking the apparatus.

One liter of distilled water was slightly acidulated with hydrochloric acid and 25 cc of a 0.04 % solution of the indicator chlorphenol red (Dichlorophenolsulfonphthalein) was added.

After boiling it to expel the dissolved carbon dioxide, traces of KOH were added to give it a pH of 5.8. At this pH the indicator shows an intermediate color and a shifting of the pH in either direction may be easily observed.

The apparatus was half-way filled with a measured quantity of this solution and subsequently filled with pure ether saturated with water, precautions being taken to leave no air-bubbles inside. By gentle shaking during several minutes the water was also saturated with ether. Subsequently the apparatus was exactly leveled horizontally, so that the interface between ether and water divided the apparatus into an upper and a lower half, as indicated by the dotted line in the figure, the water only just covering the elevations *f* and *g*.

In 25 cc of a 0.2 normal solution of potassium hydroxide 0.1 g oleic acid was dissolved. When a small quantity of this oleate solution containing excess of KOH is put into bulb *a* the orange-red color of the bulb is converted into purple. This color change is not confined, however, to the contents of bulb *a*, but immediately begins to spread along the water-ether interface. Seen in side-view, it has the shape of a sharp wedge, moving along the interface at first rapidly, afterwards more slowly. Evidently a rapid displacement of potassium oleate takes place along the interface. When the oleate comes into contact with the trace of HCl in the water it is converted into oleic acid, making room for a new spreading of oleate and resulting in a shifting of the pH towards a more alcaline reaction.

It is, in this case, not only a movement of a "two-dimensional" film. A layer of water (and, of course, of ether) is dragged along with the interface, causing a distinctly observable compensating stream of water along the bottom of the tube in opposite direction. So the movement is in fact a displacement of a certain volume of solution. The neutralisation reaction therefore will be due probably for the greater part to the excess of hydroxyde contained in this solution. However, since the oleate, according to GIBBS' rule (KRUYT (5), p. 18), accumulates in the interface, the share of hydroxyde and oleate in the transport of alcali is hardly to estimate.

If the receptacle *h* were omitted and the apparatus ended at *g*, the inevitable contaminations of the ether-water interface would accumulate in *b* and seriously interfere with the experiment. If they are allowed to escape into *h*, the spreading substance may enter into bulb *b* unhampered.

After adding a certain amount of the oleate solution to bulb *a*, one may observe the velocity with which the purple color spreads along the interface, thus stating that measurable amounts of alcali are transported over a certain distance within a certain time. In this way one obtains information about the velocity of transport but not about the quantities transported.

Therefore a measured quantity of 0.01 normal hydrochloric acid was added to bulb *b* and the time, necessary for the neutralization of the acid, was measured. In this manner the quantity transported within a certain time could be approximated.

The procedure of the experiments was as follows:

A thin graduated pipette filled with 0.01 normal hydrochloric acid was carefully introduced into bulb *b*, so that the point reached the bottom and a quantity (0.6 or 1.2 cc) of HCl was slowly added. Then the pipette was gently removed and the stirrer put in its place, so that its lower end reached beneath the water-ether level. The acid added proved to remain for the greater part unmixed in the lower part of the bulb *b*, between the elevations *f* and *g*.

Now 1 cc of the oleate solution was added to the contents of bulb *a* by running it along the inner side of the funnel. The addition took about four seconds. From the moment of the first contact of the oleate solution with the interface the time was measured, in which the purple color covered a distance of 25, 50, 75 and 95 cm from point *d*. Then the stirrer was put into action and all alcali transported into bulb *b* was immediately mixed. The time was observed at which the color change of the contents of *b* was completed after the moment that the purple color had reached the 95 cm point at e.

As a blank determinations were also made without addition of hydrochloric acid.

The determinations are, of course, rather rough. Several sources of error are not taken into account. After addition of the oleate solution it is diluted to an unknown extent by the indicator solution. Besides, the depression of the interface tension causes a slight lowering of the level and a little shifting of the water layer from *a* towards *b*. By this movement also traces of HCl may escape into *h*, so that the orange-red color of the indicator locally changes into yellow. Also the higher specific weight of the oleate solution compared to the ether-saturated water may introduce a slight error. However, these errors may hardly have exerted a serious influence upon the results, especially since these observations only intended to determine the order of magnitude of this mode of transport.

The results of several determinations are given in the next table.

HCl 0,01 N added to *b*	Distance 25 cm.	Covered 50 cm.	In seconds 75 cm.	95 cm.	Contents of *b* neutralized	Average
None	9	65	175	293	42	40
"	8	60	160	280	40	
"	8	85	232	398	37	
0,6 cc	9	85	220	368	198	186
idem	9	85	235	403	182	
"	9	80	204	353	183	
1,2 cc	9	71	205	358	232	239
idem	10	100	265	445	245	
"	9	100	313	520	240	

It is evident that the spreading-velocity is very variable. However, the time wanted to neutralize the contents of bulb *b* seemed to be fairly constant; 0.6 cc HCl 0.01 N were neutralized in $186 - 40 = 146$ seconds; 1.2 cc in $239 - 40 = 199$ seconds. Since it took 146 seconds to neutralize the first 0.6 cc, the next 0.6 cc of this 1.2 cc are evidently neutralized in $199 - 146 = 53$ seconds. This means a rate of transport of 0.006 milli-aequivalents in this time.

We may now visualize, in the same way as MASON and MASKELL did, that this transport is effected by a mere diffusion of KOH through the water layer and roughly estimate the "diffusion constant" belonging to this hypothetical process. We may assume that at this time of the experiment the oleate solution in *a* will have been considerably diluted, so that for instance the concentration of KOH will have become 0.02 milli-aequivalents per cc. The water layer connecting the bulbs is 97 cm long and (neglecting the constriction at *f*) has a cross-section of about 0.3 cm^2. Furthermore, we assume that there is a linear and constant concentration gradient from *a* to *b* during the 53 seconds concerned.

According to FICK's law we may now compute the "diffusion constant" as follows:

$$\frac{0,006}{53} \cdot \frac{1}{0,3} \cdot \frac{97}{0,02} = 1,83$$

The real diffusion constant of KOH in diluted solution at 18° C is 2.2×10^{-5} (International Critical Tables (4)). At the temperature at which the experiments were made (about 27° C) this constant may be

2.7×10^{-5}. The rate of transport observed is therefore 68000 times greater then could be expected.

If we assume that the greater part of the potassium is transported in the form of oleate, a still greater disproportionality should result from the computation. In any case, the velocity of the process is of the same order of magnitude as that found by MASON and MASKELL in the transport of carbohydrates.

Such a comparison of the velocities of the spreading and of the diffusion, however, is not correct, since the processes depend upon different factors in a different way. The spreading velocity will a.o. be dependent upon lowering of the interface tension by the interface-active substance; upon the viscosity of both fluids limiting the interfacial surface, and upon the diameter of the tube. The viscous resistance will increase with decreasing distance of the interface to the wall of the tube, so in very narrow tubes the disproportionality will not be so great. On the other hand, in narrower tubes the ratio of interface to cross section will increase, which will have an effect in opposite direction.

When we omit the ether layer from the experiment and the spreading proceeds along a water-air surface there is less viscous resistance and more lowering of the surface tension. Indeed, under these circumstances the purple color covers the distance of 95 cm in 18—20 seconds. In this case this spreading is preceded by a visible depression of the surface tension, running through the tube like a wave and reaching point *e* in only 5 seconds. In this short time traces of oleate must have been transported along this distance.

In one respect this mode of transport is similar to diffusion. As the lowering of the interface tension is dependent upon the concentration of the interface-active substance, the rate of transport will be a function of the concentration gradient, though perhaps not a linear one. In this regard as well as in regard to the order of magnitude, this is in accordance with MASON and MASKELL's experiments.

We may now look for an interface which might constitute a channel of transport in the sieve-tubes. It seems to me that the interface boundary between protoplasm and vacuole should meet the requirements. In any case it is an interface between two inmiscible liquid phases and any substance lowering its tension would tend to spread along this interface until concentration-differences are equalized. This should of course be accompanied by protoplasmic streaming which could, however, be the consequence instead of the agent of the transport. The primary cause of the transport would be only the concentration-difference of the substance to be transported.

The observed influence of narcotics upon the rate of transport of carbohydrates seems to agree with the above developed conception rather than with the theory of MÜNCH. Narcotics are all surface-active substances; so they probably accumulate in the interface and displace the substances normally to be transported.

I do not venture to pretend that, along this line, a satisfactory explanation will be at once found. Several difficulties certainly will be met with. Sugars, for instance, show a negative surface activity in the surface water-air. In accordance with GIBBS' rule they are negatively adsorbed by heat-denatured serum-albumine from their aqueous solution (BERCZELLER (1)). However, they are positively absorbed by a coal-suspension. This seems to indicate that the adsorption depends upon the nature of the interface and that the interface tension in the coal-water interface is lowered by sugars (RONA and MICHAELIS (13), VASATKO (16)). The same might be the case in other interfaces. It might also be possible that sugars were temporarily transferred into some interface-active form, in the same way as potassium is positively interface-active in the form of the oleate but negatively interface-active in the form of the hydroxide.

The relatively slow displacement of rotating protoplasm may be felt as an argument against this conception.

I will not go further than to indicate some new questions which are brought out by these experiments. For the present, a relation between the spreading of a substance along a liquid surface and the transport of organic substances through the phloem may seem to be rather theoretical. A more thorough study may prove whether the idea, indicated in this paper, is erroneous or, perhaps, suitable as a working hypothesis.

Proefstation voor de Java-Suikerindustrie.

Pasuruan, September 1932.

LITERATURE CITED.

1. BERCZELLER, L. 1918. Über negative Adsorption. Biochem. Zeitschr. **90**, 290.
2. CURTIS, O. F. 1925. Studies on the tissues concerned in the transfer of solutes in plants. The effect on the upward transfer of solutes of cutting the xylem as compared with that of cutting the phloem. Annals of Bot. **39**, 573.
3. HEYMANN, E. 1931. Neuere Untersuchungen über den Aufbau dünnster Oberflächenschichten (Filme) auf Flüssigkeiten. Zur physikalischen Chemie zweidimensionaler Systeme, Kolloid Zeitschr. **57**, 81.
4. International critical tables. New York 1926.
5. KRUSEMAN, M. W. 1931. De invloed van temperatuur en narcose op het transport der assimilaten. Dissertatie Utrecht.
6. KRUYT, H. R. Colloids, a textbook. London 1927.
7. LANGMUIR, I. 1917. The constitution and fundamental properties of solids and liquids. II Liquids. Journ. Amer. Chem. Soc. **39**, 1848.
8. MASKELL, E. J. and MASON, T. G. 1930. Studies on the transport of nitrogenous substances in the cotton plant III. Annals of Bot. **44**, 233.
9. MASON, T. G. and MASKELL, E. J. 1928. Studies on the transport of carbohydrates in the cotton plant. I and II. Annals of Bot. **42**, 189 and 571.
10. MASON, T. G. and MASKELL, E. J. 1931. Further studies on transport in the cotton plant I. Preliminary observations on the transport of phosphorus, potassium and calcium. Annals of Bot. **45**, 125.

11. MÜNCH, E. 1927. Versuche über den Saftkreislauf. Ber. d. D. Bot. Ges. **45**, 340.
12. MÜNCH, E. Die Stoffbewegungen in der Pflanze. Jena 1930.
13. RONA, P. and MICHAELIS, L. 1909. Über die Adsorption des Zuckers. Biochem. Zeitschr. **16**, 489.
14. SCHUMACHER, W. 1930. Untersuchungen über die Localisation der Stoffwanderung in den Leitbündeln höherer Pflanzen. Jahrb. f. wiss. Bot. **73**, 770.
15. SCHUMACHER, W. 1931. Über Eiweiszumsetzungen in Blütenblätter. Jahrb. f. wiss. Bot. **75**, 581.
16. VAŠATKO 1927. Die Adsorption der Saccharose an Adsorptionskohle. Zeitschr. f. d. Zuckerind. d. čechosl. Rep. **52** (9), 21.
17. VRIES, H. DE 1885. Über die Bedeutung der Circulation und der Rotation des Protoplasma für den Stofftransport in der Pflanze. Bot. Ztg. **43**, 1.
18. WEEVERS, TH. 1928. Ringwondproeven en hun beteekenis voor het stofvervoer in de plant. Vakblad voor Biologen **7**, 117.
19. WEEVERS, TH. and WESTENBERG, J. 1931. Versuche zur Prüfung der MÜNCHschen Theorie der Stoffbewegungen in der Pflanze. Proc. Kon. Akad. Wetensch. Amsterdam **34**, 1173.